DYNAMICS OF NOTCH SIGNALING IN A SELF-RENEWING TISSUE, THE *C. ELEGANS* GERMLINE

Inauguraldissertation

zur

Erlangung der Würde eines Doktors der Philosophie
vorgelegt der

Philosophisch-Naturwissenschaftlichen Fakultät der Universität Basel

von

Silvia Gutnik

aus Österreich

Basel, 2018

Genehmigt von der Philosophisch-Naturwissenschaftlichen Fakultät der

Universität Basel auf Antrag von

Prof. Dr. Susan M. Gasser

Dr. Rafal Ciosk

Prof. Dr. Alex Hajnal

Basel, 13.12.2016

Prof. Dr. Jörg Schibler

(Dekan der Philosophisch-Naturwissenschaftlichen Fakultät der Universität Basel)

Table of Content

Abbreviations

ANK	Ankyrin
ASC	Adult (somatic) stem cell
BMP	Bone morphogenetic protein
DTC	Distal tip cell
EGF(R)	Epidermal growth factor (receptor)
ESC	Embryonic stem cell
GSD	Germ cell diameter
GSC	Germline stem cell
HD	Heterodimerization domain
ICM	Inner cell mass
iPSC	Induced pluripotent stem cell
JAK/STAT	Januskinas/Signal transducers and activators of transcription
LBS	LAG-1 binding site
NICD	Notch intracellular domain
NRR	Negative regulatory region
NTC	NineTeen Complex
PCG	Primordial germ cells
PRC2	Polycomb repressive complex 2
PSC	Pluripotent stem cell
SOP	Sensory organ precursor
SRS	Substrate recognition subunit
TA	Transit-amplifying
TAD	Transactivation domain
TGF	Transforming growth factor
UPS	Ubiquitin-proteasome-system
T-ALL	T-cell acute lymphoblastic leukemia
VHL	Von Hippel Lindau

Summary

Notch signaling was in many stem cell systems shown to play not only an important role in self-renewal but also in differentiation. It is not surprising that perturbations within the pathway are associated with a variety of diseases. These range from loss-of-function mutations to activating mutations within the Notch signaling pathway and are mostly located within the Notch receptor itself. Hyperactivating mutations of Notch are often associated with auto-activation of the receptor or a failure of the activated receptor to be degraded. In the *C. elegans* stem cell system - the germline - the Notch receptor GLP-1 was shown to be absolutely essential for the maintenance of germline stem cells. Similar to the described hyperactivation found in cancer, hyperactivation of GLP-1 in the *C. elegans* germline is associated with the formation of a tumor. As in other stem cell systems the output of the signaling pathway has to be tightly controlled, which can generally happen on the various levels that assure receptor availability and its activation.

To study GLP-1 dynamics in the *C. elegans* germline we constructed a functional GFP knock-in within the intracellular domain of GLP-1, which is the form of Notch that translocates into the nucleus to activate gene expression. We found considerable differences in the receptor activation between the larval and adult germline and could show that this is likely due to differential turnover of the NICD by the ubiquitin-proteasome-system. In Notch signaling contexts in other organisms but also in Notch cell fate decisions in *C. elegans,* which are distinct from the germline stem cell fate decision, nuclear turnover of the activated Notch receptor was shown to be mediated by FBXW7/SEL-10. In contrast to the mechanism proposed for other Notch signaling events, we could show that activated GLP-1 is likely not turned over by SEL-10 but by a mechanism involving the U-box-containing E3 ligase PRP-19.

1. Introduction

1.1. Notch signaling in stem cell systems

1.1.1. Definition of stem cells and their niches

During the development of an organism cells grow, divide, migrate and adopt specific cell fates to shape organs and tissues.
Each single cell that is born contains the building plans to potentially develop into every cell type encoded in its genome. During development but also during tissue homeostasis, tightly controlled processes then safeguard the establishment of cell identities in a context dependent manner. This assures the appropriate number of cells and cell types at the right place and time in the body. Even after development in complex organisms has ceased, tissues keep being renewed throughout the organism's life.
Cells that possess this self-renewing potential are called stem cells. They are characterized not only by being undifferentiated and able to divide mitotically into more stem cells but also by having the ability to differentiate into specialized cell types. Their classification depends on their potency - the developmental options that are available to them. For example, totipotent stem cells are able to form all cell linages that support the proper development of a new organism, hence they give rise to embryonic as well as extra-embryonic cells. In mammals this characteristic is only known for the zygote - the cell that arises from the fusion of an egg with sperm - and the first cleavage blastomeres. On the other hand, pluripotent stem cells (PSCs), for example embryonic stem cells (ESCs), are able to form all cell linages of the body, while multipotent stem cells such as hematopoietic stem cells are able to acquire only a few cell fates, which correspond to one linage. In contrast, unipotent stem cells are predestinated to become one specific cell type. For example, spermatogonial stem cells differentiate only into sperm. (Jaenisch and Young 2008)
For a cell to be classified as a certain type of stem cell it has to meet the above-mentioned criteria of self-renewal and ability to differentiate according to its potency *in vitro*. In a natural context (*in vivo*) stem cell criteria are not always completely fulfilled. Thus, the definition of a stem cell depends on the context.
More broadly, stem cells can be categorized into those functioning during development of an organism, hence are required for the proper construction of the body, and stem cells that are functioning in the adult, which are referred to as adult somatic stem cells (ASCs), and hence are functioning in tissue homeostasis and repair.

However, the very same types of stem cells might function both during development and in the fully developed organism. One example here are germline stem cells (GSCs).

1.1.1.1. Stem cells of the developing organism and induced pluripotent stem cells

In sexually reproducing species a fully developed organism arises from one single cell, the zygote. Subsequent cell divisions then give rise to cells that will eventually form a full body. A complex sequence of cell divisions is thereby accompanied by a continuous commitment of newly born cells to specific cell fates. This process is called linage commitment and goes in hand with a subsequent decrease in a cell's potency.
During mammalian preimplantation development an embryo initially undergoes several rounds of cell divisions before the newly formed cell mass starts to compact and cells lying on the outside start to form an epithelium called the trophoblast. While the trophoblast will later give rise to the extra-embryonic tissues such as the placenta, the inner cell mass (ICM) will originate all three germ layers: endo-, ecto- and mesoderm. Until the formation of the so-called blastocyst each individual cell is still regarded as being totipotent since it retains the potential to either form the trophoblast or the ICM. A little later in development the very same cells might have committed to the ICM and will therefore "only" be regarded as pluripotent. However, blastomeres as well as cells of the ICM are *in vivo* not indefinitely self-renewing, even though they are regarded as stem cells. Yet those cells still retain the ability of self-renewal, since they can be cultured indefinitely *in vitro* as ESCs.
All cells that retain the ability to differentiate into the three germ layers, endoderm, ectoderm and mesoderm are defined as pluripotent cells. This does not only hold true for ESCs but also for somatic cells that were reprogrammed by *in vitro* technologies. The latter type of stem cells is called induced pluripotent stem cells (iPSCs) and is extensively used in stem cell research to understand the molecular mechanisms underlying pluripotency and reprogramming. (Jaenisch and Young 2008, Romito and Cobellis 2016)
After development of an organism has ceased and a full body was formed, stem cell identity is restricted to ASCs and GSCs.

1.1.1.2. Adult stem cells

Classically, ASCs are thought to be functioning tissue-specific to assure tissue homeostasis and regeneration of damaged tissues. Especially tissues that are somewhat in contact with the environment require a fast turnover - the various epithelia found in the body: the skin, lungs, and the intestine, to name a few. Epithelial tissues, while fulfilling tasks such as absorption of food and oxygen or secretion of enzymes and body fluids, are important barriers that shield the body against dangers from the environment such as microorganisms and carcinogens. All these tasks and the constant damage that they are confronted with require robust self-renewal.
Similar to linage commitment described for stem cells during the development of an organism, ASCs are the basis of a cells path towards differentiation. In contrast to stem cells in early development, which still possess a large developmental potential, ASCs are predestinated to give rise to only a few cell types or a single cell type. Despite the need for fast tissue-turnover, stem cells themselves are in some stem cell systems dividing only infrequently and are therefore regarded to be quiescent. Still, they are the basis for robust self-renewal by giving rise to fast-cycling transit-amplifying (TA) cells. One example for such a stem cell system is found in the small intestine. Intestinal stem cells are spatially restricted to the basis of crypts, where they divide guided by their stem cell niche (see below) and give rise to TA progenitors. The TA cells then migrate out of the crypt onto the villi and differentiate into the mature linages of the surface epithelium. (Barker, van de Wetering et al. 2008, Barker 2014)

1.1.1.3. Germline stem cells

Long-lived organisms retain the ability to self-renew in most if not all of their tissues throughout their life. The capability of repairing wounded and damaged tissues is at the basis of how the integrity of the body is retained and how a long life is supported. More simple and short-lived organisms do not require extensive mechanisms to retain the integrity of their bodies and therefore do not possess a multitude of ASCs and in some cases like in *C. elegans* none at all. However, common to all organisms is the requirement to sustain their own species. This ability is guaranteed in sexually propagating organisms by the production of gametes, which are the differentiated descendants of GSCs and can be seen as the basis of species self-renewal. Similar to ASCs that give rise to a limited number of different cell types, GCSs are predestinated to only give rise to gametes. However, they are not unipotent, since they are able to differentiate into germ cell tumors (teratomas). During normal development the potency of germ cells is restricted until after the fusion of a sperm with an oocyte,

developmental constraints are then readily eliminated to give rise to all the cell types of an organism. Thus, gametes remain developmentally plastic. In contrast, in teratomas germline cells were shown to precociously enter a pluripotent state and develop into fully differentiated tissues such as hair, teeth or neurons. (Ulbright 2005)
The self-renewing capacity of GSCs is kept in most invertebrates and vertebrates over a very long time postnatal or throughout the whole life of the organism. In mammals though, this was shown to be sex dependent. Mammalian males maintain GSCs in testis for a lifetime, while for females it still remains unclear whether they possess GSCs postnatal. (Xie 2008)

1.1.1.4. The stem cell niche

Stem cells in the adult as well as in the developing organism often reside in a localized microenvironment that is called stem cell niche (Figure 1A). Niches can be very simple and constituted by only one single cell but they can also be complex anatomical structures that are difficult to define and localize. The identification of a stem cell niche is therefore not always straightforward. The probably simplest niche consisting of only one somatic cell is found in the *C. elegans* hermaphrodite germline. It is therefore not surprising that it was amongst the first to be identified. (Xie 2008)
In the *Drosophila* ovary the stem cell niche was defined as a group of stromal cells located at the tip of the ovariole just adjacent to the GSCs (Xie and Spradling 2000). Similarly, the hub cells on the apical end of *Drosophila* testis were shown to serve as the niche (Kiger, Jones et al. 2001, Tulina and Matunis 2001).
While in *Drosophila* several somatic cells constitute the niche, in mammals GSC niches are complex anatomical structures, whose exact composition still remains unclear (Xie 2008).
GSC as well as ASC systems are often graded in regard to the differentiation status of the cells within the tissue they are residing in. A population of stem cells is found at the one end next to the niche followed by a sequence of cells that show a rising status of differentiation (as described before for intestinal stem cells within crypts). Thereby, stem cells are followed by progenitors and differentiated cells of the linage. Various reciprocal interactions between the niche and its stem cells create a dynamic system necessary for the maintenance of the stem cell pool (Figure 1A). Cues are manifold and do not only involve cell-cell interactions or cell-matrix interactions but also paracrine signals. (Scadden 2006, Barker 2014, Hsu, Li et al. 2014)

1.1.2. Modes of stem cell division

The interaction of stem cells with their niche is often required to initiate stem cell divisions, which happen symmetrically or asymmetrically.
The latter is thought to be the predominant mode of stem cell division in most systems. Thereby, after division one daughter cell retains the ability to self-renew and stays a stem cell while the other daughter cell starts its path towards differentiation. This process is referred to as asymmetric cell division. Asymmetric cell division in stem cells is not completely stochastic - though again there are exceptions -, but rather guided by either the vicinity of daughter cells to a stem cell niche, by intrinsic mechanisms or by a combination of both. During the former the cell closer to the niche remains a stem cell and cell divisions are mostly guided by external cues originating from the stem cell microenvironment. However, when intrinsic mechanisms are in play, asymmetric segregation of cell fate determinants and polarity factors define which cell remains a stem cell (Figure 1B). (Morrison and Kimble 2006, Knoblich 2008)
Asymmetric divisions seem to be an appealing strategy for stem cells to fulfill both of their tasks within only one division - namely self-renewal and differentiation. This mode of division alone cannot explain expansion of the stem cell pool, which is observed during development, wound healing and regeneration. It is therefore likely that a pool of stem cells is able to either divide symmetrically or asymmetrically depending on developmental cues or signals from the environment to assure the appropriate amount of stem cells needed at a given time. An example for a stem cell system that relies on symmetric divisions is the *C. elegans* germline (see chapter 1.2.2). In some stem cell systems, the mode of division might differ between genuine stem cells and their undifferentiated progenitors, for example the mentioned TA cells. While stem cells divide asymmetrically to replenish the pool of TA cells, TA cells themselves divide a limited number of times symmetrically. (Morrison and Kimble 2006)

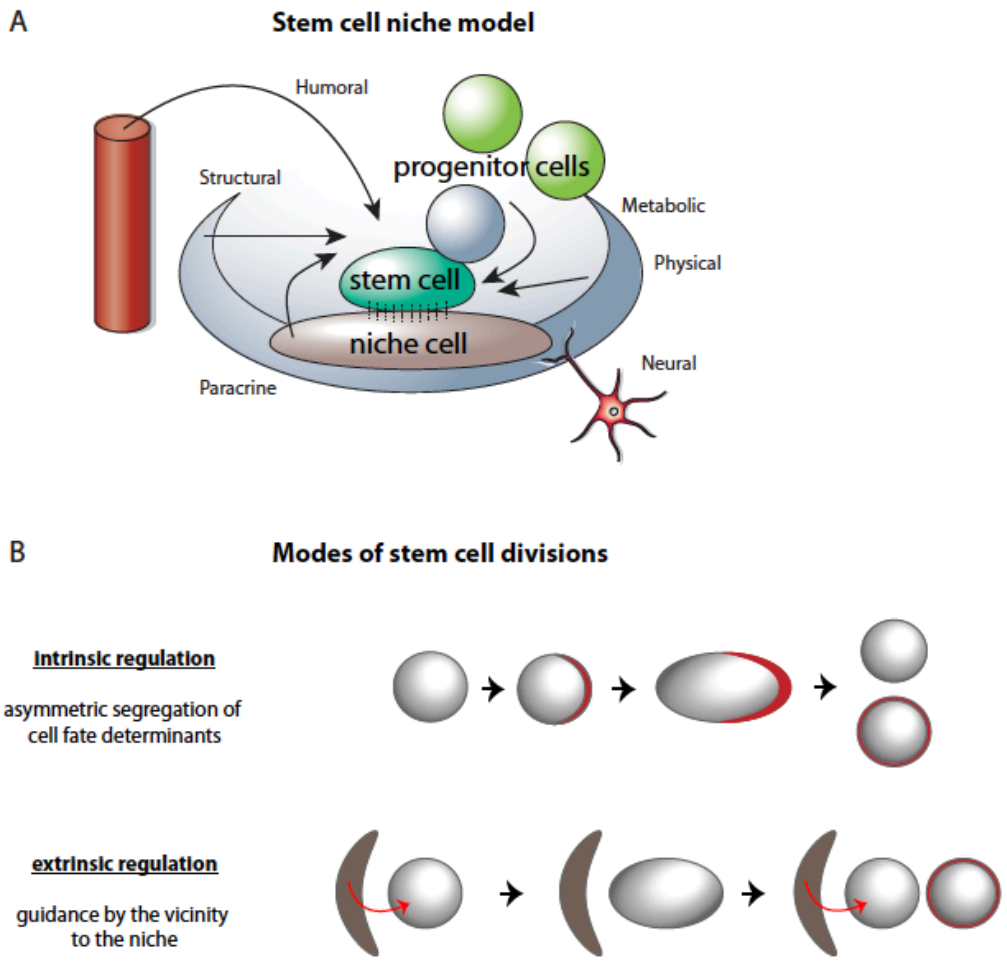

Figure 1: Stem cell niches and divisions.
(A) Schematic representation of a stem cell niche. Stem cell niches consist of cells (shown in brown) and structural components such as extracellular matrix. Communication between the niche and stem cells is manifold and ranges from cell-cell interactions to paracrine signaling molecules and input from the nervous system (adapted from (Scadden 2006)). (B) Schematic representation of ex- and intrinsically guided asymmetric stem cell divisions. Intrinsic regulation depends on the asymmetric distribution of cell fate determinants such as transcription factors, RNA binding proteins or structural proteins. Extrinsic regulation is guided by the vicinity of stem cells to their niche, whereby the niche signals to stem cells (adapted from (Knoblich 2008)).

1.1.3. Signaling pathways regulating stem cell self-renewal and differentiation with a focus on Notch signaling

Many of the mechanisms that safeguard cell fate transitions and set up cell identities are very well conserved between species. They include epigenetic branding of cells by chromatin modifiers, asymmetric division and segregation of linage determinants such as transcription factors, as well as the selective expression of cell fate determinants. Various signaling pathways guide the initiation of many of these mechanisms.

The same pathways might function to promote or inhibit certain cell fate decisions depending on the cellular context. A variety of signaling pathways have been shown to regulate stem cell self-renewal and differentiation. The Wnt signaling pathway for example has been shown to be important for cell fate specification in the human adult intestinal crypt, the nervous system and the hematopoietic system (Lowry and Richter 2007). BMP together with TGF-beta signaling is known to function in bone development and homeostasis (Wu, Chen et al. 2016). The JAK/STAT pathway was shown to regulate stem cells in *Drosophila* testis and ovaries together with BMP, though the requirements for both pathways are different in the male and female. In the testis JAK/STAT is required for GSC maintenance, while in the ovaries it is controlling the stem cell niche. Instead, BMP signaling was shown to be essential for the renewal of female GSCs. (Bausek 2013)

Probably one of the most widely studied signaling pathways in various stem cell systems is the Notch signaling pathway. Notch is believed to function during development and/or maintenance of most tissues and depending on the context promotes proliferation or differentiation. Within essentially the same tissue the function of Notch might be required during development but might be dispensable in the adult or vice versa. For example, Notch is important to induce the onset of hematopoiesis but is not required for the maintenance of hematopoietic stem cells in the adult bone marrow (Sandy, Jones et al. 2012). Notch is dispensable during embryonic development of the hair follicle, while it is required in the postnatal development for hair follicle differentiation (Aubin-Houzelstein 2012). Mechanisms that restrict Notch signaling in space and time will be introduced later (see chapter 1.1.3.3).

From the signaling pathways mentioned Notch signaling is somewhat unique. While extracellular signaling molecules such as cytokines and hormones induce BMP, TGF-beta and JAK/Stat signaling, canonical Notch signaling requires a cell-cell interaction, since the ligands are transmembrane proteins (Vassin, Bremer et al. 1987, Knust and Campos-Ortega 1989, Richards and Degnan 2009). Notably, non-canonical Notch signaling was shown to utilize secreted Notch ligands (D'Souza, Miyamoto et al. 2008).

It still remains unclear in many organisms to which extend Notch functions non-canonically. However, in the recent years it was shown that ligand- as well as transcription-independent functions of the pathway exist. One of the best-understood examples in this regard is Notch`s antagonistic function to the WNT/beta-catenin pathway in *Drosophila* (Andersen, Uosaki et al. 2012). Here, initiation of the muscle fate requires Wingless (WNT) signaling in a population of initially equal cells, which is followed by Notch-mediated lateral inhibition (see chapter 1.1.3.3) to restrict the muscle fate to only a few cells. As expected, disruption of the Wingless pathway resulted in failure of muscle cell fate specification. However, disruption of the Wingless pathway combined with the removal of the Notch receptor but not its ligand (Delta) and transcriptional activator (Su(H)) restored muscle progenitor specification. This implicates that a Notch signaling event is preceding the Wingless-dependent induction and that Notch functions independent of its ligand and transcriptional activator in this event (Brennan, Baylies et al. 1999).

1.1.3.1. Structure of the Notch receptor

The Notch receptor is a classical Type 1 single-pass transmembrane glycoprotein that can be subdivided into an extracellular part, which is responsible for ligand interaction, a short transmembrane domain and the Notch intracellular domain. Although Notch receptors are well conserved over many species from humans to worms, they differ in the sub-organization of functional domains. Common to all Notch receptors is a general building plan. The largest part of the extracellular portion of the Notch receptor consists of a series of EGF-like repeats each of which is about 40 amino acids long and contains six cysteine residues that form characteristic disulfide bonds. EGF-like repeats are responsible for ligand binding and range from 11 repeats in GLP-1 (Figure 2), 14 in LIN-12 to up to 29-36 in the four human NOTCH homologs and the *Drosophila* Notch. The EGF-like repeats are followed by three Lin12/Notch repeats (LNRs) and a heterodimerization domain (HD), which are together called the negative regulatory region (NRR) (Gordon, Arnett et al. 2008). In a non-induced receptor, the NRR acquires a conformation that buries one of the cleavage sites for membrane release of the NICD. Upon ligand-receptor interaction, a change in the conformation of the NRR allows access of proteases for cleavage and primes the receptor for signaling initiation (Gordon, Vardar-Ulu et al. 2007). The short transmembrane domain harbors a site for the second ligand-induced proteolytic cleavage, which ultimately releases the NICD.
The NICD contains several functional regions. The N-terminal RAM domain and the Ankyrin (ANK) repeats were shown to be responsible for binding to the transcriptional

activator CBF1. However, interactions between ANK repeats and CBF1 are weaker and therefore only marginally contribute to transactivation (Tamura, Taniguchi et al. 1995, Aster, Robertson et al. 1997, Kato, Taniguchi et al. 1997). In *C. elegans,* ANK repeats were additionally shown to act as an autonomous transactivation domain (TAD) (Roehl, Bosenberg et al. 1996).

The C-terminus of the NICD contains a PEST sequence, which is required for fast protein turnover. Some Notch receptors contain an additional TAD domain upstream of the PEST domain (Kurooka, Kuroda et al. 1998). Notably, activating mutations in the human Notch receptor, which are predominantly found within the membrane cleavage site or the PEST sequence, cause many forms of cancer known to be associated with altered Notch signaling (Figure 2).

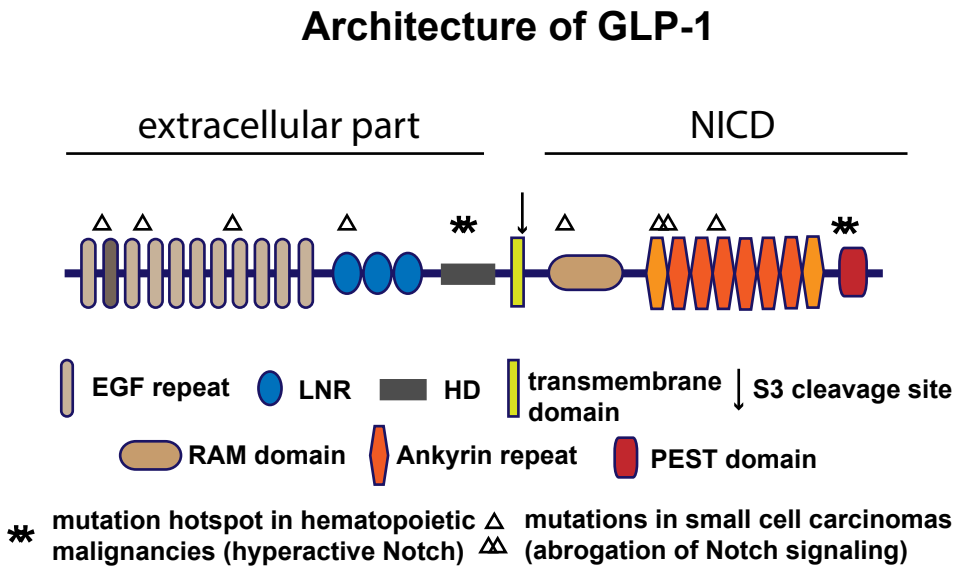

Figure 2: Notch receptor domain organization.

The Notch receptor consists of an extracellular N-terminal part, which is built up by EGF-like repeats, Lin12/Notch repeats (LNRs) and a heterodimerization domain (HD). A short transmembrane domain separates the extracellular portion from the intracellular part. The so-called Notch intracellular domain (NICD) contains a RAM (RBP-J-associated molecule) domain, Ankyrin repeats and a PEST sequence. * and Δ indicate frequent locations of mutations associated with certain types of cancer (Weng, Ferrando et al. 2004).

1.1.3.2. The mechanism of Notch signaling

Mechanistically the Notch pathway is a signaling pathway that relies on interactions between a signal-sending and a signal-receiving cell. Both cells express transmembrane proteins, whose extracellular domains need to interact in order to initiate the signaling cascade. However, the Notch pathway is quite special compared to other pathways, since it does not require any second messengers. Rather the intracellular portion of the Notch receptor itself, which is called the Notch intracellular domain (NICD), is functioning as the signaling moiety in this pathway.
The basic signal transduction pathway is strikingly similar in most Notch-dependent processes (summarized in Figure 3). The mechanisms that regulate the pathway are however different (see chapter 1.1.3.3).
Hereafter, I will give an overview of what is known about the mechanism of the core signaling pathway, which is mainly based on studies in *Drosophila* and to some extend on mammalian systems and *C. elegans.* What is known about the Notch pathway in *C. elegans* will be introduced in detail later.

Upon contact of the Notch ligand DSL (Delta/Serrate/LAG-2) with the Notch receptor a sequential cleavage reaction is initiated that subsequently leads to the dissociation of the NICD from the membrane and its translocation into the nucleus. Ligand contact thereby induces a conformational change within the NRR of the receptor, which allows for the first proteolytic cleavage (Gordon, Vardar-Ulu et al. 2007). This first cleavage is referred to as S2 cleavage and orchestrated by ADAM family proteases (Kuzbanian in *Drosophila* and ADAM10 and TACE in mammals) (Pan and Rubin 1997, Brou, Logeat et al. 2000, van Tetering, van Diest et al. 2009, Groot, Habets et al. 2014).
After the first cleavage the receptor is still residing within the membrane and finally set free during S3 cleavage by an intramembranous protease complex (the gamma-secretase complex) consisting of Presenilin and Nicastrin (De Strooper, Annaert et al. 1999, Song, Nadeau et al. 1999, Hu, Ye et al. 2002). The activated NICD then translocates into the nucleus (Schroeter, Kisslinger et al. 1998, Struhl and Adachi 1998).
In the nucleus the NICD associates with its transcriptional co-activators MAML (Mastermind, LAG-3/SEL-8) and CSL (CBF1, Suppressor of Hairless, LAG-1) to form the Notch ternary complex that initiates transcription of Notch target genes (Petcherski and Kimble 2000, Wu, Sun et al. 2002, Wilson and Kovall 2006). The NICD is thought not to directly bind to DNA but rather to CSL, which is bound to target genes and is acting as a repressor of gene expression (Wilson and Kovall 2006). CSL thereby confers specificity for Notch pathway targets. Depending on the species, CSL binds to different consensus sequences in the promoter regions of target genes. In *C. elegans* it was

shown that LAG-1 binds to the consensus sequence RTGGGAA called a LAG-1 binding site (LBS) (Christensen, Kodoyianni et al. 1996). Following this observation, a more brought definition of a LBS was suggested (YRTGRGAA) and two additional motives were proposed (RTGMGCCTYYR and CYTCMYCCW) (Yoo, Bais et al. 2004). In humans CBF1 is thought to bind to the consensus sequence GTGRGAA - a sequence with a high similarity to the putative *C. elegans* sites (Castel, Mourikis et al. 2013).

The interaction of the NICD and CSL results in CSL switching from a repressor into an activator of gene expression. The formation of the Notch ternary complex on DNA is accompanied by the eviction of a co-repressor complex and the recruitment of a co-activator complex (Wilson and Kovall 2006). Depending on the species and cell type, the co-repressor complex is built up by a variety of different proteins (Bray 2006), such as SMRT, HDAC-1, SIN3A, CIR, SAP30, SHARP, SKIP and CtBP in mammals (Kao, Ordentlich et al. 1998, Taniguchi, Furukawa et al. 1998, Hsieh, Zhou et al. 1999, Zhou, Fujimuro et al. 2000, Zhou and Hayward 2001, Oswald, Kostezka et al. 2002, Oswald, Winkler et al. 2005) or Hairless, Groucho and CtBP in *Drosophila* (Barolo, Stone et al. 2002). It was shown that SKIP might not only be part of the repressor complex but also part of the Notch activator complex. The NICD is thought to compete with the SMRT co-repressor complex for binding to CSL and SKIP, thereby displacing co-repressors and allowing for MAML recruitment. Using the respective homologs of *C. elegans* and *Drosophila* the interaction of SKIP with CSL was shown to be conserved between species at least *in vitro* (Zhou, Fujimuro et al. 2000). SKIP might therefore be an important factor mediating the switch from a repressor into an activator complex. The core activator complex was additionally shown to be joined by various co-activators, chromatin remodeling complexes (Nipped-A, Domino and Brahma in *Drosophila*, BRM in mouse) and histone acetyl transferases (p300 and/or PCAF/GCN5 in mouse) to initiate expression of Notch target genes (Wallberg, Pedersen et al. 2002, Kadam and Emerson 2003, Gause, Eissenberg et al. 2006).

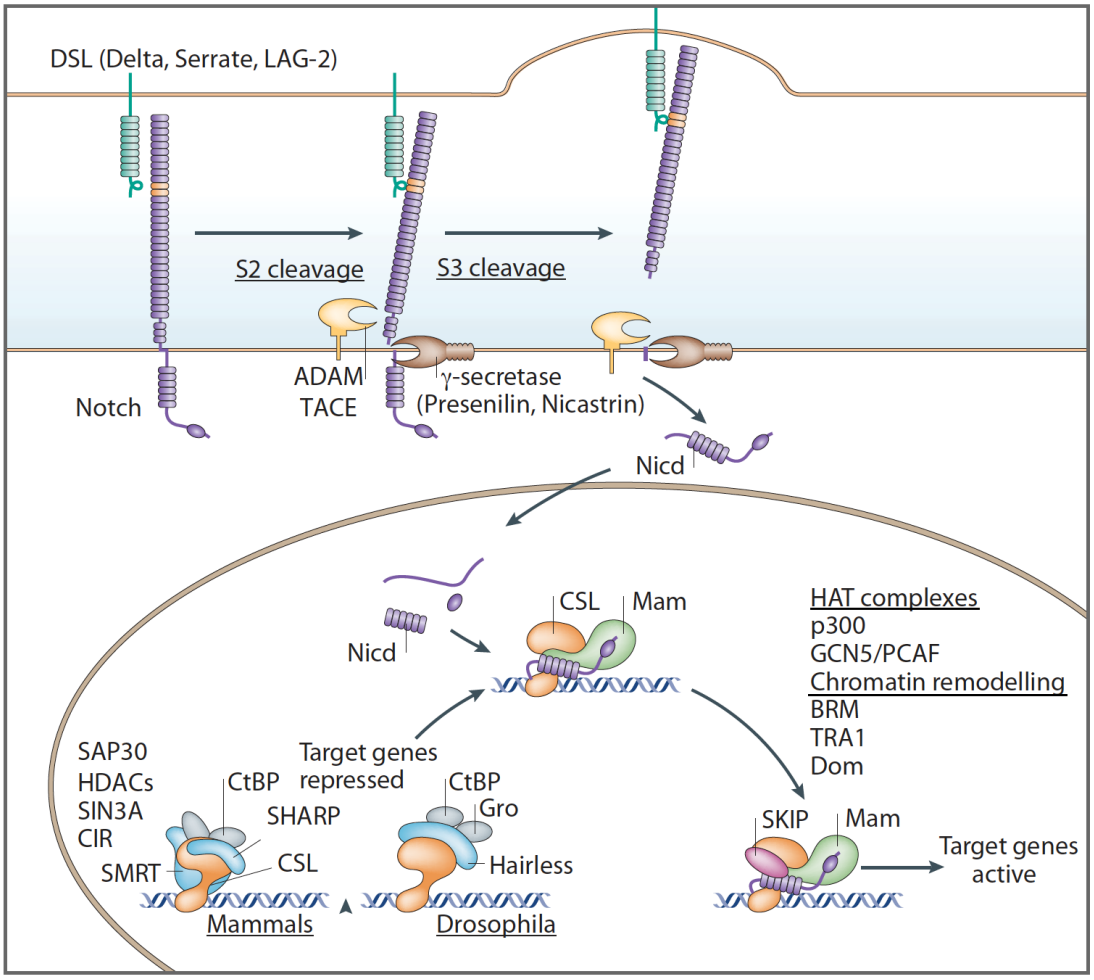

Figure 3: Notch signaling mechanism.

A schematic representation of the canonical Notch signaling pathway. Interaction of the Notch ligand DSL with the Notch receptor initiates a sequential cleavage reaction. The first cleavage occurs at the S2 site and is mediated by ADAM/TACE. This is followed by cleavage at the S3 site and mediated by the gamma-secretase complex, which is consisting of Presenilin and Nicastrin. The NICD then translocates into the nucleus and associates with transcriptional activators CSL and Mam. This displaces repressors from DNA-bound CSL, allows for binding of additional cofactors (HAT complexes and Chromatin remodelers) and initiates expression of Notch target genes. (adapted from (Bray 2006))

1.1.3.3. Mechanisms restricting Notch signaling

A very simple solution to restrict the activity of Notch signaling is the selective expression of the receptor and ligand on the surface of cells. This is a process that often depends on asymmetric inheritance of factors controlling expression or abundance of those proteins.

One simple example is the cell fate decision mediated by Notch signaling in the *C. elegans* 4-cell stage embryo, where ligand expression decides which cell acquires pharyngeal fate (Priess 2005). The first division of the worm zygote produces the AB and the P1 cell. The two descendants of AB - ABa and ABp - express the Notch receptor (Evans, Crittenden et al. 1994). However, only ABp is in contact with the ligand-expressing P2 (P1 descendant) and activates Notch signaling (Mickey, Mello et al. 1996). The spatial restriction of Notch receptor expression is thought to be regulated on the level of mRNA translation by POS-1 and SPN-4, which are two maternally provided and asymmetrically distributed RNA binding proteins (Ogura, Kishimoto et al. 2003). How the expression of the ligand is restricted still remains unclear.

Even when the Notch receptor and ligand are expressed uniformly on cell surfaces in some tissues, the activation of the pathway might still be restricted. Within such a population of equal cells, two fundamental mechanisms were shown to restrict or potentiate the ability of a cell to respond to Notch signaling - lateral inhibition and lateral induction.

In the former, Notch activation in a cell reduces the cell's ability to produce a functional signaling ligand. The negative feedback turns the cell into a signal-receiving cell and its neighbors into signal-sending cells. Which of the initially equal cells activates Notch signaling more strongly thereby depends on small differences.

The opposite is happening during lateral induction, where Notch activation in a cell leads to the ability of the cell to produce more functional ligand. Thereby, cells within a population act cooperatively as opposed to cell competition during lateral inhibition. The specification of the AC/VU cell fates and of vulva precursor cells in *C. elegans* are examples for lateral inhibition (see chapter 1.2.4).

While the above-mentioned phenomena - lateral inhibition and lateral induction - restrict and coordinate Notch signaling within a population of cells, various mechanism control ligand as well as receptor availability within a single cell. These mechanisms involve the selective turnover of the ligand and the receptor by the ubiquitin-proteasome-system, protein recycling and trafficking.

1.1.3.3.1. The ubiquitin-proteasome-system

Ubiquitin is a 76 amino acid long protein (Schlesinger, Goldstein et al. 1975), which is attached to target proteins by the E3 ligase system to mark them either for sorting within a cell, compartmentalization, recognition by other modifiers, secretion or degradation by the proteasome. Ubiquitination thereby functions in a variety of cellular processes such as cell-cycle progression, differentiation, transcription, immune response, viral infection and protein stability, trafficking and quality control. (Sun and Chen 2004, Haglund and Dikic 2005, Mukhopadhyay and Riezman 2007) Which of these functions are fulfilled by ubiquitin depends largely on the specific ubiquitin-linkage that is placed on a target protein and whether a mono- or polyubiquitin chain is added. The C-terminus of ubiquitin is thereby covalently attached to the ε-amino group of a lysine residue within the substrate protein or to a lysine within the preceding ubiquitin for polyubiquitination. For the latter, different lysine residues within ubiquitin are utilized (K6, K11, K27, K29, K33, K48 or K63) and polyubiquitin chains are typically linked via the same lysine of ubiquitin to generate for example exclusively K48- or K63-linked chains, which are referred to as homotypic chains. Heterogeneous linkage, where ubiquitin is attached to the preceding ubiquitin not strictly using the same lysine residue, is possible and might even give rise to forked chains and chains that contain ubiquitin-related proteins such as SUMO (Kirkpatrick, Hathaway et al. 2006, Kim, Kim et al. 2007, Ikeda and Dikic 2008). Monoubiquitination typically marks proteins for trafficking and sorting (Pickart and Fushman 2004), while homotypic K48-polyubiquitin marks proteins for degradation by the proteasome. The function of K6-, K11-, K27-, K29-, or K33-linked chains is not very well understood, but it might also include targeting of proteins for degradation (Xu, Duong et al. 2009). K63-linked chains are thought to be involved in a variety of non-proteolytic processes such as DNA damage response, protein trafficking, inflammatory response and translation (Pickart and Fushman 2004).

The enzymatic reaction that covalently links ubiquitin to a substrate requires the coordinated action of three classes of enzymes. An ubiquitin-activating enzyme (E1) first utilizes the energy of an ATP molecule to bind ubiquitin via a thiolester linkage (Haas, Warms et al. 1982). The activated ubiquitin is then passed on to an ubiquitin-conjugating enzyme (E2). The E2 then associates with an E3 ligase, which recognizes specific substrates and thereby brings the E2 close to the substrate. The ubiquitin is then either transferred to the E3 ligase via a thiolester linkage and then transferred to the substrate by the E3 itself. This mechanism is generally utilized by HECT domain-containing E3 ligases (see below). Or the E3 ligase confers a scaffold for bringing the E2 close enough to the substrate for ubiquitin transfer (Hershko, Heller et al. 1983, Pickart and Rose 1985) (Figure 4A). While there are usually only few or even only a

single E1 enzyme, there are many different E2s and even more E3s encoded in the genome of a species (Hershko and Ciechanover 1998). The latter confers specificity as well as the mode of ubiquitin transfer (Hershko and Ciechanover 1998, Craig and Tyers 1999). E3 ligases can either be monomeric, where specific domains of the E3 bind to the E2 and the substrate, or they can be consisting of multiple proteins and form a complex. The substrate protein is in the latter then recognized by the substrate recognition subunit (SRS) of the complex, while the E2 is bound by another subunit. Specific protein domains generally achieve substrate recognition. While monomeric E3s typically contain either a HECT domain, a U-box domain or a RING domain, SRS were shown to consist of F-box, BTB/POZ, SOCS-box and BC/VHL-box domains. Multimeric E3s generally fall into two classes, cullin-based complexes (Figure 4B) and the APC/C (anaphase promoting complex/cyclosome; not shown) (Kipreos 2005).

The *C. elegans* genome encodes only one E1, *uba-1*, and 20 *ubc* genes (**ub**iquitin **c**onjugating E2s) as well as three *uev* (**u**biquitin **E**2 **v**ariants) genes (Jones, Crowe et al. 2002). Also, the genome encodes 854 putative E3 ligases. The latter was recently re-annotated by filtering for genes that code for domains typically present in E3 ligases (F-box, HECT, U-box, BTB/POZ, RING, SOCS-box and BC/VHL-box domains) (Gupta, Leahul et al. 2015), which led to an substantial increase in the number of potential E3s compared to previous annotations (Kipreos 2005). Most of the 854 E3s can be categorized into proteins that associate with multimeric cullin-based E3 complexes. Each cullin complex consists of one of the six *C. elegans* cullin-family members (encoded by *cul-1,2,3,4,5,6*), one of their common adaptors RBX-1 (ROC1) or RBX-2 (ROC2) (Ohta, Michel et al. 1999), an E2 and an E3, and depending on the complex a variety of additional adaptor proteins. CUL-1-based complexes are typically associated with F-Box-containing E3s (449 in *C. elegans*) and SKP-related proteins (19) that function as adaptors. BTB/POZ domain-containing (168) associate with CUL-3. SOCS-box (4) and BC/VHL-box domain-containing (5) proteins are found in CUL-2-based complexes and at least in mammals in Cul5-based complexes, together with the common adaptors Elongin BC (ELB-1, ELC-1 in *C. elegans*) (Yamanaka, Yada et al. 2002, van den Heuvel 2004, Kipreos 2005, Sarikas, Hartmann et al. 2011). Most of the putative monomeric E3s encoded in the *C. elegans* genome are RING domain-containing E3s (192) and only a few contain a HECT domain (9) or a U-Box domain (Gupta, Leahul et al. 2015).

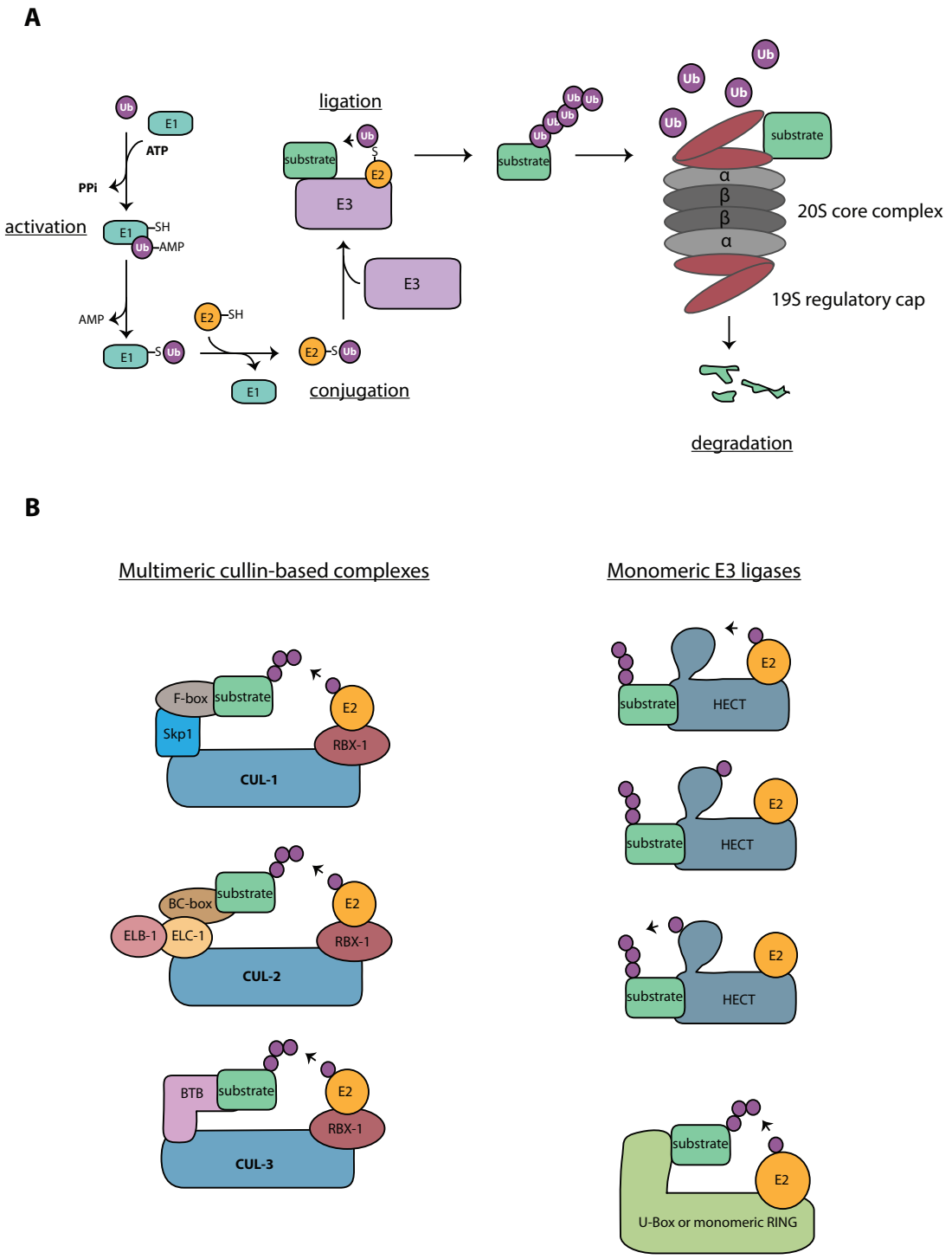

Figure 4: The ubiquitin-proteasome-system.

(A) Ubiquitination of target proteins. Ubiquitin is first activated by an E1-activating enzyme and then transferred onto an E2-conjugating enzyme, which associates with an E3 ligase to transfer ubiquitin onto a target protein. Specific polyubiquitin chains are then recognized by the 26S proteasome (built up by the 20S core complex and two 19S regulatory cap structures) and degraded.

(B) E3 ligases and their mode of ubiquitin transfer on target proteins. Most E3 ligases form a multi-subunit complex with a cullin-family member and their common adaptor proteins RBX-1/RBX-2. Monomeric E3 ligases can be subdivided into HECT-family members, U-Box and monomeric Ring domain-containing E3s. Similar to multimeric ring complexes, for the latter two ubiquitin is transferred from the bound E2-conjugating enzyme onto the substrate protein. Therefore U-Box and monomeric

Ring domain-containing E3s function more as a scaffolding structure that brings together the E2 and the substrate. HECT domain-containing E3 ligases are able to transfer ubiquitin onto the substrate by themselves (adapted from (Kipreos 2005, Pagan, Seto et al. 2013)).

Once a protein is marked for degradation it is readily recognized by the 26S proteasome, a multi-subunit complex that is performing the ATP-dependent proteolysis and resides both within the nucleus and cytoplasm (Tanaka, Kumatori et al. 1989). The proteasome is built up by one 20S core subunit and two 19S regulatory cap subunits (Figure 4A).

Four homologous rings form the 20S cylindrical core complex. Two beta-rings are sandwiched between two alpha-rings that each are built up by 7 alpha or beta subunits, respectively. The catalytic activity is conferred by three of the beta-subunits, β1, β2 and β5, which are encoded by *pbs-1*, *pbs-2* and *pbs-5* in *C. elegans* (Davy, Bello et al. 2001, Jung, Catalgol et al. 2009). The core complex is flanked by two 19S cap regulatory holoenzymes, which in *C. elegans* are built up by six ATPase subunits (*rpt-1,2,3,4,5,6*) and another 11 non-ATPs subunits (*rpn-1,2,3,5,6,7,8,9,10,11,12*). Together the components of the 19S cap form a ring-shaped base (*rpt-1-6* together with *rpn-1* and *rpn-2*) and a lid-structure (Davy, Bello et al. 2001). Some of the subunits exert specific functions. Rpt2 and Rpt5 were shown to be involved in gate opening of the 20S core complex (Smith, Chang et al. 2007). Rpn10 and Rpn13 function as ubiquitin sensors (Deveraux, Ustrell et al. 1994, Schreiner, Chen et al. 2008) and Rpn11 contains a proteolytic center that catalyzes the degradation of ubiquitin, thereby freeing single ubiquitin molecules for reuse (Verma, Aravind et al. 2002).

Ubiquitination is a powerful cellular process that regulates the abundance of proteins by selectively marking them for proteasomal degradation but also for sorting in subcellular compartments such as endoplasmic bodies. For the Notch signaling pathway both processes have been described for regulating the abundance of ligands and the receptor on the cell membranes of signal-sending and -receiving cells.

1.1.3.3.2. Restriction of ligand availability

Several studies in *Drosophila* and zebrafish identified the endocytic factor Epsin and the E3 ligases Neuralized and Mind bomb to be required for ligand activation on cell membranes (Lai, Deblandre et al. 2001, Pavlopoulos, Pitsouli et al. 2001, Itoh, Kim et al. 2003, Overstreet, Fitch et al. 2004, Tian, Hansen et al. 2004, Wang and Struhl 2004). It is thought that Neuralized and Mind bomb ubiquitinate the intracellular part of ligands on membranes. These mark primes ligands for an interaction with the ubiquitin binding protein Epsin that induces receptor endocytosis (Figure 5A). At a first

glance it seems counterintuitive that endocytosis of the ligand contributes to activation of the signaling pathway. Several models have been proposed to explain the requirement of endocytosis for ligand activation. First, it is thought that the inclusion of ligands in endocytic bodies followed by recycling to the cell surface allows for modifications and/or clustering of ligands. Second, the generation of endocytic vesicles might generate a pulling force on interacting receptors that causes the conformational change required for receptor cleavage at the S2 site. Or the pulling force removes the Notch extracellular domain to make S2 accessible. (Bray 2006, Chitnis 2006)

Ligand endocytosis is however not required for all Notch-mediated cell fate decisions and seems to be dispensable in *C. elegans* all along (Fitzgerald and Greenwald 1995). Additionally, Neuralized and Mind bomb were shown to participate in distinct Notch signaling events. In *Drosophila* Mind bomb preferentially regulates Delta activity during leg segmentation and wing vein formation, while it regulates Serrate during wing development (Le Borgne, Remaud et al. 2005). Neuralized, in contrast, was shown to be dispensable for the mentioned cell fate specification events and in return was shown to be required during peripheral neurogenesis (Lai and Rubin 2001).

1.1.3.3.3. Restriction of receptor availability

Similar to the control of ligand activity, several E3 ligases and endocytic factors have been implicated in the regulation of the Notch receptor on the cell surface (Figure 5B). *Drosophila* Numb for example was shown to interact with a component of the clathrin coats of transport vesicles (α-adaptin) and the Notch receptor, leading to receptor-mediated endocytosis of Notch. During divisions of sensory organ precursor (SOP) cells Numb is asymmetrically distributed. This generates a small difference in receptor availability within daughter cells that initially express equal amounts of the ligand and the receptor on the cell surface. This feedback leads to activation of Notch signaling in the daughter cell that did not inherit Numb (Berdnik, Torok et al. 2002). Mammalian Numb was additionally shown to mediate ubiquitination and degradation of the membrane-bound Notch1 by recruiting the HECT-type E3 ligase Itch (Qiu, Joazeiro et al. 2000, McGill and McGlade 2003). The mechanism how Numb negatively regulates Notch receptor activity on the cell surface still needs clarification since the elimination of binding domains for endocytic proteins within Numb as well as the reduction of proteasome activity proved not to influence Numb`s function in *Drosophila* SOP cell fate determination (Tang, Rompani et al. 2005).

While proteasomal degradation of the Notch receptor seems to be the predominant mechanism of turnover in most systems, an alternative mode of degradation was

postulated for the differentiation of murine skeletal myoblast cells. In this system the transmembrane receptor is thought to be targeted for lysosomal degradation by the E3 ligase c-Cbl (Jehn, Dittert et al. 2002).

Yet another mechanism involved in transmembrane protein trafficking was proposed to participate in the regulation of Notch receptor activity. Shrub - a member of the ESCRT-III complex - and the β-arrestin Kurtz are thought to cooperate with the E3 ligase Deltex to sort the Notch receptor into endosomes. In the presence of Shrub, Notch is sorted for degradation, while in the absence of Shrub and/or Kurtz, Deltex promotes monoubiquitination and activation of the receptor independent of ligand interaction (Hori, Sen et al. 2012).

Next to endocytic processes that determine receptor availability either by degradation or recycling, the extracellular portion of the Notch receptor is modified by glycosylation, which changes its ability to interact with the Notch ligand (summarized in (Bray 2006)).

A ligand-independent cleavage of the full-length Notch receptor by a furin-convertase that leads to the formation of a Notch heterodimer was for some Notch-signaling contexts shown to be required for the maturation of the receptor and activation of the pathway (Logeat, Bessia et al. 1998). For most mammalian systems the heterodimeric form of Notch seems to predominate. In *Drosophila* the functional importance of a furin-cleavage is controversial. It was suggested that both forms of the receptor might exhibit different functions depending on the developmental context (Blaumueller, Qi et al. 1997, Jarriault, Le Bail et al. 1998, Bush, diSibio et al. 2001, Kidd and Lieber 2002, Lake, Grimm et al. 2009). In *C. elegans* it is not clear whether Notch receptors are occurring as heterodimer (Greenwald 2005).

A Restriction of ligand activity

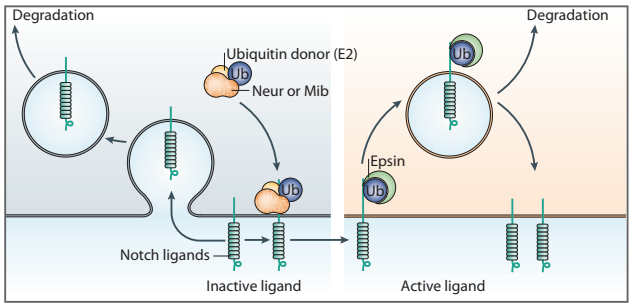

B Restriction of receptor activity

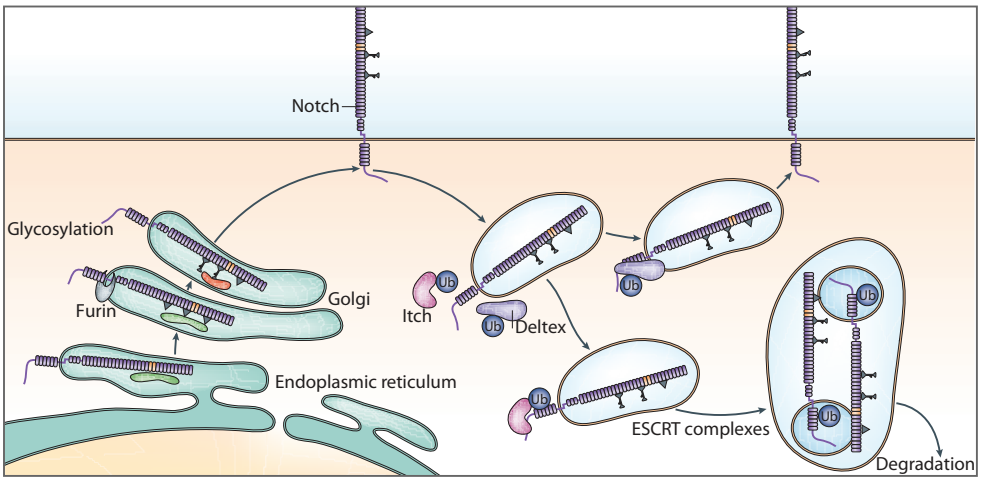

C Restriction of Notch signaling by NICD turnover

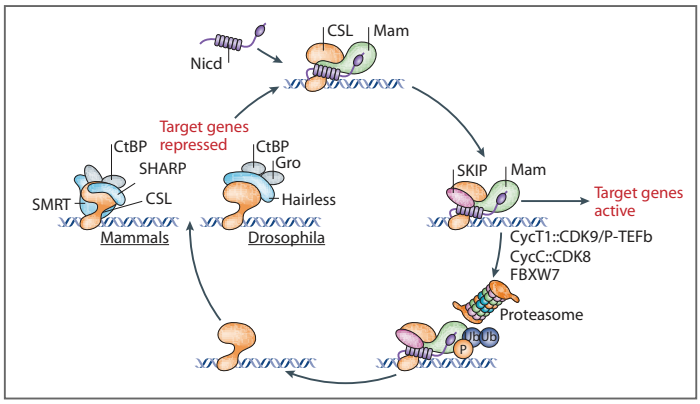

Figure 5: Restriction of Notch signaling.

(A) Neuralized (Neur) and Mind bomb (Mib) ubiquitinate the Notch ligand and thereby prevent its internalization and degradation. Ubiquitination of the ligand marks it for interaction with the endocytic protein Epsin and induces ligand internalization that is thought to be required for activation of the ligand. (B) Receptor internalization and sorting is regulated by the E3 ligases Itch and Deltex. Notch receptors are either marked for degradation by the ESCRT-complex or sorted back to the cell surface (right side). The Notch receptor is thought to be glycosylated and cleaved at the S1 site by a furin-

convertase prior to its transport to cell membranes. (C) The activated NICD is thought to be readily marked for degradation after association with the transcriptional complex and initiation of target gene expression. This process is thought to involve phosphorylation and ubiquitin-dependent degradation by the proteasome, and to be regulated by CycT1:CDK9/P-TEFb, CycC::CDK8 and FBXW7. (adapted from (Bray 2006))

1.1.3.3.4. Restriction of Notch signaling by NICD turnover

Many tightly regulated mechanisms assure that the ligand-receptor interaction happens at the right time and at the right place to initiate Notch signaling.
Notch pathway activity is rapidly changing. Once activation has occurred and the NICD mediates expression of Notch target genes, the signaling response is readily tuned down to assure the required flexibility. This implies that the activated NICD is rapidly dissociating from the Notch ternary complex allowing for an exchange of the co-activator with the co-repressor complex. One simple solution to induce NICD dissociation is the placement of protein modifications on the NICD that ultimately changes the affinity of interacting proteins. Another, though more stochastic one, is the constant competition of proteins for binding to CBF1. The latter might be exemplified by the above-mentioned competition of the NICD with the repressor SMRT for binding to CSL and SKIP (Zhou, Fujimuro et al. 2000). The former is achieved by the selective recruitment of factors that ultimately mark the NICD for turnover by the proteasome once the ternary complex has formed and has initiated target gene expression. Thereby, transcription initiation is coupled to transcription factor turnover. This was for example shown in cell culture, where CycC::CDK8 and CycT1:CDK9/P-TEFb were shown to be recruited to the HES1 promoter together with the NICD and co-activators such as Mam and SKIP. Phosphorylation of the NICD by CycC::CDK8 then promotes ubiquitination by the E3 ligase FBXW7 and proteasomal degradation (Fryer, Lamar et al. 2002, Fryer, White et al. 2004)(Figure 5C). However, FBXW7 and its homologs are not uniformly required for NICD turnover. For mammalian Notch1, Notch3 and Notch4 this seems to be the case (Gupta-Rossi, Le Bail et al. 2001, Oberg, Li et al. 2001, Wu, Lyapina et al. 2001, Tetzlaff, Yu et al. 2004, Matsumoto, Onoyama et al. 2011). The *Drosophila* FBXW7 homolog Archipelago for example was not yet implicated in regulating Notch pathway components but rather to be transcriptionally induced by Notch signaling (Bray 2006, Nicholson, Nicolay et al. 2011). In *C. elegans* the FBXW7 homolog SEL-10 seems to be required for certain cell fate decisions and to be dispensable for others (see chapter 1.2.4).

1.1.3.3.5. The functional relevance of restricting Notch signaling during disease

Since Notch is involved in many cell fate decisions during development as well as during tissue homeostasis, it is not surprising that many diseases are associated with mutations within the Notch receptor or ligand. Most of the mutations are found on the side of the receptor and either render the receptor constitutively active or non-functional, whereby the former is found more frequently (reviewed in (Andersson and Lendahl 2014)).

A famous example illustrating hyperactivation of the receptor in a disease is T-cell acute lymphoblastic leukemia (T-ALL), where more than 50% of known cases result from aberrant activation of the Notch1 receptor. The associated mutations very often lead to either an auto-activation of the receptor due to the exposure of the metalloprotease cleavage site or were shown to truncate the receptor N-terminally of the PEST domain, thus impairing degradation of the activated form of Notch. In mammals the E3 ligase FBXW7 was shown to be required for Notch1 degradation and mutations in the respective gene are accounting for 5% of T-ALL cases (Tsunematsu, Nakayama et al. 2004, Ferrando 2009). Also, in *C. elegans* hyperactivation of the GLP-1/Notch pathway was shown to result in the formation of a germline tumor. Interestingly, similar to tumors in patients, mutations that account for hyperactivation of GLP-1 are located in the NRR and are also thought to lead to ligand-independent activation of the pathway due to conformational changes that expose the S2 and S3 cleavage sites (Berry, Westlund et al. 1997, Pepper, Killian et al. 2003). In contrast to activating PEST mutations in human patients, a C-Terminal truncation of GLP-1 removing the PEST sequence was shown to lead to a phenotype otherwise observed in loss-of-function mutations at least in germline-associated and embryonic signaling events (Mango, Maine et al. 1991). This nicely illustrates that the regulatory modules fine-tuning the signaling output are versatile and context- as well as species-specific, even though the basic mechanisms of canonical Notch signaling are conserved over species. For the Notch pathway the regulatory circuits may range from the association of a multitude of transcriptional co-activators but also repressors (see chapter 1.1.3.2) to the selective recruitment of proteins that regulate the abundance of signaling components in general and more specifically of the Notch receptor itself (see chapter 1.1.3.3). In that way an elaborate regulatory circuit assures the right dosage of signaling at the right time during development and during tissue homeostasis and repair.

1.2. Notch signaling in the *C. elegans* germline stem cell niche

1.2.1. *C. elegans* as a model organism

The nematode *Caenorhabditis elegans* was first introduced as a model organism in the 1960s by Sydney Brenner and has since become one of the most important invertebrate models to study various developmental processes due to its short generation time (~96h at 15°C, ~50h at 20°C, ~40h at 25°C), transparency, large number of progeny and the ease to genetically manipulate it. (Corsi, Wightman et al. 2015)

Most of the worm`s live is devoted to reproduction. Wild-type worms produce between 200 and 300 progeny. After a period of in-uterine development the embryo is laid and hatches as a L1 larva that goes through three additional larval stages (L2-L4) intercepted by molts before finally developing into an adult worm. *C. elegans* predominantly occurs as XX hermaphrodite, which is capable of self-fertilization as it produces both sperm and oocytes. (Hubbard and Greenstein 2005)

After development has ceased, the germline is the only tissue that still divides and the only tissue capable of self-renewal. The constant divisions of GSCs thereby assure the generation of differentiated oocytes and the production of a large number of progeny. As already mentioned, the *C. elegans* germline is probably one of the simplest stem cell systems since the niche is only built up by a single somatic cell (Hubbard 2007).

1.2.2. The C. elegans germline

The adult *C. elegans* hermaphrodite germline lies within two U-shaped gonads that are attached to a single uterus. (Figure 6A). The gonad is organized as a blind-ended tube, similar to the gonad in *Drosophila,* and is graded in regard to the developmental state of each germ cell nucleus along the distal-to-proximal axis. A pool of undifferentiated GSCs (red circles in Figure 6) resides on the closed end (distal) followed by differentiating germ cells in the middle and gametes on the open end (proximal). The distal-most cells are in close contact with the stem cell niche, which consists of a single somatic cell called distal tip cell (DTC). (Hubbard 2007)

As in other stem cell systems GCSs are self-renewing and rely on the niche. The DTC was shown to be absolutely essential for GSC proliferation, since laser-ablation of the niche cell causes all GSCs to differentiate (Kimble and White 1981). While GSC divisions in the *Drosophila* male and female germline occur asymmetrically, GSCs in *C.*

elegans are dividing symmetrically during germ cell expansion in larvae and also in the adult. The divisions thereby produce daughter cells of equal potential, size and morphology. In contrast to *Drosophila*, where division planes are fixed, in *C. elegans* they are random. The ability of GSCs to divide is however still guided by the vicinity to the niche cell. (Morrison and Kimble 2006)

The *C. elegans* germline is actually a syncytium, so the term `germ cell´ refers to a germ cell nucleus surrounded by its cytoplasm and a cell membrane that retains an opening to the central core of the germline cytoplasm, called the rachis. The distal region of the germline, called the proliferative or mitotic zone, is the zone where mitotic cells can be found. By convention the proliferative zone spans up until a region, where distinctly crescent-shaped nuclei are found, a hallmark of these cells to transit into meiotic prophase. This region is called the transition zone. (Hubbard 2007)

The cells in the mitotic zone are not uniform. In accordance with the graded nature of the germline, cells closest to the niche are thought to be in the mitotic cell cycle, while cells that have moved further away from the niche are more likely to be in meiotic S-phase (Hubbard 2007). Hence, these two types of cells can be categorized into two pools - the very distal stem-cell-like pool and a proximal pool of transient-amplifying cells. While the former is kept in an immature state by the underlying regulatory network controlling proliferation in the germline and the vicinity to the niche, the pool of transient-amplifying cells gradually differentiates.

After leaving the proliferative zone, germ cells enter meiosis and start their path towards differentiation into sperm in L4 larvae or oocytes in adults (Kimble and White 1981).

1.2.3. Germline specification and development

The germline linage is specified already very early during development of the worm. After fertilization of an egg the first division of the zygote (P0) gives rise to the AB cell and the germline precursor cell the P1 blastomere, which after a couple of divisions gives rise to the P4 cell. The germline potential is segregated to the P blastomeres by several rounds of cell divisions and asymmetric partitioning events. The P4 divides the last time at around the 100-cell stage into Z2 and Z3 to generate the primordial germ cells (PCGs). In a freshly hatched L1 larva the Z2 and Z3 cells are flanked by the two somatic gonad precursor cells Z1 and Z4 (Figure 6B).

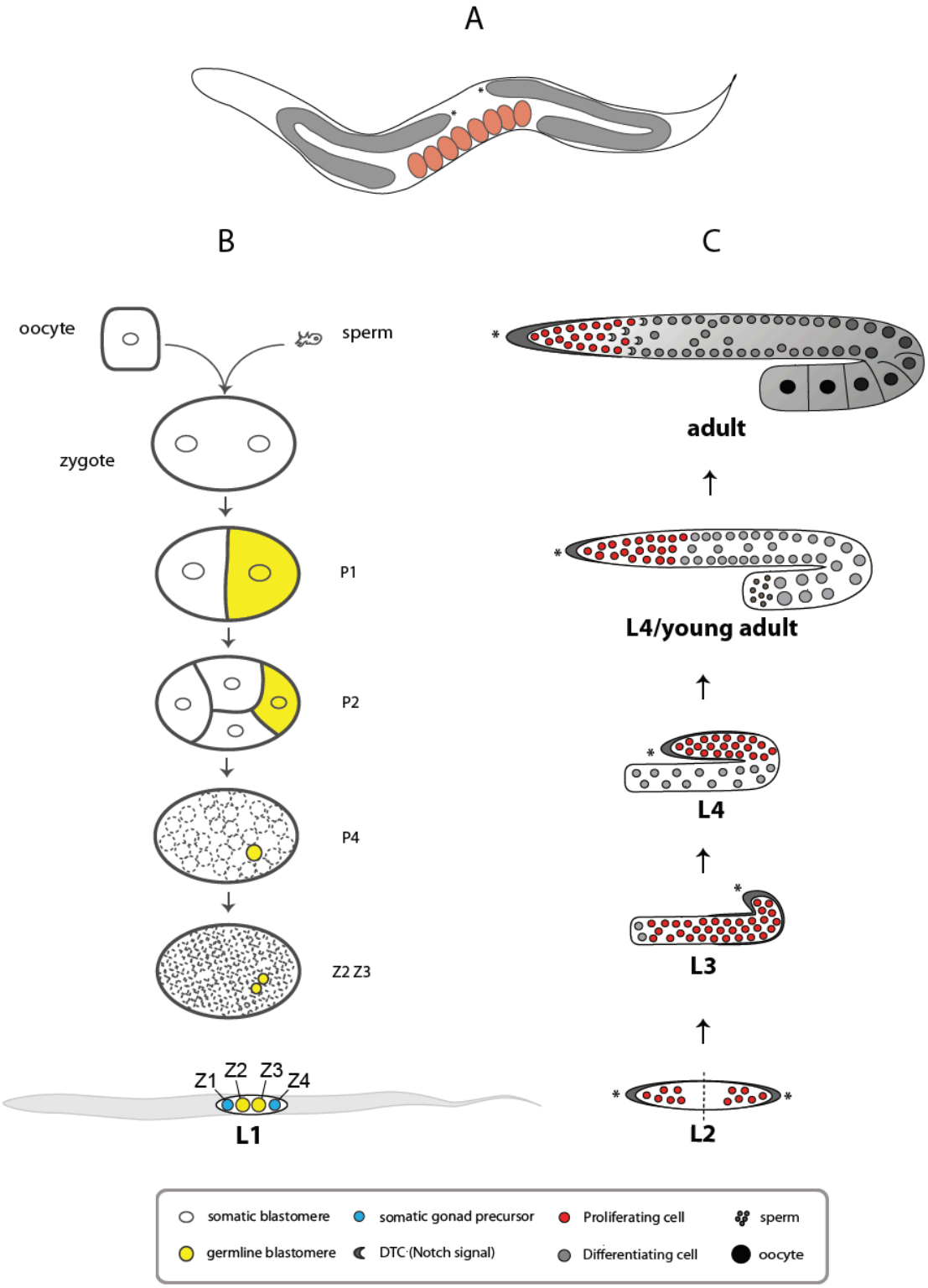

Figure 6: Germ cell specification and development in *C. elegans.*

(A) Schematic representation of an adult hermaphrodite worm. The adult worm contains two U-shaped gonads (grey), which produce oocytes that are self-fertilized when pushed through the spermatheca. The embryos (shown in orange) develop in-utero for a period of time. (B) The germline linage is specified early in development. The fusion of a sperm with an oocyte gives rise to a zygote, which divides a first time into the AB cell and the germline precursor cell, the P1 blastomere. Subsequent divisions give rise to the P2 (4-cell stage embryo), the P3 (8-cell stage embryo, not shown) and the P4

blastomere at the 16-cell stage of the developing embryo. At about the 100-cell stage the P4 cell divides a last time into two germ cell precursors called Z2 and Z3 that remain quiescent until after the L1 larva has hatched. (C) Schematic representation of germline development in larvae. The germline precursors start to proliferate and expand during mid L1 stage (not shown). The two somatic gonad precursors Z1 and Z4 will give rise to the DTCs and the somatic gonad. The germline expands along the anterior-posterior axis until late L3 and then turns to form its characteristic U-shape. During the L3 stage, meiosis is initiated and first produces sperm until the germline switches to oocyte production in adult worms. (adapted from (Hubbard and Greenstein 2005))

The somatic gonad develops in concern with the germline and gives amongst others rise to the two DTCs (marked with * throughout the thesis). PCGs stay mitotically quiescent until the mid L1 stage when they start to divide and expand the germline along the anterior-posterior axis. At around late L3/early L4 stage the germline turns and forms its characteristic U-shape. Meiosis is also initiated during the L3 stage. Thereafter, only the most distal cells in each gonad arm continue to mitotically divide. Until the end of the L4 stage the worms then produce sperm that will be stored in the spermatheca in adult worms. The germline switches from sperm to oocyte production with the last molt to adulthood - a process referred to as sperm-to-oocyte switch (Hubbard and Greenstein 2005) (Figure 6C).

1.2.4. Notch signaling in *C. elegans*

Similar to other organisms Notch signaling in *C. elegans* was shown to participate in several cell fate decisions.

The worm encodes two Notch homologs, *lin-12* and *glp-1* (Yochem and Greenwald 1989). While *lin-12* was primarily shown to function during vulva cell fate specification and *glp-1* in the maintenance of GSCs, they were both shown to be functionally redundant during embryogenesis (Sternberg and Horvitz 1989, Lambie and Kimble 1991, Fitzgerald, Wilkinson et al. 1993).

During vulva development *lin-12* functions in the AC/VU specification and together with *let-23* (EGFR) to specify the fates of three adjacent vulva precursor cells (VPCs), P5p, P6p and P7p. Both cell fate decisions are good examples for Notch acting through lateral inhibition (see chapter 1.1.3.3). The former decides which of the two initially equal cells (Z1.ppp and Z4.aaa) becomes the anchor cell (AC) or the ventral uterine precursor cell (VU). Both Z1.ppp and Z4.aaa express LIN-12 and LAG-2 (a Notch ligand in *C. elegans*). A small difference in LIN-12 activation leads to positive auto-regulation of *lin-12* transcription and to *lag-2* down-regulation in the presumptive VU (Wilkinson, Fitzgerald et al. 1994). During VPC specification LET-23 promotes the primary fate in

P6p via an inductive signal from the anchor cell and activates LIN-12 by lateral signaling in the neighboring P5p and P7p to promote the secondary fate (Sternberg 2005).

In the early embryo *glp-1* and *lin-12* function to specify the fates of AB descendants in four inductive interactions at different stages during embryogenesis. While *glp-1* is required for the first two cell specification events, *lin-12* and *glp-1* act redundantly in the latter two (Priess 2005). In the 4-cell stage embryo the two descendants of the AB cell - ABa and ABp - express the GLP-1 receptor (Priess and Thomson 1987, Evans, Crittenden et al. 1994). However, only ABp is in contact with the ligand-expressing P2 cell and activates Notch signaling (Mickey, Mello et al. 1996).

In the germline *glp-1* functions to maintain GSCs (Austin and Kimble 1987). As known for other Notch-regulated stem cell systems GLP-1 signaling in the germline represents a classical niche-stem-cell interaction. The DTC expresses one of the Notch ligands LAG-2 and the distal-most germ cells express the GLP-1 receptor (Figure 7A) (Crittenden, Troemel et al. 1994, Henderson, Gao et al. 1994).

The GLP-1 pathway is thought to be the main pathway regulating GSC proliferation in the developing as well as the adult worm and two recently discovered GLP-1 targets - *sygl-1* and *lst-1* - were shown to be essential in this context. In *glp-1 null* mutants GSCs do not proliferate already during larval stages and the few remaining cells differentiate into sperm (Austin and Kimble 1987). A phenotype that is reminiscent of the ablation of the DTC (Kimble and White 1981).

The basic mechanism of Notch signaling in *C. elegans* is strikingly similar to the canonical pathway described in other organisms (see chapter 1.1.3.2). Similar to the differences in requirements for certain Notch pathway components observed between species and during distinct cell fate decisions within the same species, genetic interaction studies suggest that some Notch pathway components interact with either *lin-12* or *glp-1*. Additionally, it was suggested that at least for certain cell fate decisions *lin-12* and *glp-1* function redundantly and *glp-1* was shown to compensate for the loss of *lin-12* activity when expressed under the control of *lin-12* regulatory sequences (Fitzgerald, Wilkinson et al. 1993). This implicates that LIN-12 as well as GLP-1 might use or at least be able to utilize the same ligands and downstream effectors of the pathway. Whether genes function in either LIN-12 or GLP-1 signaling might therefore depend to a certain extend on their expression profiles.

As in other organisms the transcriptional activator of LIN-12 and GLP-1 signaling is encoded by only one gene, *lag-1* (Csl) (Christensen, Kodoyianni et al. 1996). *sel-8* (also called *lag-3)* was identified to encode the functional counterpart of MAML in *C. elegan*s. Interestingly, *sel-8* does not share extensive sequence similarity with Mastermind (Doyle, Wen et al. 2000, Petcherski and Kimble 2000). Mutations in either *lag-1* or *sel-8* account for the loss of LIN-12 as well as GLP-1 signaling. While in other

species many components of the co-activator as well as the co-repressor complex have been identified, in *C. elegans* they are largely unknown.

C. elegans codes for four different Notch DSL ligands: APX-1*,* LAG-2*,* ARG-1 and DSL-1 (Bray 2006). *lag-2* was shown to function more broadly during LIN-12 signaling in the vulva, GLP-1 signaling in the germline and in GLP-1/LIN-12 signaling in the embryo. In contrast to that, APX-1 seems to be a maternally provided ligand for GLP-1 signaling in the early embryo (Lambie and Kimble 1991, Henderson, Gao et al. 1994, Mango, Thorpe et al. 1994, Mello, Draper et al. 1994). Recently, *apx-1* was shown to function redundantly with *lag-2* in germline proliferation starting from the L3 larval stage. However, early larval germ cell proliferation relies on *lag-2* (Nadarajan, Govindan et al. 2009). *Dsl-1* encodes the only secreted ligand and functions in vulva cell fate specification (Chen and Greenwald 2004). Similar to the observed interchangeability of the *C. elegans* Notch receptors, *apx-1* and *arg-1* were shown to substitute for *lag-2* (Fitzgerald and Greenwald 1995).

While in other organisms proper activation of the ligands was shown to be dependent on endocytic processes, in *C. elegans* this seems not to be the case. Truncated APX-1 and LAG-2, which lack the intracellular and transmembrane domains, were shown to be secreted and caused phenotypes associated with constitutive active LIN-12 and GLP-1 signaling (Fitzgerald and Greenwald 1995). In contrast, similar experiments in *Drosophila* lead to phenotypes associated with the loss of Notch signaling, demonstrating the requirement of ligand-endocytosis for proper ligand activation (Sun and Artavanis-Tsakonas 1996).

Adm-4 (TACE) and *sup-17* (Kuzbanian/ADAM10) were shown to be redundantly required for S2 cleavage in *C. elegans* for LIN-12 as well as for GLP-1 (Wen, Metzstein et al. 1997, Jarriault and Greenwald 2005) and S3 cleavage is mediated redundantly by *sel-12* and *hop-1* (Presenilin), though it was suggested that *sel-12* functions predominantly (Li and Greenwald 1997, Westlund, Parry et al. 1999). Similar to mammals and *Drosophila*, where Presenilins function together with Nicastrin in a large membrane complex (gamma-secretase complex), genetic studies in *C. elegans* showed that the Nicastrin-homolog *aph-2* functions together with *aph-1* and *pen-2* in LIN-12 as well as GLP-1 signaling. The requirements for *aph-2*, *aph-1* and *pen-2* depend again on the context. For example, while *aph-2* participates in LIN-12 signaling in the AC/VU decision, it does not influence VPC fate determination. Similarly, regarding GLP-1-mediated cell fate decisions *aph-2* is dispensable for germline proliferation but essential in the early embryo (Goutte, Hepler et al. 2000, Yu, Nishimura et al. 2000, Levitan, Yu et al. 2001). Additionally, in the germline *aph-2* was shown to genetically interact with *hop-1* but not with *sel-12*, while *aph-1* and *pen-2* interact with *sel-12*, but not *hop-1* (Francis, McGrath et al. 2002).

While the core ternary complex and many steps during Notch signaling initiation are well conserved between *C. elegans* and other species, the regulation of Notch signaling on the level of receptor turnover and trafficking is less understood.
The *C. elegans* Fbxw7 homolog *sel-10* was initially identified as a negative regulator of *glp-1* and *lin-12* and subsequently shown to encode an E3 ubiquitin ligase that targets the NICD for degradation (Sundaram and Greenwald 1993, Hubbard, Wu et al. 1997, Gupta-Rossi, Le Bail et al. 2001, Oberg, Li et al. 2001, Wu, Lyapina et al. 2001).
Sel-10 negatively regulates LIN-12 signaling in the AC/VU as well as the VPC fate decision (Hubbard, Wu et al. 1997). While *sel-10* might not be required or functions redundantly in the GLP-1-associated cell fate decisions in the germline, it might be required in the embryo. *Sel-10 (ar41)* does not suppress the germline proliferation defect of the two temperature-sensitive *glp-1* loss-of-function alleles *e2144* and *q231.* While *ar41* only weakly suppresses the embryonic lethality of *q231,* it is able to fully suppress the embryonic lethality associated with the weak temperature-sensitive *glp-1* loss-of-function allele *e2142* that shows no apparent germline defect (Sundaram and Greenwald 1993). In contrast, *ar41* enhances the overproliferation phenotype observed in *glp-1* gain-of-function mutants (Pepper, Killian et al. 2003). Interestingly, a C-Terminal truncation in GLP-1 does not result in overproliferation in the germline, indicating that the PEST sequence might not be required for Notch turnover in the germline (Mango, Maine et al. 1991). In mammals it was shown that the PEST sequence within NOTCH1 is required for NICD turnover mediated by the mammalian SEL-10 homolog (mSel-10) (Oberg, Li et al. 2001). Following this observation, it was demonstrated that the PEST and ANK repeats are required for efficient degradation of the LIN-12-ICD in VPCs (Nusser-Stein, Beyer et al. 2012). To what extend *sel-10* functions within the GLP-1-mediated cell fate decision in the germline therefore still needs clarification.
A role for receptor internalization in the regulation of receptor availability on the cell surface was in *C. elegans* so far only demonstrated for LIN-12 signaling. In the VPC fate decision Ras-activation downstream of *let-23* was shown to stimulate endocytosis and receptor down-regulation of LIN-12 via a “down-regulation targeting signal” (DTS) present in the receptor (Shaye and Greenwald 2002). WWP-1 - an Itch homolog - and ALX-1 were subsequently shown to be required for LIN-12 degradation in this context (Shaye and Greenwald 2005).

1.2.5. Regulation of germ cell proliferation and the meiotic entry decision in *C. elegans*

The main pathway regulating germ cell proliferation is, as mentioned above, GLP-1 signaling. Germ cells after a couple of rounds of mitotic division move proximal, enter meiosis and ultimately differentiate into sperm in the germline of L4 larvae and into oocytes in the adult germline (Kimble and White 1981). Recently, two targets of the Notch pathway in the *C. elegans* germline were identified that are required for germline stem cell pool maintenance. The two targets are *lst-1* and *sygl-1*, two worm specific genes (Kershner, Shin et al. 2014). However, it remains unclear how *lst-1* and *sygl-1* function on a mechanistic level. Through its two targets the GLP-1 pathway acts mainly to promote proliferation in the germline and to inhibit differentiation in the distal-most germline. It is thought that GLP-1 signaling is graded in the germline, whereby the signal is the strongest closest to the DTC. The activity of the Notch pathway coincides with the expression of two RNA binding proteins FBF-1 and FBF-2 (Figure 7B). It is assumed that *fbf-2* is a GLP-1 target gene, since its expression is restricted to the distal gonad and LBSs are present in its promoter region. However, FBF-2 is expressed in germlines lacking *glp-1*, implicating that *fbf-2* expression is not solely dependent on GLP-1 signaling (Lamont, Crittenden et al. 2004). *fbf-1 fbf-2* double mutants establish germline stem cells during larval stages, but cannot maintain them in adult worms. FBF proteins are thought to bind to and inhibit the translation of *gld-1* mRNA, thereby preventing meiotic entry in the distal gonad. (Crittenden, Bernstein et al. 2002)

Four RNA-binding proteins in two parallel pathways regulate the entry into meiosis downstream of GLP-1 signaling: GLD-1 and NOS-3 as well as GLD-2 and GLD-3 (Figure 7C). Null mutants in any single gene enter meiosis normally. However, *gld-1 gld-2* and *gld-3 nos-3* double mutants fail to enter meiosis and develop a germline tumor due to excess proliferation (Kadyk and Kimble 1998, Crittenden, Eckmann et al. 2003, Eckmann, Crittenden et al. 2004).

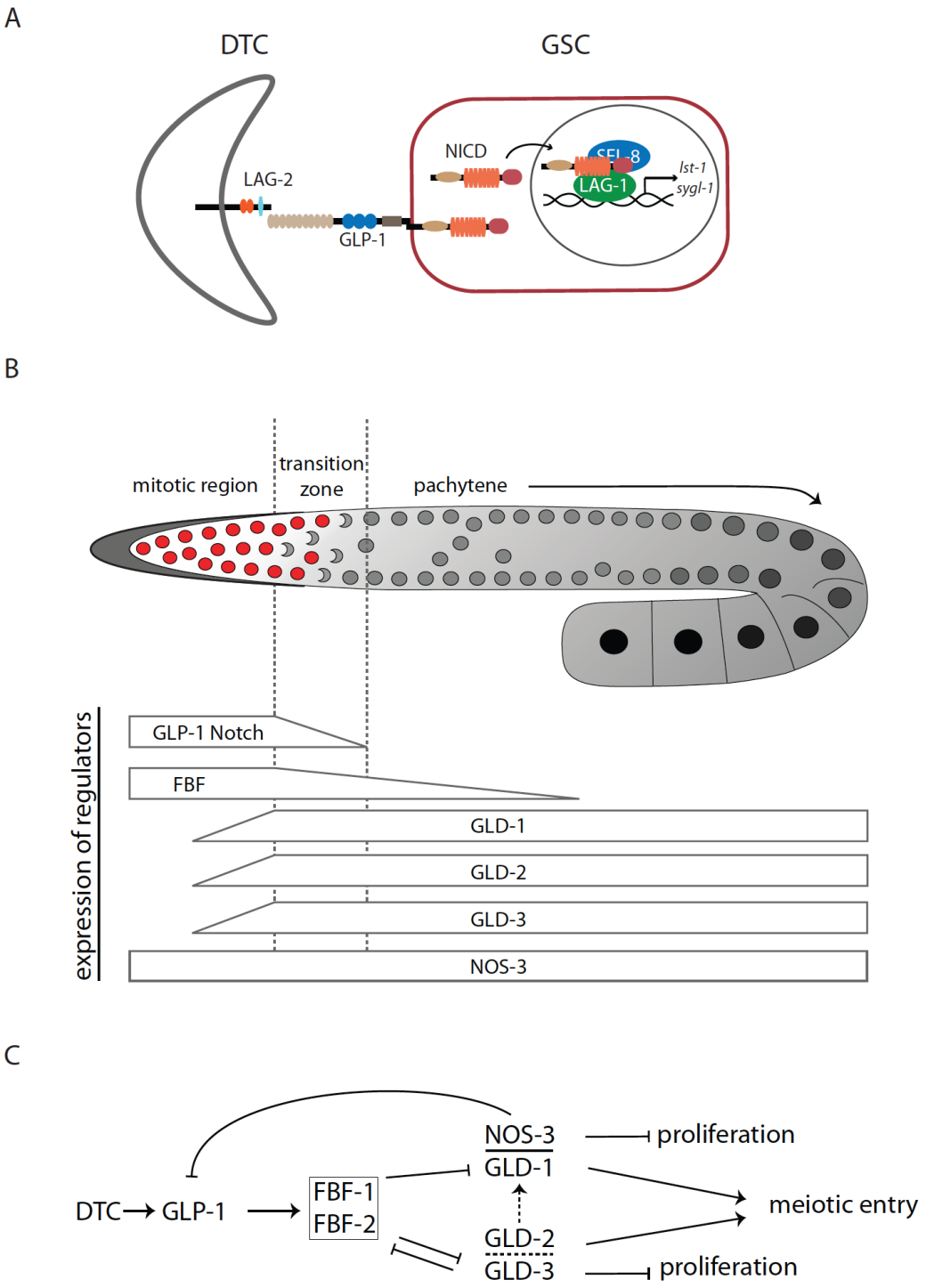

Figure 7: Regulation of the proliferation – differentiation decision.

(A) The core GLP-1 pathway in the *C. elegans* germline. The DTC expresses the ligand LAG-2 and the distal-most GSCs the receptor GLP-1. Upon contact with LAG-2 a sequential cleavage reaction leads to the translocation of the GLP-1-ICD (NICD) into the nucleus, where it associates with the transcriptional activator LAG-1 and the co-activator SEL-8 to initiate target gene expression. The two targets *lst-1* and *sygl-1* are thought to be the main targets responsible for GSC maintenance. (B) Schematic representation of the *C. elegans* germline and regions of key regulator expression. The cycling germline stem cells are located in the mitotic region (red circles). The transition zone marks where germ cells transit into meiosis, the nuclei then acquire a crescent shape. The cells translocate proximally and

differentiate into oocytes in adults. GLP-1 and FBF expression is highest closest to the DTC. Expression of GLD-1, GLD-2 and GLD-3 coincides with the transition of germ cell nuclei into meiosis. NOS-3 is expressed uniformly over the full length of the germline. (C) The regulatory circuit controlling proliferation and differentiation (see text for details) (adapted from (Kimble and Crittenden 2005)).

GLD-1 is a sequence-specific RNA binding protein of the STAR/KH family of RNA binding proteins and functions as translational repressor (Jones and Schedl 1995, Jan, Motzny et al. 1999, Ryder, Frater et al. 2004). The FBF-mediated repression of *gld-1* is released when germ cells move away from the niche. GLD-1 expression at the onset of meiosis is then thought to feedback on GLP-1 signaling by repressing *glp-1* mRNA (Marin and Evans 2003). GLD-3 binds to GLD-2, the catalytic subunit of a cytoplasmic poly(A) polymerase, and stimulates its activity (Wang, Eckmann et al. 2002). The *gld-3* mRNA also seems to be a target of FBF-mediated repression and GLD-3 protein interferes with FBF activity (Eckmann, Kraemer et al. 2002, Eckmann, Crittenden et al. 2004). *nos-3*, which encodes a Nanos family member, functions redundantly with *gld-2* to promote GLD-1 protein accumulation (Hansen, Wilson-Berry et al. 2004).

Next to the described core pathway various other factors were shown to influence the proliferation - differentiation decision.

Another RNA binding protein, PUF-8 (a Pumilio homolog), was shown to promote germline stem cell maintenance together with MEX-3, but also to inhibit the proliferative fate. Likely, *puf-8* functions as negative regulator of GLP-1 signaling or in parallel with it to inhibit the proliferative fate (Ariz, Mainpal et al. 2009, Racher and Hansen 2012).

However, germline proliferation is not only regulated on the level of RNA. RNA regulation in the *C. elegans* germline functions mainly through post-transcriptional mechanism and very often involves translational repression. Recently, it was shown that proliferation in the germline is also regulated by the proteasome, so on the level of protein turnover (Macdonald, Knox et al. 2008). This partially depends on the targeting of the chromodomain-containing protein MRG-1 for degradation by the E3 ligase RFP-1 (Fujita, Takasaki et al. 2002, Gupta, Leahul et al. 2015).

Another RNA-related process that was recently shown to contribute to the entry into meiosis is splicing. Depletion of genes functioning as splicing factors - in particular depletion of *prp*-17 - was shown to disrupt the balance between proliferation and differentiation in the germline. Knock-down of many splicing factors enhanced overproliferation of a *glp-1* gain-of-function allele (*oz264*). However, at least for *prp-17* this observation was mostly linked to a function within the GLD-1 pathway downstream of GLP-1 signaling (Kerins, Hanazawa et al. 2010).

For the sake of this thesis I will briefly give a short overview about splicing in *C. elegans*.

1.2.6. Splicing and its function in the *C. elegans* germline

Splicing is a process that removes introns from a nascent mRNA. The splicing reaction takes place in large dynamic protein complexes that form co-transcriptionally. mRNA splicing factors are thereby loaded in a stepwise fashion onto a nascent transcript (Figure 8). At the core of the complexes are snRNPs (small nuclear ribonucleoproteins), especially U-(Uridine-)rich snRNPs, which form RNA-RNA and RNA-protein interactions to recognize splice sites (illustrated in Figure 8A) as well as to catalyze the splicing reaction. First, the U1 snRNP binds to the 5`splice site followed by U2 binding to the branch point within the intron. The U4/U6•U5 tri-snRNP is then recruited. Extensive rearrangements in RNA-RNA as well as RNA-protein interactions lead to the formation of a catalytically active spliceosome containing U2, U5 and U6. With the aid of several additional splicing factors two trans-esterification reactions eventually lead to the excision of an intron (Zahler 2012). Several factors were proven to be important along the different steps of splicing. For the sake of this thesis, some of them will hereafter be introduced while emphasizing on factors that were shown to participate in the control of germ cell proliferation.

Many splicing factors have been implicated to regulated proliferation and differentiation but also germline sex determination in *C. elegans*. Genetic screens for genes that prevent the switch to oocyte production, hence masculinize the germline, identified the *mog* genes. Four of the five known *mog* genes encode splicing factors: *mog-1* (PRP16), *mog-4* (PRP2), *mog-5* (PRP22) and *mog-2* (U2A`), which participate in different steps during splicing (Zahler 2012). As mentioned above, *prp-17* was shown to influence the proliferation - differentiation decision. Similar results were shown for *teg-4* (SF3b3). Both seem to function downstream of GLP-1 signaling to influence meiotic entry (Mantina, MacDonald et al. 2009, Kerins, Hanazawa et al. 2010). PUF-8 together with TCER-1 (CA150) was shown to function redundantly to control the levels of several mRNAs in the germline. Among these are *pal-1, pos-1, oma-1* and *spn-4,* whose proteins are expressed in the developing oocytes and early embryos (Pushpa, Kumar et al. 2013). *Puf-8* itself, as mentioned above, is involved in the proliferation - differentiation decision in the germline (Ariz, Mainpal et al. 2009, Racher and Hansen 2012). It is still unclear, how on a mechanistic level splicing factors and splicing-associated proteins participate in the decision.

The splicing machinery associates with many additional factors depending on the context and stimulus, some of which are participating in various gene regulatory mechanisms. Thereby splicing might be coupled to upstream and downstream events controlling gene expression. One of the factors shown to associate with the splicing machinery is the PRP19/NTC complex, which is involved in a variety of cellular processes including transcription elongation, genome maintenance, splicing and

recruitment of ubiquitinated proteins to the proteasome (reviewed in (Chanarat and Strasser 2013)). Depending on the species and the cellular process carried out, the complex consists of a variety of subunits (Makarova, Makarov et al. 2004, Kuraoka, Ito et al. 2008, Fabrizio, Dannenberg et al. 2009, Ambrosio, Badjatia et al. 2015) (Table 4). Especially during splicing the Prp19/NTC complex was shown to dynamically associate with a variety of splicing factors (Figure 8B) (reviewed in (de Almeida and O'Keefe 2015)). The name-giving component of the PRP19 complex is a U-box-containing E3 ligase, which is capable of ubiquitinating substrate proteins (Vander Kooi, Ohi et al. 2006). The so far only identified target of PRP19 is the splicing factor PRP3, which increases its affinity to PRP8, a component of the U5 snRNP, by attaching a K63-linked ubiquitin chain (Song, Werner et al. 2010). However, it is unclear whether PRP19 promotes ubiquitination of additional proteins (Chanarat and Strasser 2013). One of the proteins shown to associate with the splicing machinery and the PRP19/NTC is SKIP (Wahl, Will et al. 2009, Chanarat and Strasser 2013, Ambrosio, Badjatia et al. 2015) (Figure 8B). This protein fulfills multiple functions including those within the Notch-repressor and -activator complex in the nucleus (Zhou, Fujimuro et al. 2000, Makarov, Makarova et al. 2002, Bres, Gomes et al. 2005, Wang, Wu et al. 2012) (see chapter 1.1.3.2).

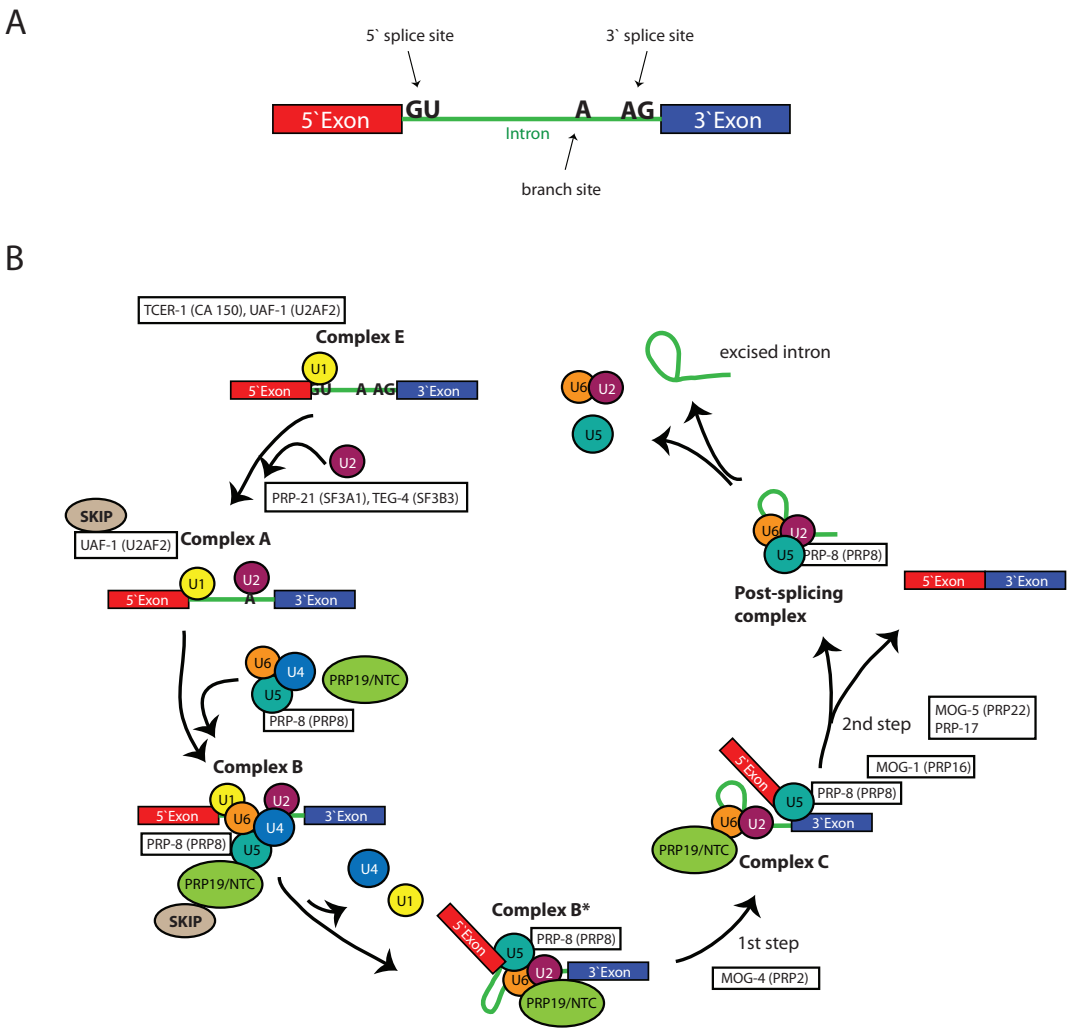

Figure 8: The splicing machinery.

(A) Schematic representation of the sequence requirements within an intron that are necessary for splicing. (B) Spliceosome formation is initiated through the recognition of the 5`splice site by the U1 snRNP, followed by U2 binding to the branch point. Subsequent association of the U4/U6•U5 tri-snRNP then leads to changes in RNA-RNA and RNA-protein interactions to catalyze the intron excision (see text for details). Splicing factors important for this thesis are boxed in black and the steps indicated, where SKIP and the PRP19/NTC complex are thought to function (adapted from (Hogg, McGrail et al. 2010, Kerins, Hanazawa et al. 2010, Chen, Zhang et al. 2011, Ambrosio, Badjatia et al. 2015)).

1.3. Aim of the thesis

The Notch pathway in *C. elegans* has been extensively studied and it is well established that GLP-1 is essential for the proliferation of germline stem cells. However, to a large extend the mechanism of Notch signaling in *C. elegans* has been studied in the context of GLP-1-mediated cell fate decisions in the embryo or LIN-12-mediated signaling events. Many aspects of the mechanism of GLP-1 signaling in the germline therefore still remain to be elucidated. It is for example still unclear, how and if GLP-1 signaling is restricted to the distal end of the germline. For targets of GLP-1 signaling it would be expected that their transcription is strongest close to the stem cell niche, where the Notch-activating signal is originating. However, GLP-1 targets have been proposed that are activated away from the niche (*lip-1*). In agreement with this observation we found that *utx-1* is a GLP-1 target in the germline, whose expression is weak in the distal-most germline and gets progressively stronger when germ cells move proximal. However, this finding implies that the activated GLP-1 receptor either enters the nucleus away from the niche or travels along with germ cell nuclei and activates particular target genes at different points during the path of a germ cell towards differentiation. Yet another possibility is that the association of the transcriptional machinery on some target genes is happening in the distal part guided by the activated Notch. The polymerase then poises until a second signal is initiating transcription away from the signal sending niche and independent of the presence of Notch. This in turn might be depending on additional factors and cues that are required for activation and/or repression of specific genes and would imply that Notch target genes are selectively utilized within the same tissue in a context specific manner. A major caveat studying GLP-1 signaling has always been the lack of a functional fluorescent transgene. To study the dynamics of signaling initiation and uncover mechanisms that are restricting GLP-1 signaling within the germline we needed a tool to follow activated GLP-1 in living animals.
My thesis aimed to study how GLP-1 signaling dynamics are regulated in the germline with the help of a fluorescently tagged GLP-1.

2. Materials and methods

Nematode culture

Animals were grown on 6 cm NG 2% plates seeded with OP50 bacteria. For immunoprecipitations and large-scale RNAi screens animals were grown on 15 cm peptone-rich plates seeded with NA22 bacteria (10 times concentrated by centrifugation). Gravid adults were then bleached and embryos allowed to hatch in M9 overnight. For immunoprecipitations, the next morning synchronized L1s were counted and a defined number of larvae was transferred to seeded plates. Animals were then grown to young adulthood and harvested in liquid nitrogen.
Temperature-sensitive strains (*glp-1(e2144), glp-1(ar202))* were maintained at the permissive temperature (15°C) and shifted to the restrictive temperature (25°), where stated. RNAi experiments were performed by feeding bacteria expressing RNAi clones from the Ahringer or Open Biosystems library (OBS; see Table 1 for details). The RNAi clone for *rfp-1* was generated by Janosch Stöcklin and contains a 1093-nucleotide long fragment of the *rfp-1* genomic region, which spans from nucleotides 876 to 1968 after the start codon, and was placed into the empty pMD3. Amplifying a 516-nucleotide long fragment from the coding region of *Y51F10.2* isoform b spanning from nucleotide 33 to nucleotide 548 similarly generated the RNAi clone for *Y51F10.2*. The *ubr-5* RNAi clone was generated by amplifying a 907-nucleotide long fragment from the *ubr-5* genomic region spanning from nucleotides 1133 to 2039 after the start codon. All RNAi clones, except for those used in the E3 ligase screen, were verified by sequencing prior to use.

Counting of progeny number

Worms of the respective genotypes were grown at 25°C, 20°C or 15°C for at least two preceding generations. Single worms were then placed on an OP50-containing plate, incubated at the respective temperature and transferred to a fresh OP50 plate after two days (25°C), three days (20°C) or four days (15°C) to avoid starvation.

RNAi experiments

Plate preparation

To prepare RNAi plates an RNAi clone was grown overnight in LB medium containing 10 µm/ml Tetracycline and 50 µg/ml Carbenicillin. The next day around 250 µl of bacteria were seeded on 6 cm NG 2% plates supplemented with 10 µm/ml Tetracycline, 50 µg/ml Carbenicillin and 1 mM IPTG. Plates were induced overnight at RT.

GLP-1::GFP localization studies

Synchronized L1 larvae of the *rrr27* (*glp-1::gfp*) strain were placed on plates containing the respective RNAi bacteria and grown to adulthood at 25°C for 48 hrs. For RNAi clones that turned out to be lethal the experiment was repeated using synchronized L3/L4 worms.

E3 ligase screen

The initial list of 854 putative E3 ligases (Gupta, Leahul et al. 2015) was filtered for U-Box domain-containing, HECT domain-containing and RING domain-containing E3 ligases. This list was then additionally filtered for genes that are enriched in the germline based on data available in the lab (Scheckel, Gaidatzis et al. 2012). For most of the screened E3 ligases the RNAi clones were not sequenced prior to use.

Temperature-shift experiments

Glp-1 (*e2144)* worms were grown on the respective RNAi plates at 15°C until they reached the young adult stage and then shifted to the restrictive temperature of 25°C.

PRC2/Notch pathway component knock-down

Two to three mid L4 worms were placed on plates containing the respective RNAi bacteria and their progeny used for experiments.

Strain list

Lab Strain #	genotype	generated by /courtesy of
342	wild type (N2)	
1540	*rrr27 (glp-1::gfp)* (III)	CRISPR-mediated genome editing
1599	*him-8 (e1489)* (IV)	CGC CB1489
1615	*rrr27 (glp-1::gfp)* (III); *him-8 (e1489)* (IV)	crossing #1540 and #1599
1898	*rrf-1 (pk1417)* (I)	CGC NL2098
1899	*rrf-1 (pk1417)* (I); *rrr27 (glp-1::gfp)* (III)	Crossing #1898 and #1615
1469	*glp-1 (e2144)* (III)	CGC JJ760

118	*glp-1 (ar202)* (III)	CGC GC833
1847	*prp-19::Strep* (*rrr25*) *glp-1::gfp (rrr27)* (III)	CRISPR-mediated genome editing
1848	*prp-19::Strep* (*rrr26*) *glp-1::gfp (rrr27)* (III)	CRISPR-mediated genome editing
786	*rrrSi185 [putx-1::gfp-H2B::tbb-2; unc-119(+)]* (II)	MosSCI
1258	*rrrSi281 [putx-1::gfp-H2B::tbb-2; unc-119(+)]* (II)	MosSCI
793	*rrrSi189 [putx-1::FLAG-GFP-linker-TEV::utx-1 ORF+3'UTR; unc-119(+)]* (II)	MosSCI
1166	*rrrSi275 [putx-1delta7::GFP-H2B::tbb-2; unc-119(+)]* (II)	MosSCI
1220	*rrrSi272 [putx-1delta5::GFP-H2B::tbb-2; unc-119(+)]* (II)	MosSCI
1188	*rrrSi260 [putx-1delta4::GFP-H2B::tbb-2; unc-119(+)]* (II)	MosSCI
1145	rrrSi247 *[pux-1delta10::GFP-H2B::tbb-2; unc-119(+)] (*II)	MosSCI
1175	rrrSi257 *[putx-1delta1::GFP-H2B::tbb-2; unc-119(+)]* (II)	MosSCI
1235	rrrSi276 *[putx-1delta13::GFP-H2B::tbb-2; unc-119(+)]* (II)	MosSCI

CRISPR-mediated genome editing

Genome editing was performed as described previously (Dickinson, Ward et al. 2013, Katic and Grosshans 2013). A sgRNA targeting nucleotides 6652 to 6671 in the *glp-1* locus was cloned into pIK111 (*PU6::NotI site::sgRNA* backbone) by Gibson assembly. The repair plasmid was generated by amplifying a homologous region spanning 1300 nucleotides upstream and 1316 nucleotides downstream of the GFP insertion site (between nucleotide 6648 and 6649 in the *glp-1* genomic region) and placed in the *L4440* plasmid by Gibson assembly. Injections were performed with 200 ng/µl *pIK82* (*peft-3::Cas9::2xNLS::tbb-2 3'UTR* in Chromosome II MosSCI targeting vector), 200 ng/µl sgRNA and 100 ng/µl repair plasmid in HT1593 (*unc-119 (ed3)*). This generated *glp-1::gfp (rrr27)*.

The Strep-tag knock-in in *prp-19* was performed as described previously (Arribere, Bell et al. 2014), whereas the very N-terminus and the very C-terminus were targeted simultaneously. SgRNAs targeting nucleotides -25 until -6 counting from the start codon and targeting from nucleotide -16 from the STOP codon until the first 4

nucleotides in the 3 `UTR of *prp-19,* respectively, were cloned into *pIK111*. For the repair a 200-nucleotide long single-stranded DNA oligo was used that contains the Strep-tag (TGGTCCCACCCACAATTCGAGAAG) in the middle and 88 nucleotides of the sequence upstream and downstream of the respective insertion site. Injections were carried out in the *rrr27* background due to the close linkage of *prp-19* and *glp-1* (2,20 cM). The injection mix contained 50 ng/µl *pIK155* (*peft-3::Cas9*; upgraded version of *pIK82*), 100 ng/µl *pIK167*, sgRNA targeting *sqt-1*, 50 ng/µl *oIK622* (99-mer oligo PAGE purified from IDT, sequence: 5'ACCAATGGATTGTGGAAGGACATAGTTGTCA TCGGAAGATCTAGCAAGTGTGTCCGTCGTCAATTGAAGAGACtAACGCTACCCCAACTCCAC ATGCT 3'), 100 ng/µl of each sgRNA and 20 ng/µl of each repair oligo. Successful insertion of the Strep-tag at the C-terminus was confirmed by PCR and sequencing. The absence of an additional insertion of the Strep-tag at the N-terminus was confirmed by sequencing.

Microscopy

Anti-HIM-3 and DAPI staining, reporter analysis (PRC2)

Images were captured with a Zeiss AxioImager Z1 microscope equipped with an AxiocamMRm REV2 CCD camera. All images were acquired in the linear mode of the Axiovision software (Zeiss) and processed using Fiji and Adobe Photoshop CS5 in an identical manner. Fluorescence intensities were quantified using ImageJ. GFP intensities were normalized to the picture background and corrected with the average autofluorescence measured in wild-type (N2) gonads at the corresponding temperatures.

Live imaging

Larval stage worms were transferred into a drop of 50% M9 in ddH2O containing 300 µM Levamisole on microscopic slides (3-well diagnostic slides, Thermo scientific). For images of dissected gonads, the head of adult worms was cut off with a syringe. Microscopic slides were covered with a cover slip, fixed with nail polish and immediately imaged.

GLP-1::GFP expression studies, anti-STREP and DAPI immuno-staining

Confocal images were captured with AxioImager M2 (upright microscope) and the Yokogawa CSU W1 Duel camera T2 spinning disk confocal scanning unit.
All images were processed using Fiji and Adobe Photoshop CS5 in an identical manner.

Protein extraction

Worms were frozen by adding an equal volume of 1,5X worm lysis buffer (WLB) (20 mM Hepes, 150 mM NaCl, 2 mM $MgCl_2$, 10 mM EDTA, 0,2% NP40; complemented with protease inhibitors - Complete™ Roche 1 tablet/10ml, PhosStop™ Roche 1 tablet/10 mL, 1 mM DTT final concentration - right before use) to each pellet and generating drops of worm suspension in liquid nitrogen. The frozen drops were ground with mortar and pestle in the presence of liquid nitrogen and 500 µl of 1,5X WLB were added immediately. The worm suspension was supplemented with 3 µl/ml benzonase nuclease (Sigma) and incubated for 30 min at 4°C under rotation.
Animal debris was removed by spinning two times at 4°C for 10 min at 20,000 x g. Protein concentrations were measured using the Bradford assay (Biorad).
For protein extracts used for mass spectrometry worms were frozen by adding equal volumes of 50 mM NaCl to each pellet and generating drops of worm suspension in liquid nitrogen. The frozen drops were ground with mortar and pestle in the presence of liquid nitrogen and two volumes of extraction buffer (50 mM HEPES, 100 mM KOAc, 5 mM MgAc, 0.1% Triton X-100, 10% (w/v) Glycerol, 20 mM β-glycerophosphate) containing protease inhibitors (7 mg/ml Complete Roche, 2 µg/ml Aprotinin, 0,2 µg/ml Pepstatin A, 2 mM DTT, 1% (w/v) Phenylmethylsulfonylfluorid) were added immediately.
Animal debris was removed by spinning two times at 4°C for 10 min at 20,000 x g. Protein concentrations were measured using the Bradford assay (Biorad).

Immunoprecipitation

10 µl of GFP-Trap®_A slurry (Chromotek) was washed once with 1X WLB, equal amounts of protein extracts were added to the beads and incubated overnight at 4°C on a rotating wheel. The next day, beads were washed once with 1,5X WLB and three times with 1X WLB, 50 µl 3X Laemmli buffer (62,5 mM TRIS pH 6.8, 10% (w/v) Glycerol, 2% SDS, 5% (w/v) β-mercaptoethanol, Bromphenolblue) was added to the beads and boiled at 95°C for 10 min. The Supernatant was carefully taken away and used for western blotting.
For IPs that were submitted for mass spectrometric analysis beads were washed once with extraction buffer containing protease inhibitors and three times with extraction buffer without Triton X-100 and protease inhibitors.

Western blotting

Protein samples containing the appropriate amount of Laemmli buffer were loaded on a gel (NuPAGE® Novex® 4-12% Bis-Tris Protein Gels, 1.0 mm) and run for 55 min at 200 V. Proteins were then transferred to a membrane with the Trans-Blot® Turbo™ system (Biorad) using the Standard transfer protocol. Membranes were shortly washed with ddH2O and blocked for 1 hr with 5% milk in TBS-T. The primary antibody was added in blocking solution and incubated overnight at 4°C. Anti-GFP (Roche Life Science) and anti-ubiquitin (P4D1, Enzo life sciences) was diluted 1:1000. The next day, membranes were washed 3 x 10 min with TBS-T before they were incubated for 1 hr at RT with the HRP-coupled secondary antibody (anti-mouse, GE Healthcare) again in blocking solution. The membranes were then again washed 3 x 10 min with TBS-T and developed using the Clarity™ Western ECL blotting substrate (BioRad).

Mass spectrometric analysis

Beads containing immunoprecipitated proteins were incubated with 0.2 µg LysC in digestion buffer (3 M GuaHCl, 20 mM EPPS pH 8.5, 10 mM CAA, 5 mM TCEP) and incubated for 4 hrs at RT. 50 mM HEPES pH 8.5 was added and 0.2 µg Trypsin and incubated overnight at 37°C. Next morning another 0.2 µg Trypsin was added and incubated for another 4 hrs at 37°C. Samples were acidified by adding 1 µl of 20% TFA before analysis by LC-MS.

Immunofluorescence

Microscopic slides (3-well diagnostic slides, Thermo scientific) were covered with subbing solution containing gelatin, chrome alum and Poly-L-Lysine, and dried for a couple of hours. Worms were then dissected with a syringe in a drop of 50% M9 in ddH_2O containing Levamisole (300 µM final concentration) and staining was performed as previously described (Burger, Merlet et al. 2013) with the exception of using Tween-20 instead of Triton-X-100. Working dilutions for the primary antibodies were 1:500 for rabbit anti-HIM-3 (M. Zetka) and 1:2000 Strep MAB classic Chromeo 546 (IBA life sciences). For the anti-HIM-3 staining, slides were later incubated for 30 min at RT with the secondary antibody goat anti-rabbit (IgG) coupled to Alexa 568 (1:500, Invitrogen). Next, gonads were mounted in Vectashield Mounting Medium with DAPI (Vector laboratories).

Statistical analysis

P-values were calculated using t-test, assuming two tailed distribution and unequal variances.

RNAi clones other than used in the E3 ligase screen

Ubiquitin-System	**RNAi Source**
pbs-5	OBS
uba-1	Ahringer
pas-5	Ahringer
Cullin complexes	
cul-1	Ahringer & OBS
cul-2	Ahringer & OBS
cul-3	Lionel Pintard
cul-4	Ahringer
cul-5	Ahringer & OBS
cul-6	Ahringer & OBS
rbx-1	Ahringer
rbx-2	Ahringer
E3 ligases Notch	
sel-10	Ahringer
ubr-5	Self-cloned
Splicing factors	
prp-17	Ahringer
prp-21	OBS
uaf-1	OBS
mog-1	Ahringer
mog-4	OBS
mog-5	Ahringer
teg-4	Ahringer
tcer-1	Ahringer
teg-1	OBS
prp-4	OBS
prp-8	Ahringer
PRP19/NTC	
C50F2.3	OBS

F53B7.3	Ahringer
cdc-5L	OBS
cpf-1	Ahringer
T12A2.7	Ahringer
M03F8.3	Ahringer
K04G7.11	OBS
ZK1307.9	Ahringer & OBS
Y17G9B.4	OBS
emb-4	Ahringer
hsp-1	Ahringer & OBS
skp-1	OBS
C07A9.2	Ahringer & OBS
cyn-12	Ahringer & OBS
PRC2/Notch	
mes-2	OBS
mes-3	Ahringer
mes-4	Ahringer
mes-6	Ahringer
glp-1	Ahringer
lag-1	Ahringer
sel-8	Ahringer
adm-4	Ahringer

Table 1: Source of RNAi bacteria used in this study.

RNAi clones used in the E3 ligase screen

Listed are all putative monomeric, germline expressed E3 ligases (Scheckel, Gaidatzis et al. 2012, Gupta, Leahul et al. 2015). Only for a subset of these genes the RNAi clone was not available or did not grow (indicated in bold).

Sequence Name	Gene Name	E3 ligase family	RNAi Source
B0281.3	.	RING-finger	Ahringer
B0393.6	.	RING-finger	Ahringer
B0416.4	.	RING-finger	Ahringer & OBS
B0432.13	**.**	**RING-finger**	**did not grow**
B0564.11	***rde-11***	**RING-finger**	**no clone**
C01G6.4	.	RING-finger	Ahringer & OBS
C02B8.6	.	RING-finger	OBS

C06A5.8	*.*	RING-finger	OBS
C06A5.9	*rnf-1*	RING-finger	OBS
C09E7.8	**.**	**RING-finger**	**no clone**
C11H1.3	*.*	RING-finger	Ahringer
C12C8.3	*lin-41*	RING-finger	Ahringer
C15F1.5	*.*	RING-finger	OBS
C16A3.7	*tag-182*	RING-finger	Ahringer
C16C10.5	*rnf-121*	RING-finger	Ahringer
C16C10.7	*rnf-5*	RING-finger	Ahringer & OBS
C17E4.3	*marc-3*	RING-finger	Ahringer & OBS
C17G1.4	*nra-3*	RING-finger	OBS
C17H11.6	*.*	RING-finger	Ahringer
C18B12.4	*.*	RING-finger	Ahringer
C28H8.9	*dpff-1*	RING-finger	Ahringer
C32D5.10	*.*	RING-finger	Ahringer & OBS
C32D5.11	*.*	RING-finger	Ahringer
C32E8.11	*ubr-1*	RING-finger	Ahringer
C34D4.14	*hecd-1*	HECT	Ahringer
C34E10.4	*wrs-2*	RING-finger	Ahringer & OBS
C36A4.8	*brc-1*	RING-finger	Ahringer
C49H3.5	*ntl-4*	RING-finger	Ahringer & OBS
C52E12.1	*.*	RING-finger	Ahringer
C53A5.6	*.*	RING-finger	Ahringer & OBS
C56A3.4	*.*	RING-finger	Ahringer
D1081.9	*.*	RING-finger	OBS
D2030.7	*.*	RING-finger	Ahringer & OBS
D2085.4	*.*	HECT	Ahringer
D2089.2	*marc-2*	RING-finger	Ahringer & OBS
EEED8.16	***brap-2***	**RING-finger**	**no clone**
F01F1.4	*rabn-5*	RING-finger	Ahringer & OBS
F10D7.5	*.*	RING-finger	Ahringer
F10G7.10	*.*	RING-finger	Ahringer
F11A10.3	*mig-32*	RING-finger	Ahringer
F14D12.2	*unc-97*	RING-finger	Ahringer & OBS
F16A11.1	*.*	RING-finger	Ahringer & OBS
F19G12.1	*.*	RING-finger	Ahringer
F20H11.1	*.*	RING-finger	Ahringer & OBS
F26E4.11	*hrdl-1*	RING-finger	Ahringer

F26F12.7	*let-418*	RING-finger	Ahringer
F26F4.7	***nhl-2***	**RING-finger**	**did not grow**
F26G5.9	*tam-1*	RING-finger	OBS
F32A6.3	*vps-41*	RING-finger	Ahringer
F35G12.9	*apc-11*	RING-finger	OBS
F36A2.13	*ubr-5*	HECT	Self-cloned
F36F2.3	*tag-214*	RING-finger	Ahringer
F36F2.3	*tag-214*	U-Box	Ahringer
F44D12.10	**.**	**RING-finger**	**no clone**
F53F8.3	*.*	RING-finger	OBS
F53G2.7	*mnat-1*	RING-finger	OBS
F54B11.5	*.*	RING-finger	OBS
F55A11.3	*hrd-1*	RING-finger	**did not grow**
F55A11.7	*.*	RING-finger	OBS
F55A12.10	*.*	RING-finger	OBS
F55A3.1	*marc-6*	RING-finger	Ahringer
F55G1.6	*.*	RING-finger	Ahringer & OBS
F56A3.2	*slx-1*	RING-finger	Ahringer & OBS
F56D2.2	*.*	RING-finger	Ahringer & OBS
F58B6.3	*par-2*	RING-finger	Ahringer
F59E10.2	*cyp-4*	U-Box	Ahringer
H05L14.2	*.*	RING-finger	Ahringer
K01G5.1	*tag-331*	RING-finger	Ahringer
K02B12.8	*zhp-3*	RING-finger	Ahringer
K04C2.4	*brd-1*	RING-finger	OBS
K08E3.7	*pdr-1*	RING-finger	Ahringer & OBS
M02A10.3	*sli-1*	RING-finger	Ahringer & OBS
M110.3	*.*	RING-finger	Ahringer & OBS
M142.6	*rle-1*	RING-finger	Ahringer
R05D3.4	*rfp-1*	RING-finger	Janosch Stöcklin
R05G6.4	*.*	U-Box	Ahringer & OBS
R06F6.2	*vps-11*	RING-finger	Ahringer
T01C3.3	*.*	RING-finger	**did not grow**
T01G5.7	*.*	RING-finger	**did not grow**
T02C1.2	**.**	**RING-finger**	**no clone**
T05A12.4	*.*	RING-finger	Ahringer & OBS
T05H10.5	*ufd-2*	U-Box	Ahringer & OBS
T08D2.4	*.*	RING-finger	Ahringer & OBS

T09B4.10	*chn-1*	U-Box	Ahringer
T10F2.4	*prp-19*	U-Box	Ahringer
T12E12.1	*.*	RING-finger	Ahringer & OBS
T13A10.2	*.*	RING-finger	Ahringer & OBS
T13H2.5	*spat-3*	RING-finger	Balazs Hargitai
T14G8.1	*chd-3*	RING-finger	Ahringer & OBS
T20F5.6	*.*	RING-finger	Ahringer
T20F5.7	*.*	RING-finger	Ahringer & OBS
T24D1.2	*.*	RING-finger	Ahringer
T24D1.3	*.*	RING-finger	Ahringer
T24D1.5	***har-2***	**RING-finger**	**no clone**
W02A11.3	*toe-4*	RING-finger	Ahringer & OBS
W04H10.3	*nhl-3*	RING-finger	Ahringer
W06B4.3	*vps-18*	RING-finger	Ahringer
W09G3.6	*.*	RING-finger	Ahringer
Y105E8A.14	*.*	RING-finger	Ahringer & OBS
Y119C1B.5	***.***	**RING-finger**	**no clone**
Y2H9A.1	*mes-4*	RING-finger	Ahringer
Y37E11AR.2	*siah-1*	RING-finger	Ahringer & OBS
Y38H8A.2	*.*	RING-finger	OBS
Y39A1C.2	*oxi-1*	HECT	Ahringer
Y45F10B.8	*.*	RING-finger	Ahringer & OBS
Y45F10B.9	*.*	RING-finger	Ahringer & OBS
Y45G12B.2	*.*	RING-finger	Ahringer & OBS
Y47D3A.22	*mib-1*	RING-finger	Ahringer
Y47G6A.14	*.*	RING-finger	Ahringer
Y48G8AL.1	*herc-1*	HECT	Ahringer
Y49F6B.9	*.*	RING-finger	Ahringer & OBS
Y4C6A.3	*.*	RING-finger	Ahringer
Y51F10.2	*.*	RING-finger	Self-cloned
Y52E8A.2	*.*	RING-finger	OBS
Y53G8AR.5	*.*	RING-finger	Ahringer & OBS
Y54E10A.11	***.***	**RING-finger**	**no clone**
Y54E10BR.3	*.*	RING-finger	Ahringer library
Y55F3AM.6	*.*	RING-finger	Ahringer & OBS
Y57A10A.31	*.*	RING-finger	Ahringer & OBS
Y59A8A.2	***phf-14***	**RING-finger**	**no clone**
Y59A8B.13	***slr-2***	**RING-finger**	**no clone**

Y65B4BR.4	*wwp-1*	HECT	OBS
Y67D8C.5	*eel-1*	HECT	OBS
Y71F9AL.10	.	RING-finger	OBS
Y92H12A.2	**.**	**HECT**	**no clone**
ZC13.1	.	RING-finger	Ahringer & OBS
ZK637.14	.	RING-finger	Ahringer & OBS

Table 2: Source of RNAi bacteria used in the E3 ligase screen.

Utx-1 reporter dissection

Motifs used in the *utx-1* promoter dissection

MOTIF1

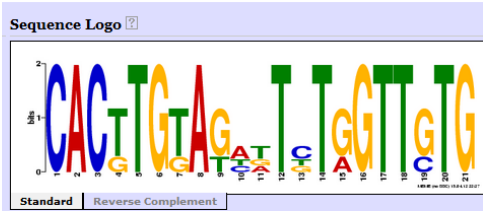

Name	Strand	Start	*p*-value	Sites
Crem	+	175	5.81e-13	ACTCAAATTT CACTTGTAGCTTCTGGTTGTG TCCTCAAAAA
Cbrig	+	134	1.78e-12	TTTCAATGTT CACTTGTAGTTTCTGGTTGTG CCCTTCCCCT
Ce	+	216	6.43e-11	TGAGATACTT CACTTGTATAATTTGGTTGTG AAAAGATTT

MOTIF2

Name	Strand	Start	*p*-value	Sites
Cbrenn	+	1081	4.07e-12	CGACCCCGCA CATTGGCAACGACACTCCG ATATTCCGCC
Ce	+	1026	4.00e-11	GAACGCACGG CAATGGCAACGATACTCCG TTTCTAACGT
Cjap	+	500	5.22e-11	AAGCGAGCTC CAACGCAAACGACACTCCG TACTTACGCT
Cbrig	+	1169	1.33e-10	CGGGCAGAAA AATCGACAACGACGCTCCG ATATAACAGG

MOTIF3

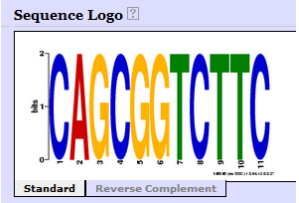

Name	Strand	Start	p-value	Sites
Crem	+	469	9.71e-08	GTTCATCTAT CAGCGGTCTTC TATTATTCTC
Ce	+	497	9.71e-08	CTTTTTTTTC CAGCGGTCTTC CTGTTGTTAA

MOTIF4

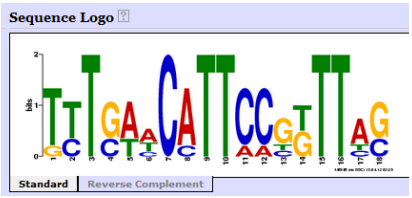

Name	Strand	Start	*p*-value	Sites
Crem	+	251	3.76e-11	TTACTCGTCT TCTGAACATTCCGGTTAG TTTTTACATT
Ce	+	300	2.16e-10	TGTTAAACTT TTTGTACATTCCGGTTAG AATCAAGTGC
Cbrig	+	217	1.92e-09	ATTATTCTTG GTTCAACATTCCGGTTAG TTTGAACATT

MOTIF5

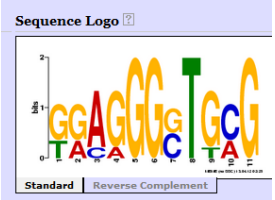

Name	Strand	Start	p-value	Sites
Ppa	+	686	8.21e-08	CTATTGTATG GGAGGGCTGCG GTGCTATGCG
Crem	-	1118	5.14e-07	TTCTGGCGTA GGAGGGGTGAG GGGAATCGGG
Cjap	+	702	5.14e-07	TATTTTATTT TGAGGGCTGCG TGT
Ce	+	1006	1.59e-06	GCACAGTAGA GACGGGCTGCG AACGCACGGC
Cbrig	+	506	2.92e-06	TGCTCTTGGG GAAAGGGTGCG CGGGAGAATC
Cbrenn	-	1005	6.34e-06	CAGAGACAAG TGAGGGGTTAG ACAAAAATCG

Transgenic animals and reporter GFP quantifications

The transcriptional reporter *putx-1::gfp-h2b::tbb-2* (*rrrSi185* and *rrrSi281*) was constructed from the 1302-nucleotide long putative promoter region of the gene *utx-1* and fused to sequences coding for *gfp-h2b* (*pBMF2.7*) and the ubiquitously expressed *tbb-2 3'UTR* (*pCM1.36*) using the Gateway Reporter Cloning System (Merritt, Rasoloson et al. 2008).

Reporter versions 7 and 5 were similarly constructed by amplification of 253 base pairs and 1195 base pairs, respectively, downstream of the *utx-1* start codon. Version 1 was generated by cutting the 5`entry clone containing the full-length *utx-1* promoter with restriction enzymes *AvaII* and *BglII* and Version 4 was similarly generated by cutting with restriction enzymes *AvaII* and *BglI*, which removes 376 base pairs and 974 base pairs, respectively, from the *utx-1* promoter. Version 10 was constructed as full-length *utx-1* promoter with mutations introduced in the two LBSs in the 5`UTR by changing ttcccaaa and ttctcaca for ggaaaga in the primer. Version 11 was constructed by amplifying the Version 5 promoter with the Version 10 mutations in the LBS of the 5`UTR. Version 13 was constructed by cutting Version 10 with *AvaII* and *BglII* and exchanging this region with a PCR-generated insert that harbors a mutation in the upstream LBS (cttgagaa to ggaaagac).

All Transgenic animals were produced as single-copy integrant in Chromosome II using the MosSCI protocol (Frokjaer-Jensen, Davis et al. 2008).

Primer list

sgRNA *glp-1::gfp*

SG176_sgRNA_NICD_V3_F
AATTGCAAATCTAAATGTTTGTGAAGAATATCAAAAGAGCGTTTTAGAGCTAGAAATAGC

SG177_sgRNA_NICD_V3_R
GCTATTTCTAGCTCTAAAACGCTCTTTTGATATTCTTCACAAACATTTAGATTTGCAATT

***Glp-1::gfp* repair plasmid**

SG161_V3_L440_GLPup_F
GATCCCCCGGGCTGCAGGCATTTTTGGCTTTTGGAACTG

SG162_V3_GFP_GLPup_R
TCCTTTACTTTGTCGCCCAGACTTAGC

SG163_V3_GLP-1up_GFP_F
GGCGACAAAGTAAAGGAGAAGAACTTTTCAC

SG164_V3_GLP-1down_GFP-R
CTTCACAGTTTTGTATAGTTCGTCCATGC

SG165_V3_GFP_GLP-1down_F
ACTATACAAAACTGTGAAGAATATCAAAAGAG

SG166_V3_L440_GLP1-down_R
TTCGCTATTACGCCAGTGATTGATTGGAAAGGACTC

RNAi clone *Y51F10.2*

SG073
AGTCCCCGGGTATTTCATTCCTCGCGTGTG

SG074
AGTCCCCGGGGCTGGTGGTCTTTCCATCTC

RNAi clone *ubr-5*

SG534_ubr-5_RNAiF1
ACGTAGTGCGGCCGCGGTGCGTCCGGTAGTAAAAA

SG535_ubr-5_RNAiR1
ACGTAGTGCGGCCGCCCATGGGGTTGCTAGTGTCT

sgRNA *prp-19::Strep*

SG474_sgRNA_prp19_F1
AATTGCAAATCTAAATGTTTGTGTATATTTTGCTACTTTCGTTTAAGAGCTATGCTGGAA

SG475_sgRNA_prp19_R1
TTCCAGCATAGCTCTTAAACGAAAGTAGCAAAATATACACAAACATTTAGATTTGCAATT

SG476_sgRNA_prp19_F2
AATTGCAAATCTAAATGTTTACAATTAGAAAGAGAATACTGTTTAAGAGCTATGCTGGAA

SG477_sgRNA_prp19_R2
TTCCAGCATAGCTCTTAAACAGTATTCTCTTTCTAATTGTAAACATTTAGATTTGCAATT

repair oligo *prp-19::Strep*

SG478_prp19_N
TCCTACAAAATTCGCATTGAAACTTTCTTCGTTTATGTCCCACGTCAATCAAGCGGTTTCGT
GTATATTTTGCTACTTTCAGGAGATGTGGTCCCACCCACAATTCGAGAAGTCTTTCGTGTGC
GGAATCAGTGGTGAACTGACCGAAGACCCAGTCGTCTCTCAAGTCTCAGGGCACATCTTTG
ATCGTCGGCTGATCG

SG479_prp19_C
TGGACCAGTCACTGGAGTTAGATTCGGAGAAAATGCTCGTTCATTGGTGACGTGTTCATTG
GATAAGAGTCTCCGAGTATTCTCTTTCTGGTCCCACCCACAATTCGAGAAGTAATTGTTTTT
ATTACCATTTATTACTAAGTTATTCAAAATTTCACCACATTTTTCCCGTTTCGTTTCCTTGTTT
TTTTTGTATTCCG

putx-1 dissection

putx-1::gfp-h2b::tbb2

putx-attB4
GGGGACAACTTTGTATAGAAAAGTTGGGATTTTATCTTCATCGGACCTG

putx-attB1
GGGGACTGCTTTTTTGTACAAACTTGTGGCGGTGTGAGAAGCGATAC

Version 7

543 putxSHORTESTL+attb4
GGGGACAACTTTGTATAGAAAAGTTGTAACGTTGATCTTTGTTTAATAAACCATACTATTTG
AATTAAGACACAGTATTGACC

putx-attB1
GGGGACTGCTTTTTTGTACAAACTTGTGGCGGTGTGAGAAGCGATAC

Version 5

541 - putx1stLBSdelL+attb4
GGGGACAACTTTGTATAGAAAAGTTGAATACTTGTAAATGTGAATCAGAAACC

putx-attB1
GGGGACTGCTTTTTTGTACAAACTTGTGGCGGTGTGAGAAGCGATAC

Version 10

putx-attB4
GGGGACAACTTTGTATAGAAAAGTTGGGATTTTATCTTCATCGGACCTG

546 - putxRmut5'LBSAB R+attB1
GGGGACTGCTTTTTTGTACAAACTTGTGGCGGGTCTTTCCGCGATACGGTGTTCATGCACA
AGACTTGTCTTTCCTTATACAAATCTGGAAAAACTGCAGCGATTTAG

Version 11

541 - putx1stLBSdelL+attb4
GGGGACAACTTTGTATAGAAAAGTTGAATACTTGTAAATGTGAATCAGAAACC

546 - putxRmut5'LBSAB R+attB1
GGGGACTGCTTTTTTGTACAAACTTGTGGCGGGTCTTTCCGCGATACGGTGTTCATGCACA
AGACTTGTCTTTCCTTATACAAATCTGGAAAAACTGCAGCGATTTAG

Version 13

SG021_putx13_F
TTCATCGGACCTGAAAAACTTGCCCTGCTCCCCGGATTTTTCAAAGGAAAGACTCAAAACTT
TTCTATGGCATAACAAATC

SG022_pux13_R
AAAAAGAGATCTCGGAAATACGC

3. Results

GLP-1 signaling dynamics in the *C. elegans* germline

GLP-1::GFP is expressed as expected on the membranes in the distal-most germline but does not localize to nuclei in adult gonads.

With the advances of genome editing tools and the availability of CRISPR for *C. elegans* we generated a GFP knock-in in the endogenous *glp-1* locus, henceforth called *glp-1::gfp*. The domain architecture of GLP-1 is rather modular, which made it feasible to place GFP between functional domains (Figure 9A).
We placed GFP within the NICD to visualize both the transmembrane form and the activated receptor in the nucleus. (Nusser-Stein, Beyer et al. 2012) successfully constructed a single-copy-integrated *lin-12-icd:gfp* transgenic worm strain, where GFP was placed between the Ankyrin repeats and the PEST domain of LIN-12. We therefore decided to integrate GFP in the *glp-1* locus at a similar position. With the help of Heinz Gut (Protein structure facility - FMI) we placed GFP between amino acids 1189 (Q) and 1190 (T), which corresponds to a position between the Ankyrin and PEST domains (Figure 9A).
Glp-1::gfp worms are viable and look superficially wild-type when grown at 15°C, 20°C or 25°C. However, we noticed that *glp-1::gfp* worms produce less viable progeny compared to the N2 wild-type strain (Figure 9B), and this cannot be rescued by mating *glp-1::gfp* worms to N2 wild-type males. Additionally, male induction by heat-shock does not work, because heat-shocked L4 worms become sterile. The GFP knock-in at this specific location might therefore cause a weak reduction-of-function of *glp-1* and temperature-sensitivity at high temperatures.
As expected *glp-1::gfp* worms showed GFP expression on the membranes in the distal part of adult gonads in hermaphrodites and males (Figure 9C-F). The GFP signal is strongest close to the stem cell niche and gets weaker along the distal-proximal axis. The expression pattern and localization we observed is in agreement with previous observations with antibody stainings on dissected gonads (Crittenden, Troemel et al. 1994).
Additionally, and again in agreement with published antibody stainings using an antibody raised against the Ankyrin repeats of GLP-1, we were unable to detect a nuclear GFP signal in the adult germline in hermaphrodites and males (Figure 9C and F). However, a nuclear signal would be expected from the mechanism of Notch signaling and its function in regulating germ cell proliferation.
Interestingly, and as observed already previously in the same antibody stainings against GLP-1 as mentioned before (Crittenden, Troemel et al. 1994), we also found GLP-1::GFP expressed in the hermaphrodite spermatheca. GLP-1::GFP was not only

visible on the membranes of the most distal spermatheca cells (distal constriction) but also in the nucleus of those cells (Figure 9D). Expression of GLP-1::GFP in the spermatheca was not restricted to the adult spermatheca, but was also visible during late L4 when terminally differentiated cells form a spermatheca with a lumen (Figure 9E) (wormatlas). However, to our surprise we could see a very weak nuclear GFP signal again in the distal-most germ cells in late L4 hermaphrodites and males (Figure 9E and F, arrows), suggesting that the localization of activated GLP-1 differs between the adult and larval germline in hermaphrodites and males. While looking at male *glp-1::gfp* worms we noticed that a substantial number of males did not contain a germline (63%, N=30). This could either be caused by the background mutation in the "male" strain (the actual genotype is *rrr27 (glp-1::gfp), him-8 (e1489)*) and would then suggest that *him-8* genetically interacts with the presumed reduction-of-function of *glp-1::gfp.* Or the reduced function of *glp-1* in *glp-1::gfp* worms is more severe in males and would then suggest that the GLP-1 pathway in the germline shows some kind of sex-specificity, for example, differences in protein partners that bind to the NICD.

For the remaining thesis we therefore focused on hermaphrodites.

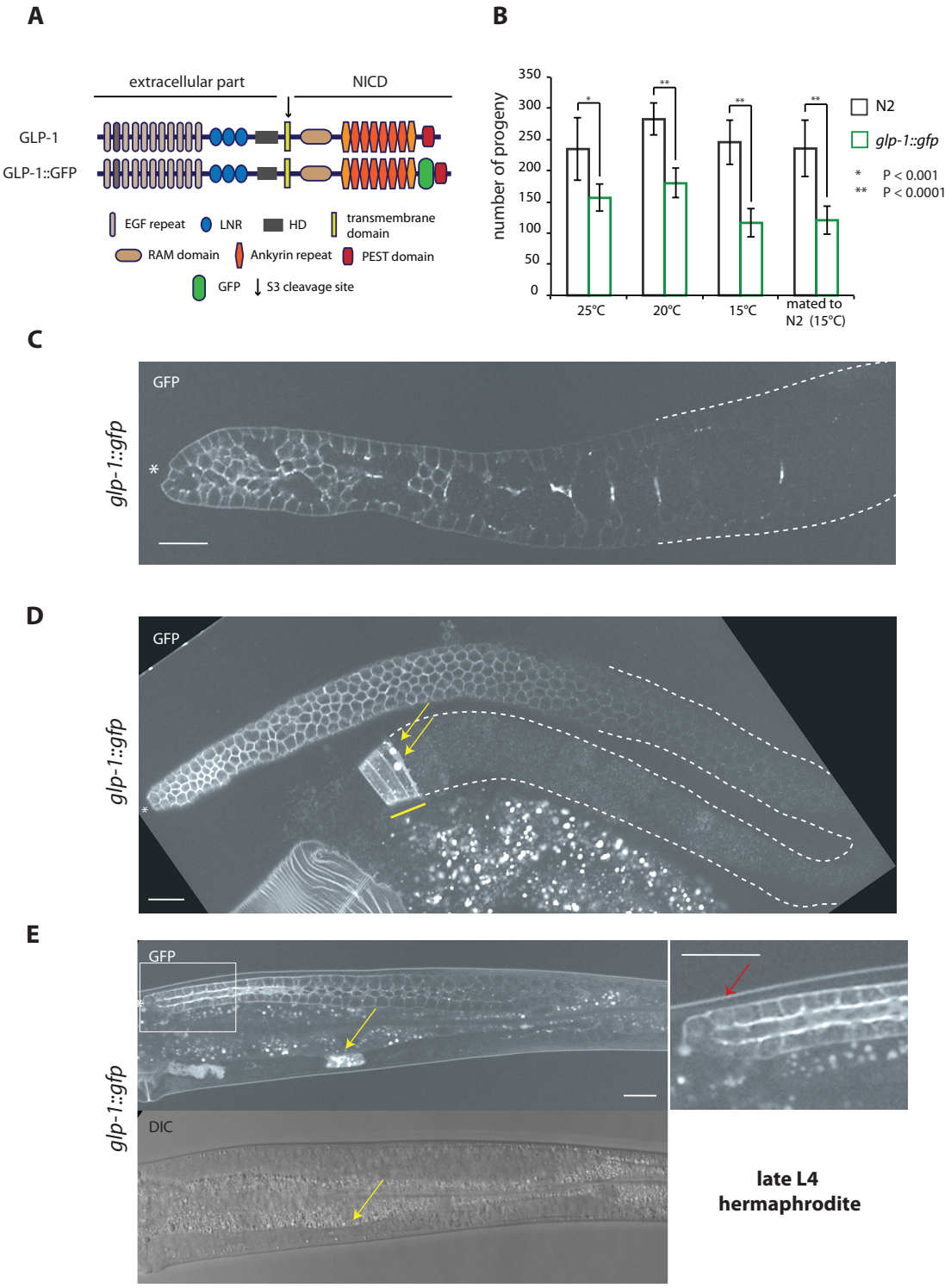
A
extracellular part
NICD
GLP-1
GLP-1::GFP
EGF repeat
LNR
HD
transmembrane domain
RAM domain
Ankyrin repeat
PEST domain
GFP
S3 cleavage site
B
number of progeny
350
300
250
200
150
100
50
0
25°C
20°C
15°C
mated to N2 (15°C)
N2
glp-1::gfp
* P < 0.001
** P < 0.0001
C
GFP
glp-1::gfp
D
GFP
glp-1::gfp
E
GFP
DIC
glp-1::gfp
late L4 hermaphrodite

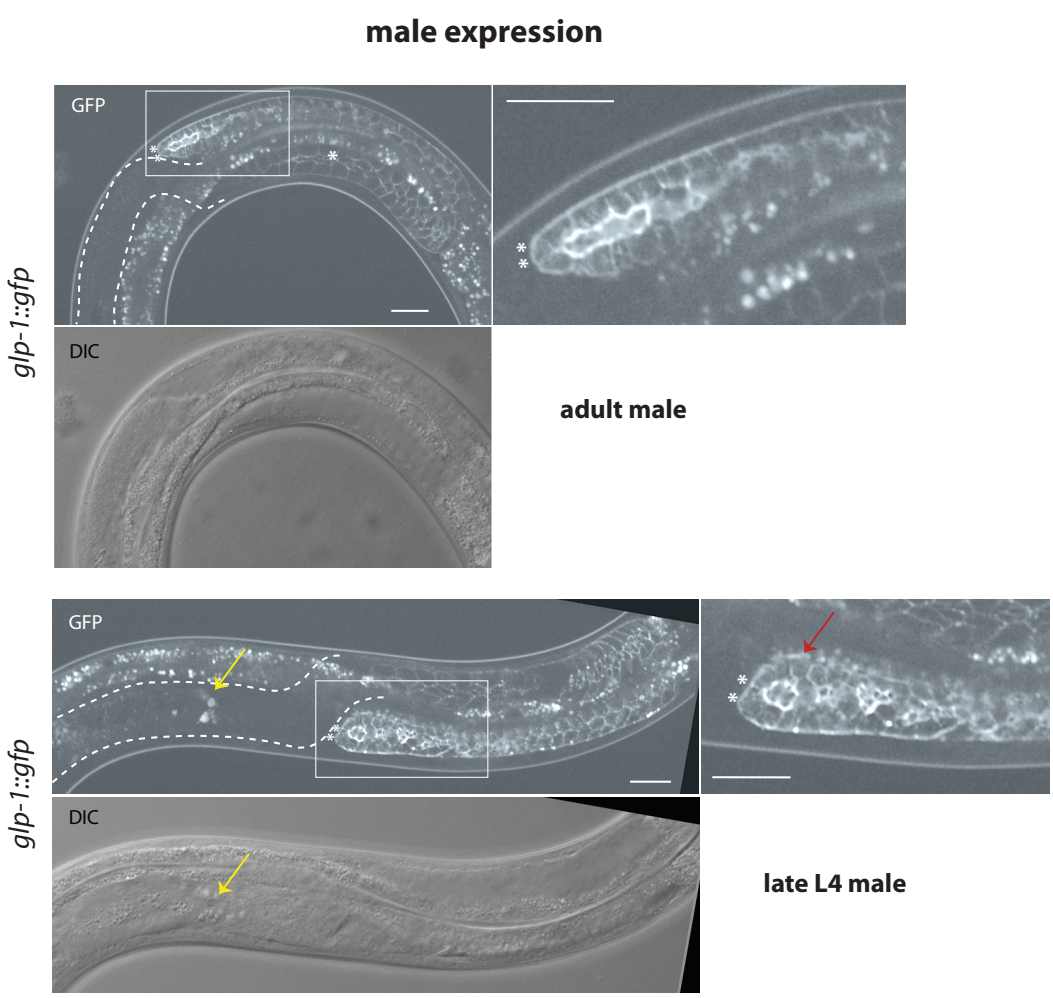

Figure 9: Knock-in of GFP within the intracellular part of GLP-1 by CRISPR shows an expected expression pattern.

(A) A schematic representation of GLP-1 and GLP-1::GFP proteins. The GFP was inserted between the Ankyrin repeats and the PEST domain within the intracellular domain (NICD) of GLP-1. (B) *glp-1::gfp* worms produce less viable progeny than N2 wild-type worms independent of the temperature they are grown at. Mating to N2 males does not rescue the reduced progeny size in *glp-1::gfp* worms (N=10 for all conditions). (C) Confocal image of a representative dissected adult gonad expressing GLP-1::GFP. Only the distal half of the gonad is shown. GLP-1 localizes to the distal-most membranes of germline cells, where germline stem cells undergo mitosis. Note that no nuclear signal is detected. (D) Surface view of a representative dissected adult gonad. GLP-1::GFP expression is strongest closest to the stem cell niche and gets weaker along the distal – proximal axis. GLP-1::GFP is detected on the membranes of the most distal spermatheca cells (distal constriction (Gissendanner, Kelley et al. 2008) yellow line). A strong nuclear signal can be detected in spermatheca cells (arrows). (E) A confocal image of a late L4 *glp-1::gfp* worm is shown. Expression of GLP-1::GFP is visible in the developing spermatheca (yellow arrow) before mature sperm is present. Additionally, a very weak nuclear GFP signal can be detected in the distal-most germ cells (red arrow). (F) Confocal images of *glp-1::gfp* males (actual genotype is *rrr27 (glp-1::gfp), him-8 (e1489)*). No nuclear GLP-1::GFP is detected in adult males (up), but similar to hermaphrodites a weak nuclear GFP signal is detectable in late L4 males (red arrow). Note that a strong nuclear signal is detected in unidentified cells in the somatic gonad (yellow arrow). Scale bars represent 20 µm. * and ** mark the distal end of hermaphrodites and males, respectively.

GLP-1 signaling is not only needed for the maintenance of germline stem cells in the adult germline, but was also shown to be required for germ cell proliferation already early during larval stages (Austin and Kimble 1987). In freshly hatched L1 larvae the germline precursor cells Z2 and Z3 are still mitotically quiescent and start dividing midway through the L1 stage. From there on germ cells proliferate and start to initiate meiosis during the L3 larval stage (Figure 10A). Since we detected a weak signal for GLP-1::GFP in late L4 worms (Figure 9) we speculated that GLP-1 localization might differ between the adult and larval germline.

In larvae starting from mid L1 the nuclear signal was detectable in the developing germline and the signal was in later larval stages, when germ cells start to undergo meiosis (L3/L4), restricted to the mitotic, distal end of the gonad (Figure 10B). The absence of a nuclear signal in freshly hatched L1 larvae is in agreement with earlier findings that *glp-1* is not required for the first mitotic division in L1 larvae (Austin and Kimble 1987). Nuclear GLP-1::GFP seems therefore to correlate with the occurrence of mitotic divisions during larval germline development, when the germline is expanding.

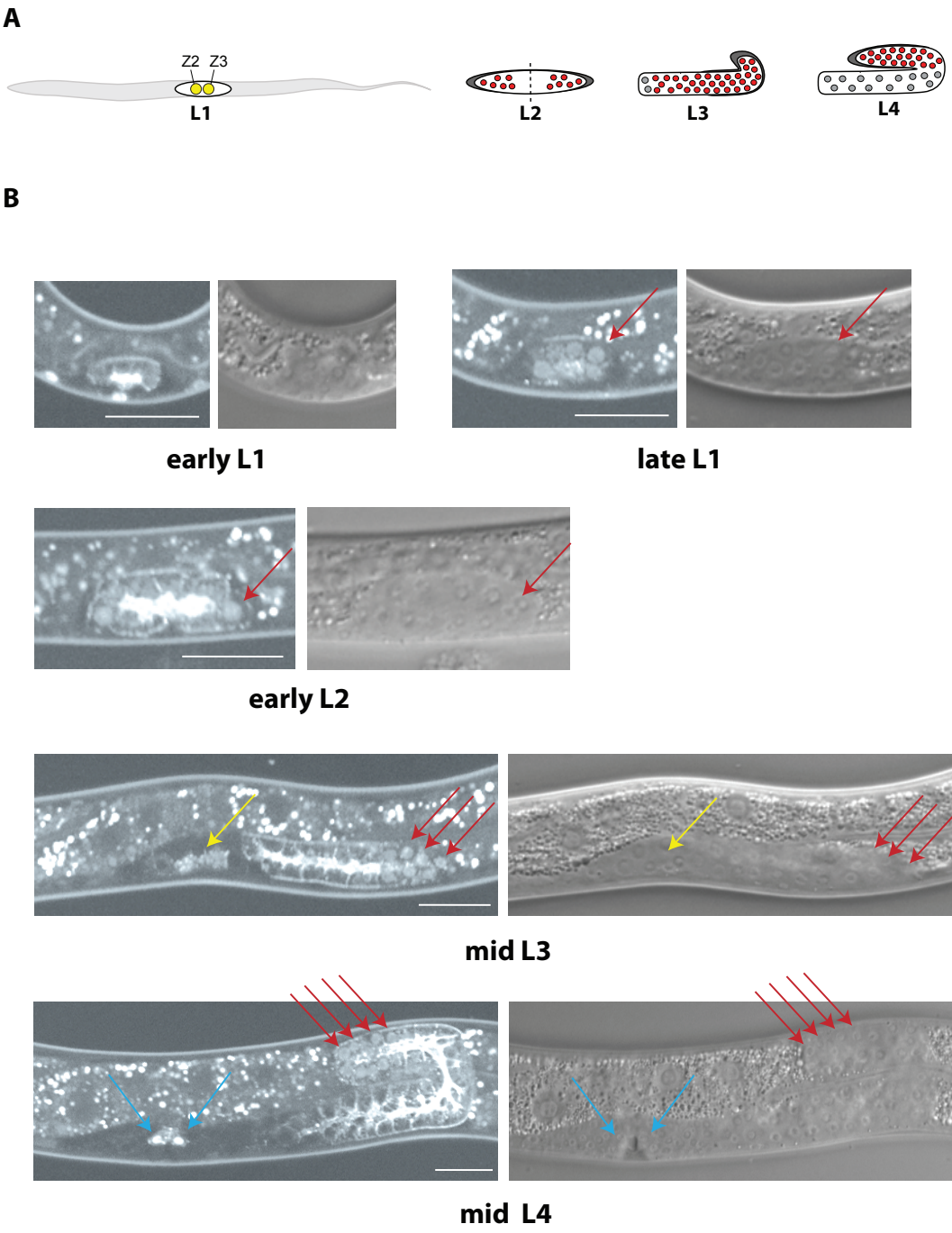

Figure 10: GLP-1::GFP is located in the nucleus of mitotic germ cells in larvae.
(A) Development of the germline during larval stages. After hatching, the germline consists of only 4 germline founder cells, of which Z2 and Z3 are giving rise to the actual germline cells. Z1 and Z4 (not shown) will form the somatic gonad. Germ cell divisions start already in the L1 stage and after horizontal expansion until the L3 stage the gonad turns to form the characteristic U-shape. Midway through the L3 larval stage germ cells furthest away from the DTC will transit into meiosis to produce sperm (not shown) until the switch to oocyte production in the adult. Red circles represent proliferating germ cells and grey circles represent cells that progress into meiosis, thus start to differentiate into sperm or oocytes. (B) Expression of GLP-1::GFP during larval stages. Nuclear GLP-1::GFP is detected in mitotically dividing germline cells (red arrows) and during L3/L4 stages in cells of the somatic gonad (yellow arrows) and in vulva precursor cells (blue arrows). Scale bars represent 20 µm.

In addition to germline cells, GLP-1::GFP is also expressed in the developing larval somatic gonad (yellow arrows Figure 10B), where it localizes to the nucleus, and in specific vulva precursor cells during vulva development (blue arrows Figure 10B). To our knowledge no function for GLP-1 was descripted so far during the development of the somatic gonad and the vulva. However, it was shown previously that a C-terminal truncation of GLP-1 and a strong *glp-1* gain-of-function allele (*oz112*) cause a multivulva phenotype as normally observed in a *lin-12* gain-of-function allele (Mango, Maine et al. 1991, Berry, Westlund et al. 1997), suggesting that GLP-1 might indeed play an unappreciated role in vulva development.

GLP-1-ICD localization is dynamically regulated by the ubiquitin-proteasome-system.

Since previously two GLP-1 target genes were found to be required for the function of Notch signaling in the adult germline (Kershner, Shin et al. 2014) and temperature-shift experiments with temperature-sensitive *glp-1* loss-of-function alleles showed a requirement for *glp-1* in the maintenance of germ cell proliferation also in the adult germline (Austin and Kimble 1987), it is unlikely that its role as activated transcription factor, and therefore its nuclear localization, is not required to generate a signaling output in the adult germline. Therefore, either very little GLP-1 is activated on the membranes in the adult and translocates into the nucleus and cannot be detected or activated nuclear GLP-1 has a rapid turnover in order to restrict the signaling output.
To test this idea, we knocked down the proteasome component *pbs-5* as well as the only E1 ligase encoded in the *C. elegans* genome *uba-1* by RNAi. Because removing the proteasome is lethal, we could only perform RNAi transiently by feeding worms from the L4 stage on for 48 hrs. Knock-down of either gene resulted in nuclear localization of GLP-1::GFP with a penetrance of 97% for *pbs-5* RNAi (N=30) and 96% for *uba-1* RNAi (N=24), while in mock-treated worms nuclear localization was never observed (N=47) (Figure 11A). Interestingly, nuclei that showed nuclear GLP-1::GFP were only found in the first approximately 6 rows of germline cells counting from the DTC. This is in accordance with previous observations, where the existence of two distinct pools of proliferating cells in the distal germline was proposed. The very distal pool reaching until 6-8 germ cell diameters from the DTC was suggested to contain genuine stem cells (Cinquin, Crittenden et al. 2010, Lee, Sorensen et al. 2016). It is therefore likely that we observe nuclear translocation of GLP-1::GFP upon *pbs-5* or *uba-1* knock-down in those stem cells. Even though we observe nuclear-localized GLP-1::GFP we did not see overproliferation in these germlines. This result was not very surprising, since a mutant of the proteasomal component *pas-5 (oz237)* was shown to have a normal extend of proliferative zone. However, it was also demonstrated that

the respective mutant is able to enhance the overproliferation phenotype of a *glp-1* gain-of-function allele (*ar202*) (Macdonald, Knox et al. 2008). Similar to *pbs-5* RNAi, *pas-5* RNAi also caused nuclear localization of GLP-1::GFP (data not shown).

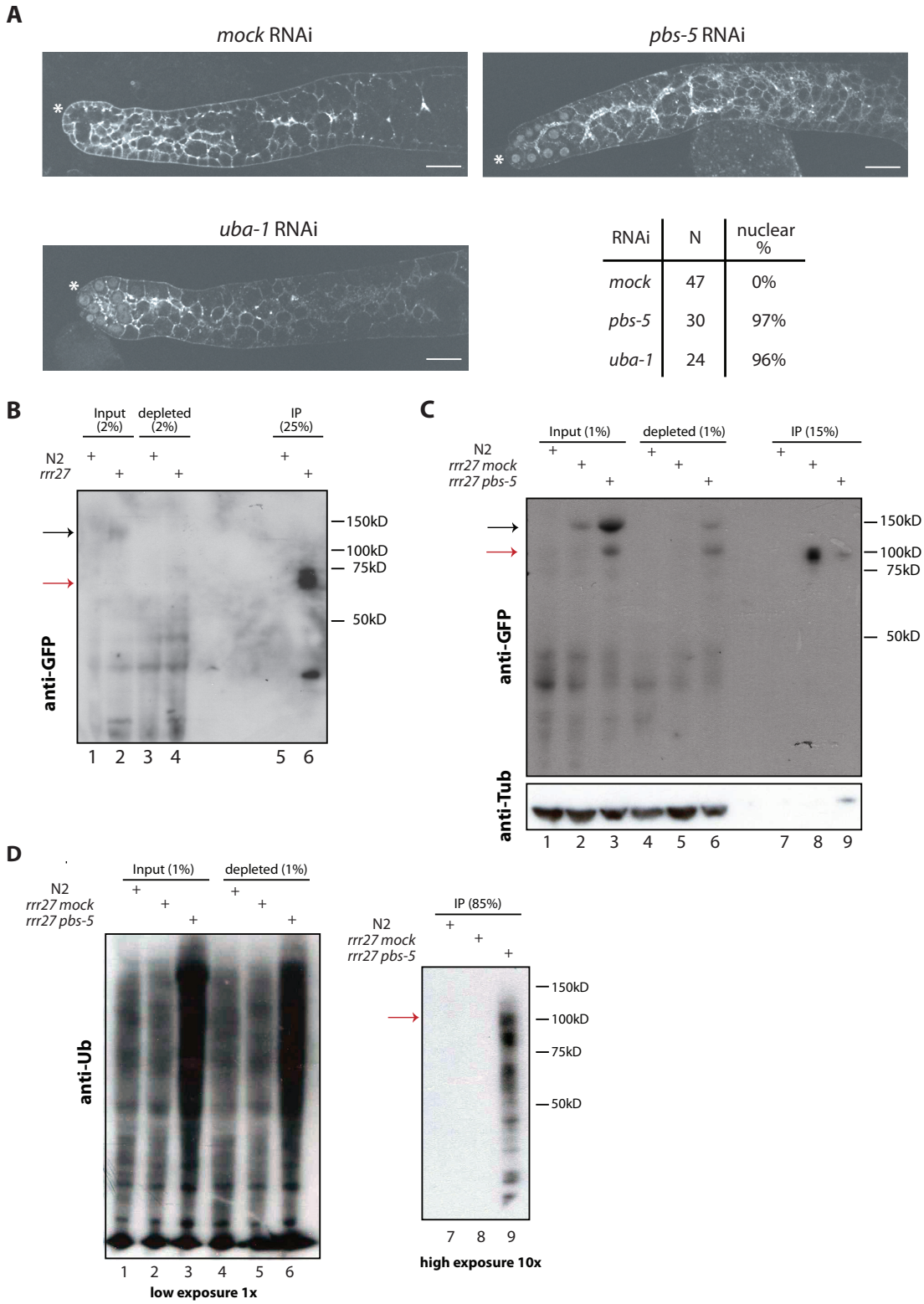

Figure 11: The stability of the GLP-1-ICD is regulated by the ubiquitin-proteasome-system.

(A) Shown are confocal images of dissected gonads from *glp-1::gfp* worms. While mock-treated adult germlines do not show nuclear GLP-1::GFP (N=47), a nuclear signal is observed after depleting *uba-1* (E1 ligase) (96%, N=24) and the proteasomal component *pbs-5* (97%, N=30) by RNAi. Scale bars represent 20 µm. (B) Western blot detection of GLP-1::GFP after GFP-IP from wild-type or *glp-1::gfp* worms. (C) Western blot detection of GLP-1::GFP (up) and tubulin (bottom) in total protein extracts and after GFP-IP from wild-type or *glp-1::gfp* worms treated or not with *pbs-5*(RNAi). Note that GLP-1::GFP

accumulates in *pbs-5* (RNAi) total extracts. GLP-1::GFP is more easily immunoprecipitated from mock-treated worms than from *pbs-5* (RNAi) worms. (D) Western blot detection of ubiquitinated proteins from total extracts (left) and immunoprecipitated GLP-1::GFP (right) with an anti-ubiquitin antibody. *pbs-5* (RNAi) stabilizes ubiquitinated proteins on total extracts as expected (lane 3). Ubiquitinated forms are detected only after GFP-IP from *pbs-5* (RNAi) worms.

Our observation of a nuclear localization of GLP-1::GFP in worms depleted from the E1 ligase *uba-1* as well as the proteasomal component *pbs-5* suggests that the GLP-1-ICD might indeed be ubiquitinated to be turned over. Using immunoprecipitations with agarose GFP-traps (Chromotek) we were able to successfully enrich for the nuclear form of GLP-1 in untreated worms (Figure 11B). The GLP-1 receptor has a full-length size of 1295 amino acids corresponding to around 142 kD (Crittenden, Troemel et al. 1994). In input samples we were able to detect a weak signal around 150 kD in protein extracts from *glp-1::gfp* worms, which is absent in extracts from wild-type (N2) worms (Figure 11B lane 2). This band might therefore correspond to full-length GLP-1. However, including GFP the full-length receptor should run at around 169 kD. The nuclear form of GLP-1::GFP is 512 amino acids long and should therefore run around 83 kD (Rudel and Kimble 2001). In immunoprecipitations from protein extracts of *glp-1::gfp* worms we were able to reproducibly enrich for GLP-1::GFP at around 75 kD. Additionally, we always detect a second band that is running a little lower. To identify potential interaction partners of GLP-1 we performed mass spectrometric analysis on immunoprecipitated GLP-1::GFP against wild-type control samples but could not significantly enrich for interaction partners (Figure 12). When we looked at GLP-1-derived peptides in the mass spectrometric analysis, we could see that out of 118 identified peptides, which are corresponding to 17 peptide sequences, 110 mapped to regions within the NICD and predominantly within the Ankyrin repeats (
Table **3**). This confirmed that we indeed enrich for the nuclear form of GLP-1 by immunoprecipitations.

If GLP-1::GFP is turned over very quickly by the ubiquitin-proteasome-system, we hypothesized that we would see an accumulation of the nuclear form in *pbs-5* RNAi-treated worms and would be able to detect a ubiquitin signal. Indeed, in protein samples from *pbs-5*-depleted *glp-1::gfp* worms, we were able to enrich for the nuclear form of GLP-1::GFP (lane 3 Figure 11C) and were able to detect a signal for ubiquitin in immunoprecipitated GLP-1::GFP at about the size where we detect a signal for GFP (compare lane 9 Figure 11D right panel and lanes 8 and 9 Figure 11C). We do not only see the presumptive nuclear form of GLP-1 enriched in protein extracts from *glp-1::gfp* worms treated with *pbs-5* RNAi but also the full-length GLP-1. The accumulation of the full-length form is in agreement with the accumulation of membrane-associated GLP-1::GFP upon *pbs-5* depletion observed in confocal images (Figure 11A).

We noticed, however, that the signal for the immunoprecipitated nuclear form of GLP-1::GFP in *pbs-5*-depleted worms is much weaker than for immunoprecipitated mock-treated worms (compare lane 8 and 9 Figure 11C). Additionally, the putative nuclear form of GLP-1::GFP differs in size between worms grown on OP50 (75 kD) and grown under RNAi condition (100 kD) (compare lane 6 Figure 11B and lane 8 and 9 Figure 11C). One possibility for the former could be that the affinity of the agarose beads for the nuclear form of GLP-1 changes due to modifications that are stabilized. The latter might be due to differences in GLP-1 processing when the RNAi pathway is triggered, a hypothesis we were not able to follow up at this point. One possibility we followed up on was that GLP-1 is differentially processed depending on the bacteria worms are fed with. RNAi is performed using the bacterial strain HT115(DE3), while maintenance and large-scale production of *glp-1::gfp* worms was done on OP50 bacteria or NA22. Using immunoprecipitations with agarose GFP-traps on *glp-1::gfp* worms grown on the four different bacterial strains OP50, NA22, HT115 and DA837 we could not detect differences in the size of GLP-1::GFP by western blot (Figure 13). At this point we therefore cannot explain why the nuclear form of GLP-1::GFP runs differently on protein gels.

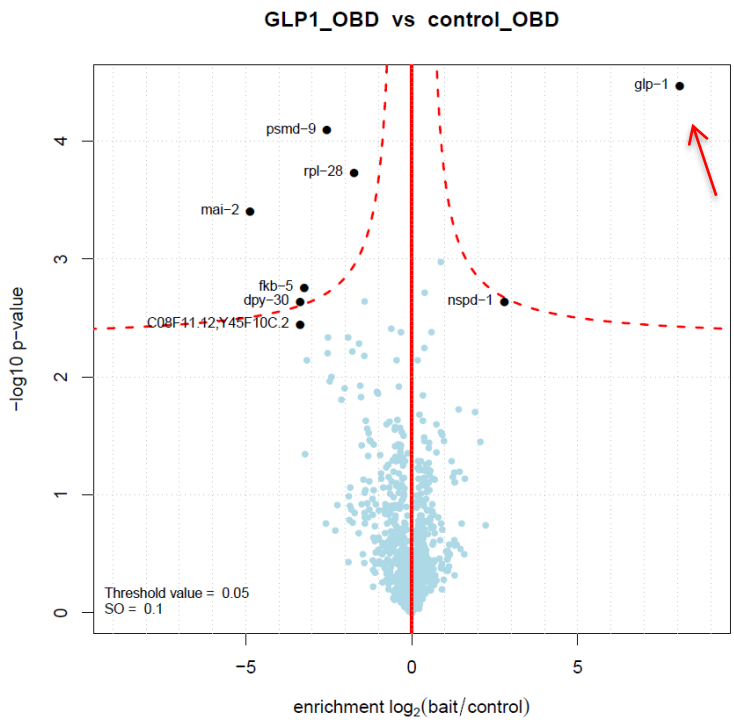

Figure 12: Quantitative comparison of the on-beads-digested GFP IPs from protein extracts of *glp-1::gfp* worms compared to control (N2). The only significantly enriched protein is GLP-1 (red arrow).

Peptide sequence	Peptide count	Location within GLP-1
(K)LIETYWcR(C)	1	EGFR
(K)YcEEAIDMcK(D)	1	EGFR
(R)DELGPLVFR(W)	1	NRR
(R)MSLGLPITEAMVAVPK(R)	5	NRR
(K)MVNATVWMPPMESTNEK(G)	3	RAM
(R)NQSNHSSQcSLLDNSAYYHPNTK(R)	8	RAM
(R)VLHWLAANVR(G)	7	ANK
(R)GKPEDVITTEAIR(C)	15	ANK
(R)DcDENTALMLAVR(A)	8	ANK
(R)EGANPTIFNNSER(S)	5	ANK
(R)SALHEAVVNK(D)	3	ANK
(K)EIDELDRNGMTALMLVAR(E)	6	ANK
(R)NGMTALMLVAR(E)	4	ANK
(K)HQVEMAELLLSK(G)	23	ANK
(K)LDYDGAAR(K)	19	ANK
(K)DKQDEDGRTPIMLAAK(E)	8	ANK
(K)QDEDGRTPIMLAAK(E)	1	ANK

Table 3: GLP-1-peptide sequences identified in mass spectrometric analysis of GFP-IPs from protein extracts of *glp-1::gfp* worms. Note that no GLP-1-peptides were detected in control samples. Peptides are ordered according to their location within GLP-1, whereby peptides mapping to the N-terminus are listed first. Only 8 out of the 118 total peptides identified map to the EGFR or NRR domains of the extracellular part of GLP-1. The remaining 110 predominantly mapped to the Ankyrin repeats (ANK) and a few peptides to the RAM domain of the NICD.

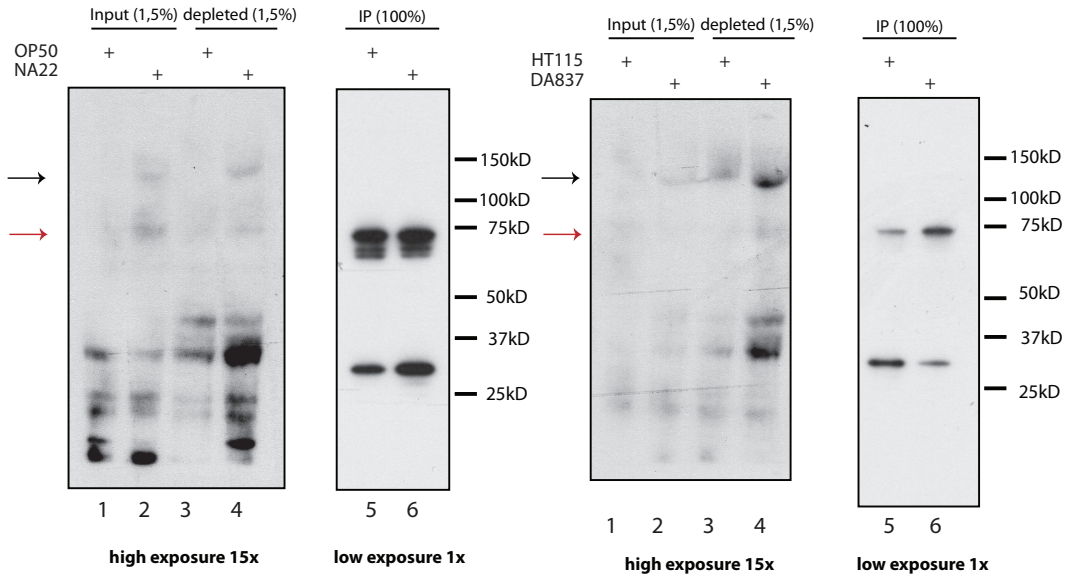

Figure 13: GLP-1 processing is not influenced by differences in the types of the bacteria *glp-1::gfp* worms are grown on.

Western blot detection of GLP-1::GFP after GFP-IP from *glp-1::gfp* worms grown on OP50 or NA22 (left panels) and HT115 or DA837 (right panels). GLP-1-ICD runs at the same size for all treatments (red arrows). Note that we can detect full-length GLP-1 (black arrows). Samples generated from worms grown on OP50 and NA22 were run on a separate gel than those generated from worms grown on HT115 and DA837.

Depletion of the U-Box E3 ligase PRP-19 leads to nuclear stabilization of GLP-1::GFP.

Nuclear localization of GLP-1::GFP upon *uba-1* or *pbs-5* knock-down prompted us to dissect the mechanism of GLP-1 turnover in the germline.

In mammals the E3 ligase FBXW7 - the homolog of SEL-10 - was shown to target the NICD for proteasomal degradation. In *C. elegans sel-10* was initially identified as negative regulator of LIN-12 signaling and subsequently shown to target Notch for degradation (Sundaram and Greenwald 1993, Gupta-Rossi, Le Bail et al. 2001, Wu, Lyapina et al. 2001).

However, several observations suggested that GLP-1 is degraded by different means in the *C. elegans* germline than in the embryo and distinct from mechanisms functioning for LIN-12 degradation. For example, mutations in *sel-10* only weakly suppress the germline proliferation defects of two temperature-sensitive *glp-1* loss-of-function alleles (*e2144* and *q231*) (Sundaram and Greenwald 1993).

To test this hypothesis, we first knocked down *sel-10* by RNAi, but could not observe nuclear stabilization of GLP-1::GFP. A very recent study presented evidence that *sel-10* might function together with *ubr-5*, which encodes a HECT-type E3 ligase, to negatively regulate GLP-1 signaling in the germline (Safdar, Gu et al. 2016).

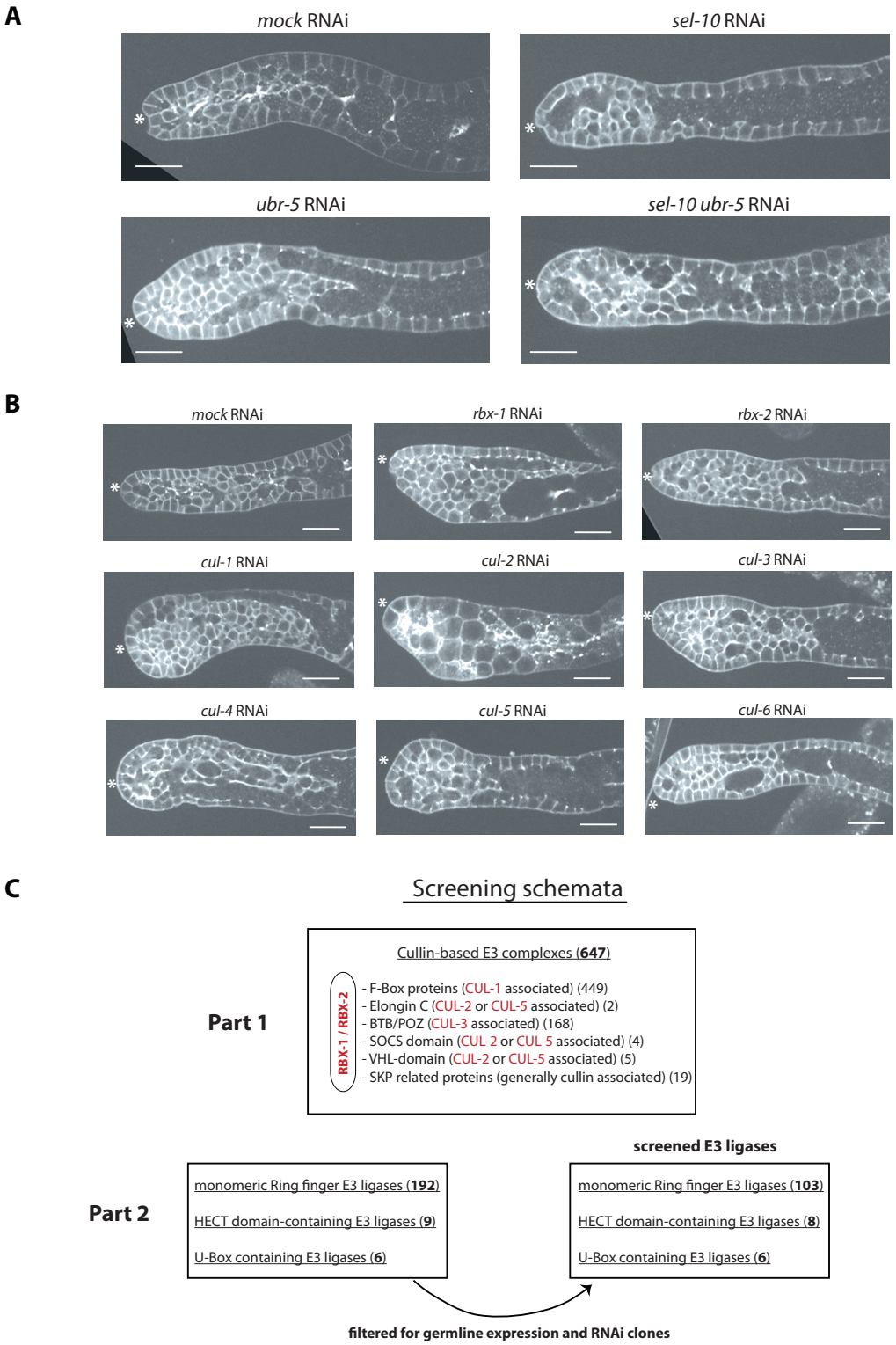

Figure 14: GLP-1 is turned over by a different E3 ligase in the germline than proposed for embryonic GLP-1 and LIN-12.

(A) Confocal images of dissected adult gonads expressing GLP-1::GFP and treated with the indicated RNAi are shown. In none of the shown RNAi experiments nuclear GLP-1::GFP was detected (N=10 for *sel-10, ubr-5* RNAi and *sel-10 ubr-5* double RNAi; N=47 for *EV* RNAi). (B) Confocal images of dissected gonads of *glp-1::gfp* worms treated with the indicated RNAi. Nuclear localization was not observed (N=30 for all conditions). (C) Screening schemata applied to narrow down the E3 ligase mediating GLP-

1 nuclear turnover in the germline. Depletion of all cullin-family members (*cul-1,2,3,4,5*, or -*6*) as well as their common adaptors *rbx-1* and *rbx-2* did not show nuclear stabilization of GLP-1::GFP (part 1). In a second step, filtering for germline expression and for availability of RNAi clones was applied to generate a candidate list of E3 ligases (Part 2). Numbers in parenthesis indicate the number of E3 ligases (according to (Gupta, Leahul et al. 2015)) encoded in the *C. elegans* genome that fall into a specific subclass of E3s. For part 1 classification was done according to the presence of domains that typically associate with a specific cullin-member. * marks the distal end of gonads and scale bars represent 20 µm.

However, knock-down of *ubr-5* alone and double knock-down of *sel-10* and *ubr-5* by RNAi did not result in nuclear-localized GLP-1::GFP (Figure 14A).

This prompted us to perform a screen for the E3 ligase that is required for GLP-1 turnover in the *C. elegans* germline. (Gupta, Leahul et al. 2015) generated a list of 854 putative E3 ligases by looking for genes that code for domains typically present in E3 ligases: F-box, HECT, U-box, BTB/POZ, RING finger, SOCbox and VHL-box domains. Most of them can be categorized into proteins that are typically present in multimeric cullin-based E3 complexes, while the remaining are thought to function as monomers (reviewed in (van den Heuvel 2004, Sarikas, Hartmann et al. 2011)). *C. elegans* codes for 647 E3 ligases that are part of a cullin-based complex. Those fall into 449 F-Box proteins that typically associate with CUL-1-based complexes and 168 BTB/POZ domain-containing that associate with CUL-3. Another 4 SOCbox as well as 5 VHL-box domain-containing proteins that are usually found in CUL-2 or CUL-5 complexes are present in the *C. elegans* genome, as well as two Elongin BC proteins that serve as adaptors. SKP-related proteins (19) were shown to interact with different cullin-family members. Common to all cullin-based complexes are the adaptor proteins RBX-1 and RBX-2 (Figure 14C). To test whether the NICD is turned over by a multimeric E3 complex, we first knocked down all cullin-family members encoded in the *C. elegans* genome, *cul-1, cul-2, cul-3, cul-4, cul-5, cul-6* or the common adopters *rbx-1* and *rbx-2.* None of the RNAi treatments resulted in nuclear localization of GLP-1::GFP (Figure 14B). This implicates that GLP-1 is likely turned over by a monomeric E3 ligase.

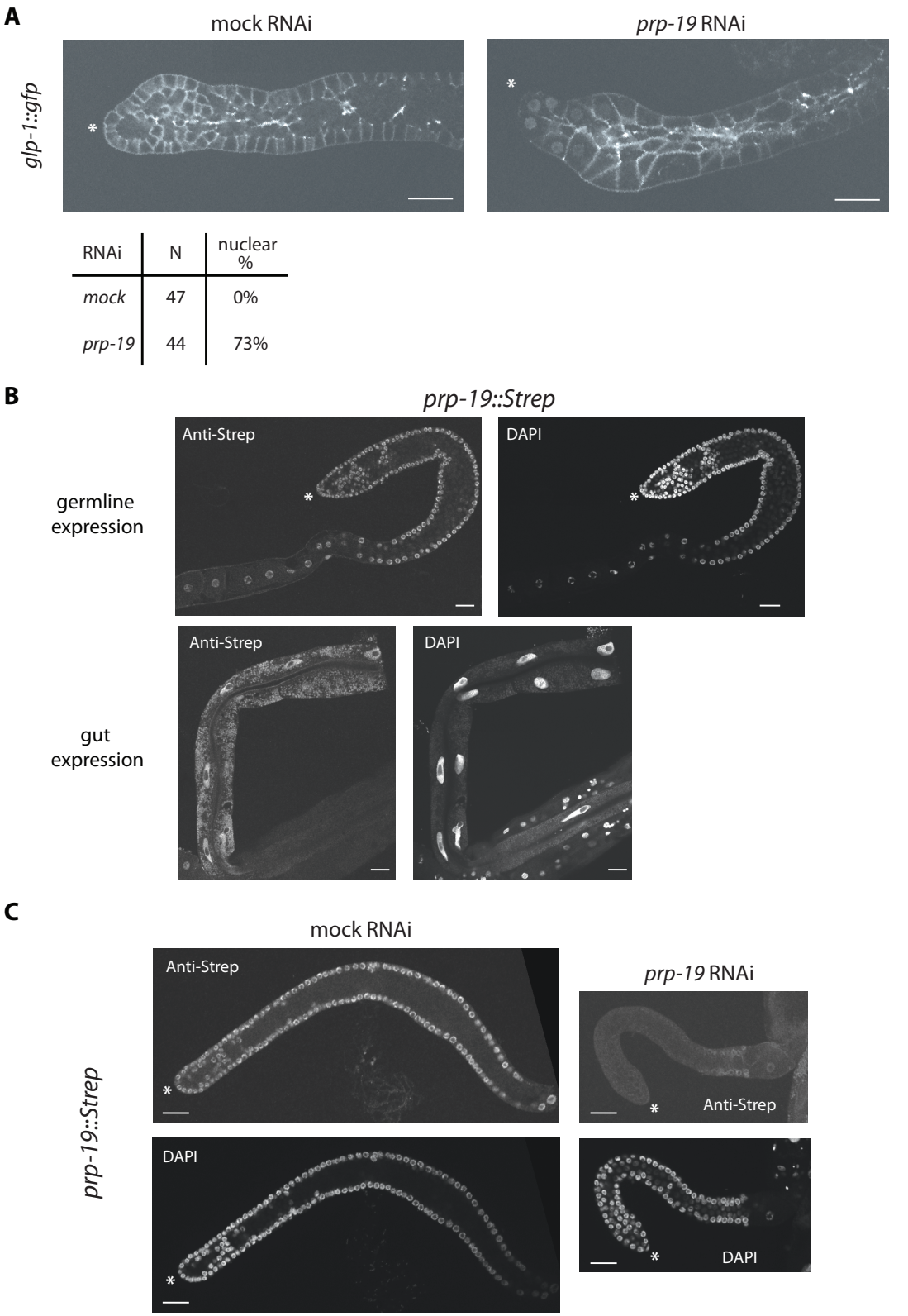

Figure 15: The U-box domain-containing putative E3 ligase *prp-19* mediates GLP-1 nuclear turnover. (A) Worms depleted for *prp-19* showed nuclear stabilization of GLP-1:GFP with a penetrance of 73% (N=44). Shown are representative confocal images of dissected gonads of *glp-1::gfp* worms treated with the indicated RNAi. (B) Expression of a Strep-tagged PRP-19 in germline nuclei and gut nuclei. Dissected gonads and the gut were stained with anti-StrepMAB classic Chromeo 546 (IBA life sciences) and DAPI. Expression of PRP-19 is not restricted to a certain germline region. (C) The anti-Strep

immuno-staining is specific for strep-tagged PRP-19. While in mock-treated worms (EV RNAi) staining can be seen in all germline nuclei, *prp-19*-depleted worms lose the staining almost entirely. Scale bars represent 20 µm. * mark the distal end of the germline.

We first generated a candidate list from the remaining 207 putative E3 ligases, which had been categorized as RING fingers (192), HECT domain- (9) or U-Box-containing E3 ligases (6). We focused on those genes that are germline-expressed (Scheckel, Gaidatzis et al. 2012), which resulted in 127 remaining candidates (Table 2). RNAi clones in either the Ahringer or OBS library were available for 114 of them (Figure 14C).

Among the 114 E3 tested only knock-down of *prp-19* (*T10F2.4*), a U-Box domain-containing putative E3 ligase, resulted in nuclear localization of GLP-1::GFP in 73% of analyzed gonads (N=44), while mock-treated worms never showed nuclear localization (N=47) (Figure 15A).

Prp-19 is the name-giving component of the PRP19 complex, which at least in humans and yeast was shown to function in a variety of cellular processes. To test whether the observed phenotype is resulting from knock-down of *prp-19* in the germline and not caused by secondary effects coming from somatic tissues, we crossed *rrr27* (*glp-1::gfp)* into *rrf-1 (pk1417*), which has been widely used to restrict RNAi mainly to the germline. In *rrf-1* mutants RNAi is functioning only in some somatic tissues, for example the intestine (Kumsta and Hansen 2012). In this background GLP-1::GFP also localized to distal germline nuclei in the absence of *prp-19* (data not shown). At least for *C. elegans* it was not known so far where PRP-19 localizes. The function of PRP19 in mouse suggests a nuclear as well as a cytoplasmic localization, while yeast Prp19 was so far only associated with a nuclear function (reviewed in (Chanarat and Strasser 2013)). To study PRP-19 localization and link it to its function in *C. elegans* we were aiming to generate a functional PRP-19 expressing transgenic line, but could not obtain a fluorescently tagged strain either by single-copy-integration by MosSCI or by CRISPR-mediated genome editing. However, introducing a Strep-tag by CRISPR at the C-terminus of *prp-19* was successful. Immuno-stainings against the Strep-tag in dissected gonads showed expression of PRP-19 in all germline nuclei, in oocytes as well as in gut nuclei (Figure 15B) and embryonic cells (data not shown). No staining was detected in *prp-19*-depleted worms, confirming the specificity of the antibody (Figure 15C).

Knock-down of *prp-19* suppresses the loss of mitotic nuclei in a temperature-sensitive *glp-1* loss-of-function allele.

GLP-1 signaling was shown to be the main pathway that regulates germ cell proliferation in the *C. elegans* germline (Kimble and White 1981, Austin and Kimble 1987). The development of the germline is severely affected in *glp-1* loss-of-function mutants. Germ cells do not proliferate already during early stages in development and the few remaining germ cells develop into sperm (Austin and Kimble 1987). The same can be observed in worms carrying a temperature-sensitive (ts) loss-of-function (lf) allele of *glp-1*, when those worms are shifted to the restrictive temperature early in development.

However, *glp-1* is not only required for the establishment of a germ cell pool during development, but also for its maintenance. *Glp-1 lf ts (e2144)* worms grown on the permissive temperature have a wild-type germline, however shifting those worms to the restrictive temperature during the adult stage results in the continuous loss of mitotic germ cells (Figure 16A). We reasoned, if PRP-19 regulates GLP-1 stability in the nucleus, knock-down of *prp-19* in *glp-1 lf ts (e2144)* worms would lead to a deceleration of the germ cell loss. To test this hypothesis, we raised synchronized L1 worms on RNAi plates at the permissive temperature until they reached the young adult stage. Worms were then shifted to the restrictive temperature for 4 hrs and 7 hrs, a time point when in mock-treated worms the proliferative zone is almost entirely gone (Figure 16B). To identify proliferative germ cells we stained dissected gonads in two independent experiments with DAPI to visualize nuclear morphology and counted starting from the distal tip the number of germ cell diameters (gcd) until the appearance of the first row of crescent-shaped nuclei (a respective nucleus is marked in Figure 16B with a yellow arrow), which is a hallmark of those cells to transit into meiosis (MacQueen and Villeneuve 2001). In wild-type germlines the mitotic region spans between 15-20 gcd (Hansen, Hubbard et al. 2004). Similarly, for *glp-1 lf ts* worms raised under mock RNAi conditions at the permissive temperature we observed an average of 15 gcd. Worms grown on *prp-19* RNAi at the permissive temperature showed a slight increase in gcd (16 and 17 on average in two independent experiments) compared to mock-treated worms. When we shifted those worms to the restrictive temperature, mock-treated worms contained on average only 2 gcd after 7 hrs, while worms treated with *prp-19* RNAi retained an average of 10 or 12 gcd in the respective experiment (Figure 16B and C). This corresponds to a loss of proliferative zone length of 84,5% in mock-treated worms, while *prp-19*-depleted worms only lose an average of 34%.

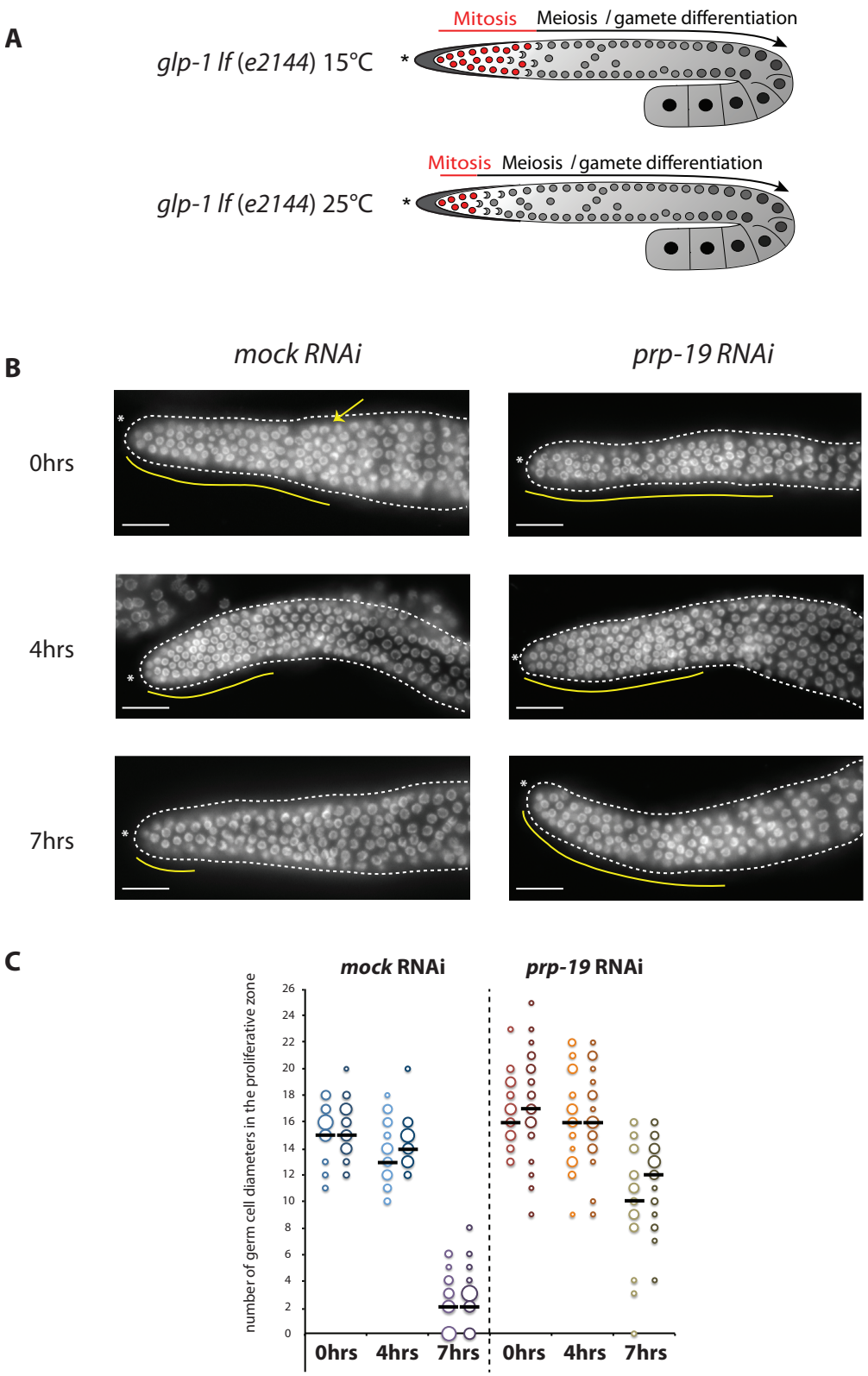

Figure 16: Depletion of *prp-19* slows down the loss of mitotic nuclei in a temperature-sensitive *glp-1* loss-of-function allele.

(A) The temperature-sensitive *glp-1* loss-of-function allele *e2144* behaves wild-type when it is grown at the permissive temperature of 15°C. Shifting these worms to the restrictive temperature in the late L4 or young adult stage leads to the sequential loss of mitotic germ cells (red circles) in the distal gonad

due to loss of GLP-1 signaling. (B) DAPI-stained representative dissected gonads from animals of the indicated genotype treated with mock or *prp-19* RNAi and time shifted to 25°C are shown. The proliferative zone (yellow line) is per convention defined to reach from the DTC until the appearance of the first row of germ cell nuclei that contains at least two crescent-shaped nuclei (arrowhead), a hallmark of those nuclei to transit into meiosis (transition zone). Note that *prp-19 (RNAi)* worms retain mitotic cells even after 7 hrs at 25°C. * marks the distal end of the germline. Scale bars represent 20 µm. (C) Quantification of two independent experiments after the shift to the restrictive temperature for 4 hrs and 7 hrs (N>20 in all cases). Blotted are the germ cell diameters (gcd) of the proliferative zone of the respective condition and for two independent experiments. The size of the circle is relative to the number of gonads with the same gcd-count. Worms depleted for *prp-19* show a longer mitotic zone at all three time points.

Knock-down of *prp-19* enhances overproliferation of mitotic nuclei in a temperature-sensitive gain-of-function allele of *glp-1.*

It was previously shown that disruption of the proteasome enhances a temperature-sensitive (ts) gain-of-function (gf) allele of *glp-1* (ar202). (Macdonald, Knox et al. 2008). It was further shown that the observed enhancement might partially be due to a decrease in GLP-1 degradation. Similarly, we reasoned that depletion of the E3 ligase, which is targeting GLP-1 for degradation, should enhance the overproliferation phenotype of *glp-1 gf ts* (ar202). This allele behaves wild-type when grown at the permissive temperature. Shifting those worms to the restrictive temperature induces the formation of a germline tumor (Figure 17A). We depleted *prp-19* by RNAi from *glp-1 gf ts* (*ar202*) worms and grew them on the permissive temperature. Consistent with a putative function of PRP-19 in GLP-1 turnover, *prp-19* RNAi-treated worms showed an enhancement of the overproliferation phenotype at the permissive temperature (Figure 17). Mock-treated worms grown on the permissive temperature showed a normal extent of the mitotic zone (15-20 gcd) in 95% (N=37) of dissected gonads as determined by anti-HIM-3 staining and nuclear morphology (Figure 17B and C). In contrast, 67% (N=43) of dissected gonads from *prp-19*-depleted worms showed phenotypes otherwise observed in *glp-1 gf ts* (*ar202)* worms grown on the restrictive temperature (*pro* or *tum* phenotypes) (Pepper, Killian et al. 2003) (Figure 17B and C).

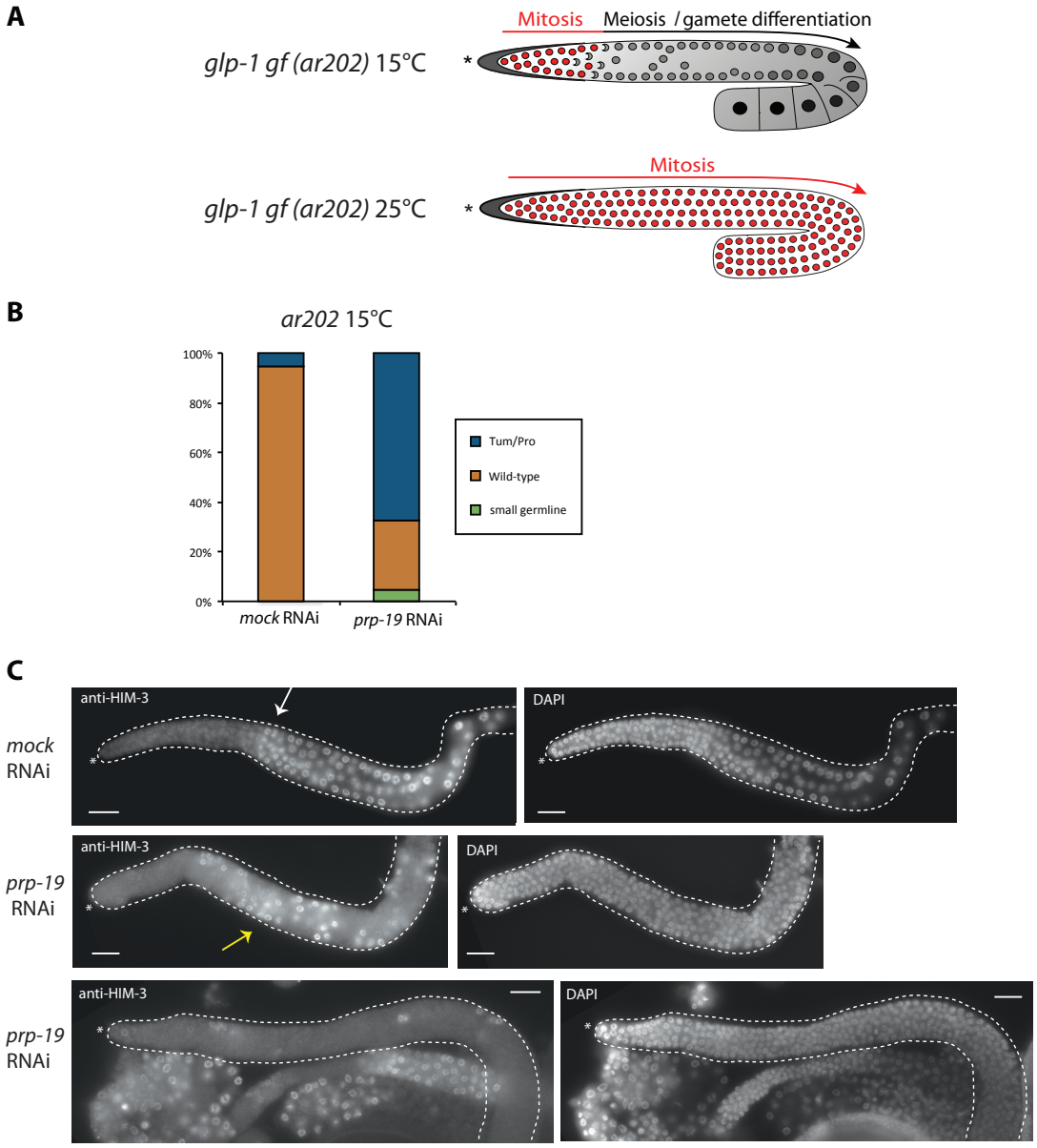

Figure 17: Depletion of *prp-19* enhances the overproliferation phenotype in a temperature-sensitive *glp-1* gain-of-function allele (*ar202*) at the permissive temperature.

(A) The temperature-sensitive *glp-1* gain-of-function allele *ar202* behaves wild-type when it is grown at the permissive temperature of 15°C. Shifting these worms to the restrictive temperature of 25°C leads to the development of a tumorous gonad due to hyperactivation of GLP-1 signaling. (B) While 95% (N=37) of dissected gonads of mock-treated worms contain a wild-type length of proliferative zone at the permissive temperature, 67% (N=43) of dissected gonads from *prp-19*-depleted worms show overproliferation of germline cells at this temperature, which is manifested either by a *pro* (extended proliferation and/or proximal proliferation) or *tum* phenotype. (C) Representative pictures of phenotypes observed in the experiment. Dissected gonads were stained with DAPI for nuclear morphology and anti-HIM-3, a meiotic marker. In mock-treated worms HIM-3 staining coincides with germ cell nuclei transiting into meiosis (white arrow marks the beginning of the transition zone) roughly 15-20 gcd away from the DTC. *Prp-19*-depleted worms that show a tumor phenotype exhibit excess proliferation and proliferative cells away from the niche, which are occasionally intermingled with

meiotic cells (marked with a yellow arrow). * marks the distal end of the germline. Scale bars represent 20 µm.

Knock-down of putative PRP-19/NTC complex members and splicing factors results in nuclear stabilization of GLP-1::GFP.

Prp-19 is the homolog of PRP19, which is the name-giving component of the large protein complex PRP19/NTC. At least in other organisms such as yeast and humans the complex is known to function in a variety of processes including splicing, genome maintenance, transcription elongation and the recruitment of ubiquitinated proteins to the proteasome (Chanarat and Strasser 2013). We therefore wanted to know if the putative function of PRP-19 in GLP-1 turnover is dependent on the complex.
In *C. elegans* the complex has not been as well studied as in other species. Therefore, we first generated a list of homologs based on the yeast, *trypanosoma* and the human counterpart of the complex (Table 4). For the human PRP19/NTC complex, different compositions of the complex have been identified, which largely depend on the particular cellular process the complex is involved in (Makarova, Makarov et al. 2004, Kuraoka, Ito et al. 2008, Fabrizio, Dannenberg et al. 2009, Ambrosio, Badjatia et al. 2015). We reasoned that if PRP-19 functions within the complex to regulated GLP-1 localization, we would also observe nuclear localization upon depletion of putative complex member homologs.
We again knocked-down putative PRP-19 complex members in *glp-1::gfp* worms by RNAi starting at the L1 stage and screened the same generation for nuclear stabilization of GLP-1::GFP in adult dissected gonads. For RNAi clones that resulted in larval arrest, we repeated the experiment placing synchronized L3/L4 larvae on RNAi plates for 48 hrs. For a subset of the tested RNAi clones we saw no phenotype including no changes in GLP-1::GFP localization (*T12A2.7, K04G7.11,* ZK1307.9 Y17G9B.4, *cyn-12)*, even though RNAi-mediated phenotypes have been reported previously (*T12A2.7, K04G7.11, cyn-12)* (wormbase).
For most of the RNAi conditions that resulted in larval arrest (*C50F2.3, cdc-5L, M03F8.3, hsp-1, skp-1*) when worms were grown from a synchronized L1 population, we could observe nuclear GLP-1::GFP with varying penetrance (Table 5 and Figure 18). Especially knock-down of *cdc-5L*, *skp-1* as well as *hsp-1* resulted in nuclear-localized GLP-1::GFP in a large proportion of analyzed gonads (60%, 91% and 78%, respectively), while knock-down of *C50F2.3* resulted only in 17% of analyzed gonads in nuclear localization. Additionally, knock-down of *F53B7.3* as well as *prp-17* and *C07A9.2* resulted in nuclear stabilization of GLP-1::GFP with a penetrance of 80%, 21% and 10%, respectively.

S. cerevisiae	*H.sapiens I*	*H.sapiens II*	*H.sapiens III*	*T. brucei*	*C. elegans*
S.c. Prp19C	PRP19/CDC5L	PRP19-associated	XAB2		
Prp19/Pso4	**PRP19/PSO4/SNEV**		PRP19/PSO4/SNEV	**PRP19**	*prp-19*
Syf1/Ntc90		XAB2/SYF1/HCRN	XAB2/HCRN		*C50F2.3*
Isy1/Ntc30		ISY1/FSAP33	ISY1/FSAP33		*F53B7.3*
Cef1/Ntc85	**CDC5L**			**CDC5**	*cdc-5L*
Prp46/Ntc50	**PRL1/PRP46/CWC1**			**PRL1**	*cpf-1*
Snt309/Ntc25	**SPF27/SNT309/DAM1**			**SPF27**	*T12A2.7*
Cwc15	AD002/CWF15				*T10C6.5**
Clf1/Ntc77/Syf3		SYF3/CRNKL1/CLF			*M03F8.3*
Syf2/Ntc31		SYF2/fSAP29/p29			*K04G7.11*
Cwc2/Ntc40		RBM22/fSAP47/CWC2			*T11G6.8**
Ntc20					
Yju2					*ZK1307.9*
PRP17				PRP17	*prp-17*
		PPIE/CypE/Cyclophilin-33	PPIE/Cyclophilin-33		*Y17G9B.4*
		hAquarius/fSAP164	hAquarius/fSAP164		*emb-4*
			CCDC16/ZNF830		
	CTNNB1 (beta-catenin)				
	HSP73				*hsp-1*
		PRP45/SKIP/SNW1		SKIP	*skp-1*
		G10/CWC14/fSAP17/BUD 31			*C07A9.2*
		CCDC12			*Y69A2AR.21**
		PPIL1/CYPL1		PPIL1	*cyn-12*
		GCIP			

Table 4: PRP19/NTC complex composition in yeast, humans and *trypanosoma*, as well as the respective homologs encoded in the *C. elegans* genome.

Note that in humans three different complexes have been identified, which largely depend on the function executed. Homologs marked with * are not available as RNAi clone in our libraries and were therefore not used in experiments.

PRP19/NTC component	RNAi phenotype (from L1)	GLP-1::GFP localization (from L1)	RNAi phenotype (from L4)	GLP-1 ::GFP localization (from L4)
prp-19	germline morphology defects	**73% nuclear (N=44)**	n.A.	n.A.
C50F2.3	larval arrest	n.A	germline morphology defects	**17% nuclear (N=12)**
F53B7.3	germline morphology defects	**80% nuclear (N=10)**	n.A.	n.A.
cdc-5L	larval arrest	n.A	germline morphology defects	**60% nuclear (N=10)**
cpf-1	emb (80%)	wild-type	n.A.	n.A.
T12A2.7	wild-type	wild-type	n.A.	n.A.
M03F8.3	larval arrest	n.A	germline morphology defects	wild-type-like
K04G7.11	wild-type	wild-type	n.A.	n.A.
ZK1307.9	wild-type	wild-type	n.A.	n.A.
Prp-17	germline morphology defects	**21% nuclear (N=33)**	n.A.	n.A.
Y17G9B.4	wild-type	wild-type	n.A.	n.A.
emb-4	emb (100%)	wild-type	n.A.	n.A.
hsp-1	larval arrest	n.A	germline morphology defects	**78% nuclear (N=9)**
skp-1	larval arrest	n.A	germline morphology defects	**91% nuclear (N=11)**
C07A9.2	germline morphology defects	**10% nuclear (N=10)**	n.A.	n.A.
cyn-12	wild-type	wild-type	n.A.	n.A.

Table 5: Phenotypes and penetrance of nuclear-localized GLP-1::GFP observed in dissected gonads of worms treated with RNAi against putative *C. elegans* Prp-19/NTC complex members.
Worms were either treated from the L1 stage onwards with the respective RNAi or if this resulted in larval arrest from the L3/L4 stage. Nuclear stabilization of GLP-1::GFP was analyzed in dissected gonads and observed with varying penetrance.

Some components of the PRP19/NTC complex were shown not only to be part of the complex but also to participate in specific steps during splicing or to be required for transcription-related events. *Prp-17,* the homolog of one of the complex members in *trypanosoma* was even in *C. elegans* shown to participate in the proliferation - differentiation decision and SKIP, the homolog of *skp-1,* was shown to interact with the intracellular domain of NOTCH (Zhou, Fujimuro et al. 2000).
We tested the involvement of the spliceosome in the nuclear localization of GLP-1::GFP by knocking-down several splicing factors that were shown to be required during different steps in the splicing cascade (Figure 8). Among the tested splicing factors, knock-down of *uaf-1, prp-21, mog-4, mog-5, teg-4* and *prp-8* resulted in nuclear stabilization of GLP-1::GFP with varying penetrance (Table 6 and Figure 18).

Depletion of *mog-1* and *tcer-1* did not show the phenotype. However, *mog-1* (RNAi) worms also did not show masculinization of the germline (Graham and Kimble 1993), making it likely that RNAi did not work.

splicing factor	RNAi phenotype (from L1)	GLP-1::GFP localization (from L1)	RNAi phenotype (from L4)	GLP-1::GFP localization (from L4)
prp-19	germline morphology defects	**73% nuclear (N=44)**	n.A.	n.A.
uaf-1	larval arrest	n.A.	germline morphology defects	**100% nuclear (N=37)**
prp-21	larval arrest	n.A.	germline morphology defects	**93% nuclear (N=28)**
mog-1	wild-type-like	wild-type	n.A.	n.A.
mog-4	larval arrest	n.A.	germline morphology defects	**100% nuclear (N=10)**
mog-5	larval arrest	n.A.	germline morphology defects	**40% nuclear (N=10)**
prp-17	germline morphology defects	**21% nuclear (N=33)**	n.A.	n.A.
teg-4	larval arrest	n.A.	germline morphology defects	**86% nuclear (N=14)**
tcer-1	wild-type	wild-type	n.A.	n.A.
prp-8	larval arrest	n.A.	germline morphology defects	**57% nuclear (N=14)**

Table 6: Phenotypes and penetrance of nuclear-localized GLP-1::GFP observed in dissected gonads of worms treated with RNAi against *C. elegans* splicing factors.
Worms were either treated from the L1 stage onwards with the respective RNAi or if this resulted in larval arrest from the L3/L4 stage. Nuclear stabilization of GLP-1::GFP was analyzed in dissected gonads and observed with varying penetrance.

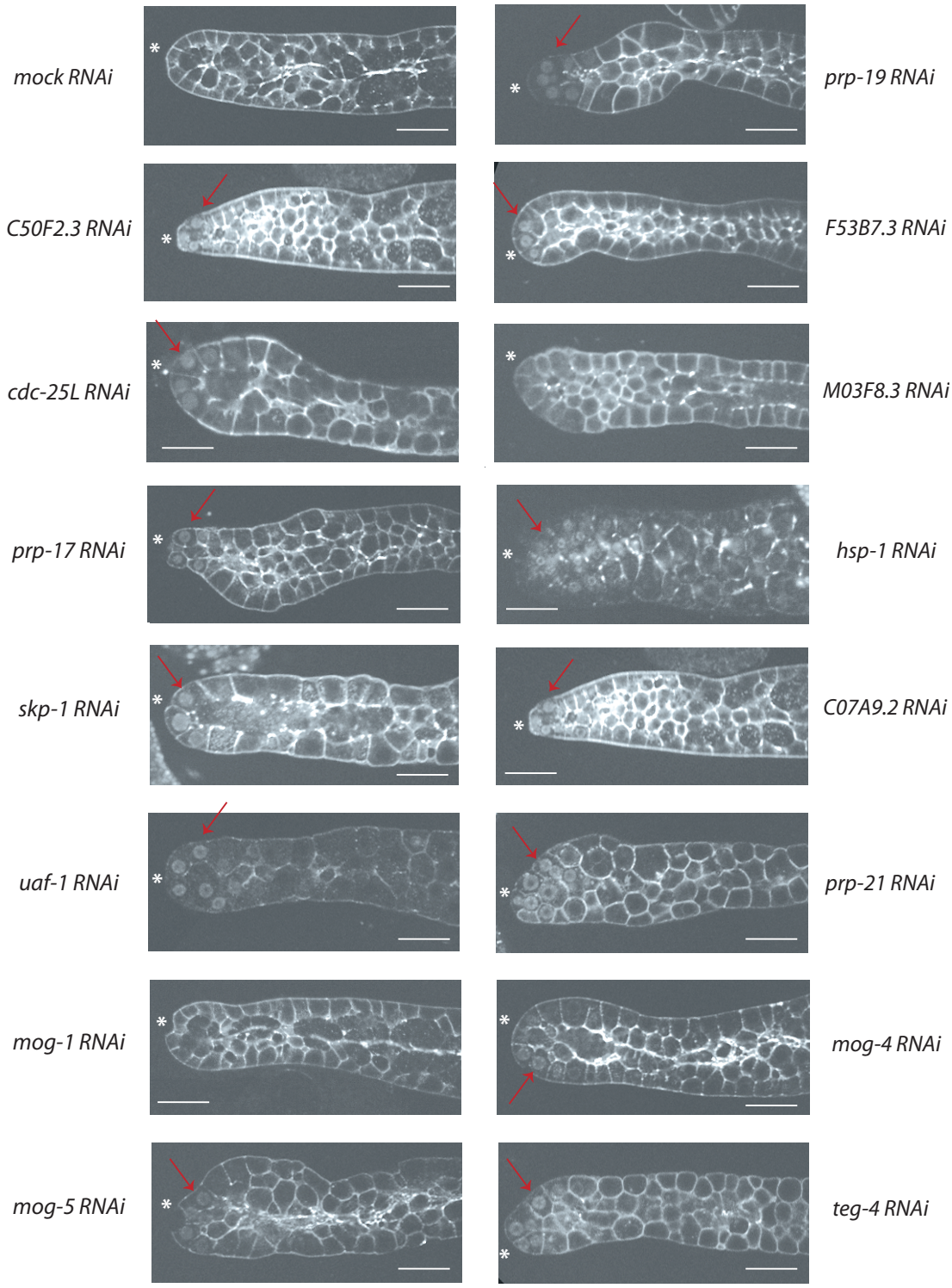

Figure 18: Nuclear stabilization of GLP-1::GFP upon knock-down of putative *C. elegans* PRP19/NTC complex members and splicing factors.

Shown are representative confocal images of dissected gonads treated with the indicated RNAi. For penetrance of the phenotype see Table 5 and Table 6. Similar to *prp-19*-depleted *glp-1::gfp* worms, RNAi-mediated knock-down of several putative *C. elegans* PRP-19/NTC members and splicing factors resulted in nuclear stabilization of GLP-1::GFP. Red arrows point to nuclear-localized GLP-1::GFP.

* marks the distal end of gonads. Scale bars represent 20 µm.

The abundance of PRP-19 is altered upon knock-down of splicing factors and putative *C. elegans* PRP-19/NTC complex members.

One possibility that would explain why the knock-down of splicing factors and putative PRP-19 complex members resulted in nuclear stabilization of GLP-1::GFP is that PRP-19 localization and/or abundance is dependent on the integrity of the splicing machinery and/or the integrity of the putative PRP-19 complex. To test both hypotheses, we treated *prp-19::Strep* worms with RNAi against *uaf-1, prp-21*, *prp-17* and *skp-1* and assessed PRP-19 localization and abundance by anti-Strep immuno-stainings in dissected gonads as done before. As expected, the Strep-staining was nicely visible in all germline nuclei in mock-treated worms and was almost entirely gone when we depleted *prp-19*. In worms depleted for the proteasomal component *pbs-5,* PRP-19::Strep was also detectable in all germ cell nuclei at a level comparable to mock-treated worms. However, depletion of *skp-1, prp-21* and *uaf-1* decreased PRP-19::Strep abundance, while wild-type-like PRP-19::Strep was retained when *prp-17* was depleted (Figure 19).

It is possible that the decrease of PRP-19 under this RNAi conditions fosters nuclear stabilization of GLP-1::GFP and implicates that the abundance of PRP-19 might be dependent on at least one putative PRP-19 complex member and the splicing machinery.
However, since at this point we do not know the composition of the PRP-19 complex in *C. elegans,* we can only speculate how the tested putative members are involved in the regulation of GLP-1 localization (see discussion). One possibility is that they are indeed part of the complex also in *C. elegans* and the disruption of the complex changes the integrity of PRP-19 and thereby its function in regulating GLP-1 localization. Since we only looked at changes in PRP-19::Strep localization in the absence of the two putative complex members *skp-1* and *prp-17*, which both were shown to function also independent of the complex, we cannot answer at this point whether PRP-19 functions within or independent of the complex to regulate GLP-1 localization.
Even though we do not see a decrease of PRP-19::Strep abundance in *prp-17*-depleted worms, the activity of PRP-19 and not its abundance might be dependent on PRP-17 to a certain extent, since we see GLP-1 localized to distal germline nuclei in some *prp-17*-depleted *glp-1::gfp* worms (Figure 18). Additionally, the change in PRP-19::Strep abundance in gonads of splicing-factor-depleted worms might again be a result of the multiple interplays between the splicing machinery and the PRP19/NTC, and the integrity of the spliceosome might be required for the integrity of the PRP19 complex. SKIP, the homolog of SKP-1, was not only shown to be part of the splicing machinery,

but also to be part of the Notch co-activator and co-repressor complex and may be involved in targeting the NICD co-transcriptionally for degradation (Fryer, White et al. 2004). Whether *skp-1* knock-down indirectly leads to nuclear stabilization of GLP-1 by changing the abundance of PRP-19 or the nuclear localization of GLP-1 in the absence of SKP-1 is a result of SKP-1 not recruiting protein modifiers to the NICD for turnover, we don't know at this point. However, the latter still might be dependent on recruitment of PRP-19 to the NICD (see discussion).

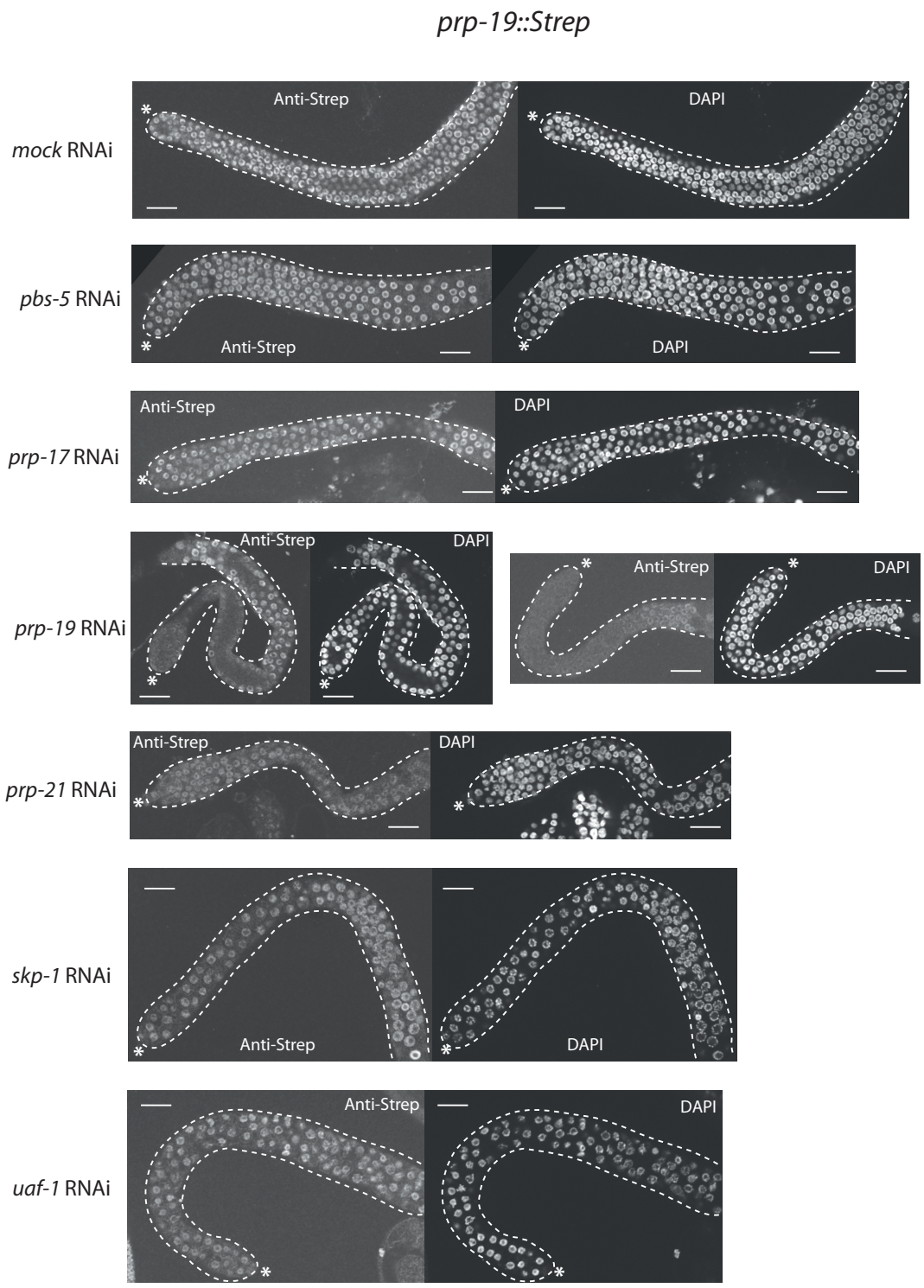

Figure 19: PRP-19 abundance changes in worms depleted for putative PRP19/NTC complex members and depleted for *C. elegans* splicing factors.

Shown are representative confocal images of dissected gonads stained with anti-Strep Chromeo 546 (IBA life sciences) and DAPI. A Strep-staining is visible in all germline nuclei of mock-treated worms. No staining is visible for worms depleted for *prp-19* and stainings are decreased in worms treated with *skp-1, hsp-1, uaf-1* and *prp-21* RNAi. Germlines of *pbs-5*- and *prp-17*-depleted worms show staining intensities similar to mock-treated worms. All images are surface views of dissected gonads. * marks the distal end of gonads. Scale bars represent 20 µm.

4. Discussion

Dynamic regulation of GLP-1 in the *C. elegans* germline

Though the Notch pathway is well studied in *C. elegans* and the function of GLP-1 in the germline as master regulator of the decision proliferation versus differentiation is well established, many aspects of the signaling pathway were and are still unclear. For example, when I started my PhD project it was still unclear what the germline targets of GLP-1 that are required for the maintenance of the germline stem cell pool are. A question that had been resolved recently with the finding of the two redundant targets *lst-1* and *sygl-1* that account for the function of *glp-1* in promoting proliferation (Kershner, Shin et al. 2014). Also, it was not clear how GLP-1 signaling is restricted to the distal-most region of the germline, where activation of Notch-dependent gene expression can happen and how the signaling response is tuned down again. Interestingly, transcriptional activation of GLP-1 targets was shown to occur away from the niche, this was observed for the Notch target *lip-1* (Hajnal and Berset 2002). In accordance, we observed that *utx-1*, a target of GLP-1 in the germline, is only weakly expressed closest to the signal initiating stem cell niche and strongly expressed when germ cells start to differentiate (see Appendix, Figure 20). This initially prompted us to investigate the dynamics of GLP-1-dependent activation of gene expression.

For this purpose, we generated a GFP knock-in by CRISPR-mediated genome editing within the intracellular part of GLP-1 in order to follow the activated form within the germline and particularly within germline nuclei. Despite the fact that GLP-1 is well studied, a functional fluorescently tagged transgene was never successfully generated. With the generation of the GFP knock-in we were for the first time able to visualize GLP-1 in live animals. *Glp-1::gfp* worms are viable and behave superficially wild-type. However, we noticed a reduction of viable progeny in those worms compared to wild-type worms (Figure 9). The GFP knock-in within the *glp-1* locus might cause a reduction-of-function of *glp-1*. It is unlikely that the germline function is reduced since we see a normal extend of proliferative zone in *glp-1::gfp* worms (data not shown). The differences in viable progeny of *glp-1::gfp* worms compared to wild-type worms might be due to a reduction-of-function in the GLP-1-mediated cell fate decision of the embryo since we occasionally observed the presence of arrested early embryos in OP50-grown worms and especially during mock RNAi treatments. Why we observe this more often in RNAi-treated worms, we don't know (see below for another RNAi-related observation). The GFP knock-in of *glp-1::gfp* worms is located in the C-terminal part of the NICD, upstream of the PEST domain. Similar to this, a C-terminal truncation of GLP-1 found in the *glp-1* allele *q35* causes a *glp-1* loss-of-function phenotype (sterility and embryonic lethality) (Mango, Maine et al. 1991). It is therefore possible that GFP at the C-terminus mimics the loss of the C-terminal part

to a certain extend and GFP might interfere with motives/domains within C-terminal GLP-1 that are required for its regulation in the embryo. Since we were mainly interested in the germline dynamics of GLP-1 signaling, we did not follow up these observations, also because the germline expression pattern we observed was in agreement with antibody stainings on dissected gonads (Crittenden, Troemel et al. 1994). As previously reported we could detect a strong signal for GLP-1::GFP on the membranes of the distal-most germline, which gets weaker in regions where germ cells start to transit into meiosis. Also consistent with previous reports we were not able to detect the nuclear form in adult germlines, but detected it in larval stages (Figure 9 and Figure 10).

One explanation for the observed differences of GLP-1::GFP localization and presumably activation could be differences in the length of the mitotic cell cycle between the adult hermaphrodite germline (16-24 hrs or around 8 hrs depending on the study) and during the proliferative phase of germline development (around 4 hrs) (Kipreos, Lander et al. 1996, Crittenden, Leonhard et al. 2006, Fox, Vought et al. 2011). However, the length of the mitotic cell cycle also differs between male and hermaphrodite germline, whereby males have a substantially shorter or comparable cell cycle of around 10 hrs depending on the study to compare with (Morgan, Crittenden et al. 2010). When we looked at GLP-1::GFP localization in adult male germlines we could also not detect a nuclear signal, making it unlikely that cell cycle length governs the stability. On the contrary, more intuitive is a scenario where a fast cell cycle requires a faster turnover of the NICD. It was already shown in mammals that the turnover of the NICD is mediated by CycC::Cdk8-dependent phosphorylation (Fryer, White et al. 2004). Cdk8 itself was implicated in regulation of the G1- to S-Phase progression and also G2- to M-phase and mitotic progression (Szilagyi and Gustafsson 2013). This might therefore constitute a link between cell cycle progression and transcriptional output generated by the Notch pathway. Additionally, for LIN-12 in the *C. elegans* vulva, it was shown that degradation of the NICD is linked to cell cycle progression. While the G1 cyclins CYD-1 and CYE-1 were shown to stabilize LIN-12-ICD, the G2 cyclin CYB-3 promotes its degradation (Nusser-Stein, Beyer et al. 2012). When we depleted several factors that are involved in the cell cycle by RNAi (*cdk-1, cdk-2, cdk-9, cdk-7, wee-1.3, cyb-1, cyb-2.1, cyb-2.2, cyb-3*) we could not see changes in GLP-1 localization in the adult (data not shown).

The differences we see in the nuclear stability of GLP-1 between larvae and adults might depend on different requirements of the developing and adult gonad in the dosage of expression of Notch-dependent genes. The developing gonad is still expanding its stem cell pool and rapidly growing and might therefore simply be dependent on a higher expression level of Notch targets, while the adult germline somewhat remains in a steady-state level regarding the stem cell pool. This

explanation is not completely speculative since there are examples, where differences in the levels of Notch target gene expression were shown to be decisive for the outcome of developmental processes. It was, for example, shown that pancreatic progenitors in the zebrafish intrapancreatic duct remain quiescent when Notch levels are high and their amplification is induced when Notch signaling levels remain low (Ninov, Borius et al. 2012).

Two possibilities on the mechanistic level arise from the observed differences in larval and adult GLP-1 signaling.
Either very little GLP-1 gets activated at the membranes in the adult worm and translocates into the nucleus or activated nuclear GLP-1 is readily turned over.
The lack of a nuclear signal for the activated receptor in adult germline in our *glp-1::gfp* worms and in previous antibody stainings is somewhat surprising, though not uncommon to the pathway. Several other studies reported difficulties in the detection of the nuclear form and it was suggested that the levels of activated Notch are simply too low to be detected since target gene expression is occurring nevertheless (Schroeter, Kisslinger et al. 1998). Even though we cannot visualize the nuclear form of GLP-1 in the adult, several observations implicate that its nuclear translocation is required also in the adult germline to generate a signaling output. First of all, the two key germline GLP-1 targets *lst-1* and *sygl-1* were shown to be expressed in the adult germline and at least for *sygl-1* this was shown to depend on the presence of LBSs within the promoter (Kershner, Shin et al. 2014, Lee, Sorensen et al. 2016). Similar to this, we could show that expression of *utx-1* in the adult germline is dependent on GLP-1 and on LBSs within the promoter (Seelk, Adrian-Kalchhauser et al. 2016) (Figure 22).

To test our hypothesis of rapid turnover or differences in signaling initiation on membranes, we depleted components of the ubiquitin-proteasome-system (UPS), the key machinery utilized for targeted protein turnover. Indeed knock-down of the only E1 ligase encoded in the *C. elegans* genome (*uba-1*) and the proteasome subunit *pbs-5* resulted in nuclear localization of GLP-1::GFP with close to full penetrance (Figure 11A). We did not only observe accumulation of the nuclear form, but also an accumulation of GLP-1::GFP on internal membrane-structures in the gonad, while GLP-1::GFP was reduced on membranes surrounding the gonad upon *pbs-5* and to a lesser extend upon *uba-1* depletion (Figure 11). It is therefore possible that the UPS, as shown for Notch in other organisms, does not only regulate the stability of activated nuclear GLP-1, but also the abundance of the full-length receptor on the cell surface and might be involved in receptor trafficking and recycling of GLP-1. The accumulation of the nuclear form of GLP-1::GFP upon *pbs-5* and *uba-1* depletion implicates that the

stability of the activated form of GLP-1 might be regulated by the UPS. At this point we do not know how the differences in GLP-1::GFP localization between larval stages and the adult arise.

It is still likely that a combination of reduced ligand-induced activation of the receptor on the cell surface in adults and changes in the dynamics of nuclear turnover generates the observed differences between adult and larval gonads. We do not only see a stronger nuclear signal for GLP-1::GFP in larvae, but also an accumulation of presumably the full-length receptor at internal membrane structures (Figure 10B), similar to the observation of an accumulation of full-length receptor upon depletion of *pbs-5* in adult *glp-1::gfp* worms. This supports the above-mentioned hypothesis that the GLP-1 receptor, as seen for other Notch receptors (Bray 2006), is extensively sorted.

In agreement with the observed enrichment of nuclear GLP-1::GFP and the full-length receptor on internal membranes of the gonad in *pbs-5*-depleted *glp-1::gfp* worms, we saw an enrichment of both forms in protein extracts derived from *pbs-5*-RNAi-treated *glp-1::gfp* worms by western blot (Figure 11C). In immunoprecipitations we were then able to enrich for the nuclear form of GLP-1::GFP and to detect a signal for ubiquitin (Figure 11B-D).

The nuclear stabilization of GLP-1::GFP upon depletion of factors mediating protein degradation within the UPS (Figure 11A) together with the accumulation of the nuclear form of GLP-1::GFP in western blots of whole protein extracts upon knock-down of *pbs-5* (Figure 11C), the selective enrichment of the NICD by immunoprecipitations (Figure 11B and C,

Table **3**) and the detection of a ubiquitin signal in immunoprecipitated GLP-1::GFP within the same sample (Figure 11D) brought us to the conclusion that the activated and nuclear GLP-1 is dynamically regulated by the UPS.

When we performed western blots on immunoprecipitated GLP-1::GFP we noticed a reproducible size difference of the presumed nuclear form between protein extracts generated from *glp-1::gfp* worms grown on OP50 and RNAi bacteria.

This could implicate that GLP-1 is differently processed depending on the growth condition and to our knowledge this has not been reported before. There are several possibilities that might cause these differences. One possibility is that the type of bacteria used for RNAi changes the processing of the GLP-1 receptor. To test this, we grew *glp-1::gfp* worms on OP50 and NA22, which are both commonly used to grow *C. elegans*, as well as on HT115, which is used in RNAi feeding experiments, and DA837. Immunoprecipitated GLP-1::GFP was running at the same molecular weight independent of the bacteria used (Figure 13). Due to time constraints we did not

further follow up on this peculiarity, the following explanations therefore remain purely speculative.

Another possibility for the observed size differences is changes in GLP-1 processing due to the antibiotics (Carbenicillin and Tetracycline) and IPTG used on RNAi plates. Indeed, it was shown that Tetracycline inhibits the function of certain types of metalloproteinases (Pasternak and Aspenberg 2009). The full-length Notch receptor is known to be cleaved at three specific sites - S1, S2 and S3. The two cleavage reactions at the S2 and S3 site are ligand-induced and were shown to free the NICD from the membranes to allow for nuclear translocation (Bray 2006). Evidence from mammalian studies revealed a ligand-independent cleavage at the S1 site, yet again located within the HD domain (Lake, Grimm et al. 2009). This cleavage is thought to contribute to maturation of the protein and to lead to a heterodimeric form of the receptor that is presented at the cell-surface (Blaumueller, Qi et al. 1997, Logeat, Bessia et al. 1998).

Even though the position of S1 and S2 cleavage sites within GLP-1 are not well annotated, they are likely also occurring somewhere within the HD domain (Brou, Logeat et al. 2000). The size observed for GLP-1::GFP in RNAi-treated worms, hence worms subjected to Tetracycline, is in agreement with a protein fragment spanning from the HD-domain until the C-terminus. This would imply that S2 cleavage is not happening and the GLP-1 receptor is activated independently of S3 cleavage on membranes but still requires a ligand interaction.

A third hypothesis for differences in protein sizes is that triggering the RNAi pathway itself changes processing of the receptor. The RNAi pathway in *C. elegans* involves the function of *ego-1* (**e**nhancer **o**f ***g****lp-1*), a RNA-dependent RNA polymerase, which is required for the amplification of small RNAs. *Ego-1* was previously shown to function in the germline in parallel with *glp-1* to promote proliferation and/or inhibit meiotic entry (Qiao, Lissemore et al. 1995, Vought, Ohmachi et al. 2005). In the absence of *ego-1* GLP-1 localizes normally on the membranes on the surface of gonads in antibody stainings against the LNG repeats of GLP-1, though an increase of internalized GLP-1 is observed, indicating that the trafficking of the full-length receptor might be altered (Vought, Ohmachi et al. 2005). However, to what extend RNAi directly influences Notch receptor-processing, remains unclear.

Early studies in Drosophila suggested an involvement of the proteasome in the degradation of the NICD. Expression of a dominant-negative mutant version of the beta6 subunit of the proteasome was shown to lead to the stabilization of an ectopically expressed nuclear form of Notch (Schweisguth 1999). Following this observation, several E3 ligases were shown to be involved in Notch turnover, and in particular FBXW7 was shown to mediate Notch turnover in the nucleus (Gupta-Rossi,

Le Bail et al. 2001, Oberg, Li et al. 2001, Wu, Lyapina et al. 2001, Tetzlaff, Yu et al. 2004, Matsumoto, Onoyama et al. 2011). For the GLP-1-mediated cell fate decision in the germline the involvement of the *C. elegans* homolog of FBXW7, SEL-10, remains unclear.

Several observations suggested that GLP-1 is degraded by different means in the *C. elegans* germline. For example, mutations in *sel-10* fail to suppress the germline proliferation defects of two temperature-sensitive *glp-1* loss-of-function alleles (*e2144* and *q231*) (Sundaram and Greenwald 1993). In accordance with these findings, we do not see nuclear stabilization of GLP-1::GFP upon knock-down of *sel-10* in dissected gonads. The mammalian homolog of SEL-10, FBXW7, is part of a multimeric cullin-based E3 ligase complex, which is amongst other proteins constituted by CUL-1 and RBX-1 (Krek 1998, Tsunematsu, Nakayama et al. 2004). Consistently, we did also not observe nuclear GLP-1::GFP in worms depleted for those two factors (Figure 14B). The absence of a nuclear signal in *rbx-1*-depleted worms, which is one of the common adaptors of multimeric cullin-based E3 ligase complexes, made it unlikely that GLP-1 localization is regulated by any other cullin-family member. In agreement with this, when we knocked down *cul-1,-2,-3,-4,-5* and *-6* we did not observe nuclear localization of GLP-1::GFP. Additionally, as expected from earlier findings, where inactivation of the gene coding for the second common adaptor for cullin-based complexes *rbx-2* was shown to cause no apparent defects, we did not observe GLP-1::GFP stabilization upon knock-down of *rbx-2* and no apparent phenotype (Moore and Boyd 2004) (Figure 14B). Additionally, it was recently suggested that SEL-10 might function redundantly with the HECT-type E3 ligase UBR-5 to coordinate GLP-1 turnover. However, we did not see nuclear stabilization of GLP-1::GFP in neither *ubr-5*-depleted nor in double knock-down against *sel-10* and *ubr-5*. These observations suggested that activated GLP-1 is likely turned over by a monomeric E3 ligase in the germline.

When we then screened candidate E3 ligases by RNAi against genes containing domains that are typically present in monomeric E3 ligases and that are germline-expressed, we identified the U-box domain-containing E3 ligase PRP-19 as putative regulator of GLP-1-ICD turnover (Figure 15A). However, we did not observe nuclear-localized GLP-1::GFP in all analyzed gonads. It is possible that RNAi is not completely penetrant or that a second redundant factor exists that functions together with PRP-19. Double RNAi of *prp-19 sel-10*, *prp-19 rbx-1* and *prp-19 cul-1* to *cul-6* showed no enhancement of the penetrance we observed in *prp-19* RNAi treatments. It is therefore unlikely that PRP-19 functions together with a multimeric cullin-based E3 complex in general and in particular with a SEL-10-based complex (data not shown). It still remains possible that PRP-19 functions together with any other monomeric E3 ligase.

The screening strategy we applied might have missed factors that are equally important, since for a large subset of screened genes we did not sequence the RNAi clone prior to use. Additionally, we filtered the list of putative E3 ligases for germline-expressed genes (Scheckel, Gaidatzis et al. 2012, Gupta, Leahul et al. 2015), making it possible that we used too stringent cut-offs and left out very lowly expressed genes.
Since the PRP19/NTC complex is only very little studied in *C. elegans* and was proposed to fulfill nuclear as well as cytoplasmic functions (Chanarat and Strasser 2013), we wanted to understand where PRP-19 localizes within germline cells. In agreement with a putative function in the turnover of the nuclear form of GLP-1, we see PRP-19::Strep expression in germline nuclei (Figure 15B and C). We then aimed to confirm an interaction by performing co-immunoprecipitations on *prp-19::Strep glp-1::gfp* worms. However, attempts to co-immunoprecipitate GLP-1 and PRP-19 by either using Strep-Tactin beads (IBA life sciences) or GFP-IPs, as done with *glp-1::gfp worms*, did not work due to technical problems, including the detection of the Strep-tag in western blots.
The finding that depletion of *prp-19* causes nuclear stabilization of GLP-1::GFP, the fact that PRP-19 contains a U-box domain and is located within the nucleus of germline cells in *C. elegans* and the finding that PRP19 at least in human cells was shown to ubiquitinate proteins (Song, Werner et al. 2010), prompted us to propose that *prp-19* in *C. elegans* is involved in the turnover of the GLP-1-ICD and might thereby act as E3 ubiquitin ligase on the GLP-1-ICD.

In agreement with a function of *prp-19* as a negative regulator of the activated form of GLP-1, we could see suppression of a temperature-sensitive *glp-1* loss-of-function allele (*e2144*) and enhancement of a temperature-sensitive *glp-1* gain-of-function allele (*ar202*) when we depleted *prp-19* by RNAi (Figure 16 and Figure 17). The latter was particularly observed already at the permissive temperature.

PRP-19 homologs were in various organisms shown to be part of a multisubunit complex that is dynamically associating with different co-factors termed PRP19-associated proteins depending on the particular function it executes. The Prp19/NTC complex can in that way be seen as a hub that bridges and integrates various proteins depending on the specific context in a dynamic fashion to fulfill a multitude of cellular functions (Chanarat and Strasser 2013).
To understand if the putative PRP-19 complex in *C. elegans* that we deduced from homologs in other organisms (Table 4) is required to regulate GLP-1 localization, we knocked-down candidate homologs by RNAi and again screened for GLP-1::GFP localization. Indeed, we could observe nuclear-localized GLP-1::GFP in worms

depleted for *C50F2.3, F53B7.3, cdc-5L*, *prp-17*, *hsp-1* and *skp-1* with varying penetrance. Several possibilities arise from these observations.

First, the stability of PRP-19 is dependent on the integrity of the complex. That would mean that the nuclear localization we observe upon knock-down of putative complex members arises due to a decrease of PRP-19. This was for example shown for the BRCA1–Rap80 complex, a complex required for DNA double-strand break recognition, and the SAGA chromatin remodeling complex. The integrity of the former was demonstrated to be dependent on the subunit MERIT40 (Shao, Patterson-Fortin et al. 2009). Similarly, the integrity of SAGA depends on the presence of distinct components of the complex (Sterner, Grant et al. 1999).
Second, some subunits of the PRP19 complex were shown to function in a multitude of cellular processes. Especially SKIP is a versatile protein that functions in splicing but also co-transcriptionally for example as part of the Notch co-repressor and the co-activator complex (Zhou, Fujimuro et al. 2000, Makarov, Makarova et al. 2002, Bres, Gomes et al. 2005, Wang, Wu et al. 2012). Moreover, PRP-17 was shown to be a splicing factor (Sapra, Khandelia et al. 2008). From several biochemical as well as genetic interaction studies it is known that PRP-19 is associated with components of the spliceosome (for example RSR-*2*) also in *C. elegans* (Fontrodona, Porta-de-la-Riva et al. 2013, Shiimori, Inoue et al. 2013). Additionally, the PRP19 complex as a whole was also shown to dynamically associate with the splicing machinery on various steps in the splicing cascade (Figure 8) (Hogg, McGrail et al. 2010, de Almeida and O'Keefe 2015). It might therefore be possible that GLP-1::GFP localization upon *prp-19* knock-down results from the disruption of the splicing machinery.
Indeed, upon knock-down of several splicing factors we observed nuclear localization of GLP-1::GFP (Figure 18) with varying penetrance. This could either mean that splicing directly effects GLP-1 localization or the stability of the PRP-19 complex and possibly PRP-19 itself depends on the integrity of the spliceosome (so the opposite as stated above).
To answer if the abundance of PRP-19 changes upon knock-down of putative PRP-19 complex members - so to answer the first hypothesis stated above - and to answer if the abundance of PRP-19 depends on splicing factors and/or the integrity of the splicing machinery, we used *prp-19::Strep* worms to assess PRP-19 levels in dissected gonads upon depletion of candidate genes among the complex members and splicing factors. This initial list was mainly chosen depending on the penetrance of nuclear-localized GLP-1::GFP (two high: *prp-21* and *uaf-1*, one low: *prp-17)* and *skp-1* was added because of its known association with Notch in other organisms.

The observed decrease in anti-Strep staining in *uaf-1*-, *prp-21*- or *skp-1*-depleted *prp-19::Strep* worms together with the unchanged levels of PRP-19 in *prp-17*-depleted worms again allow for several explanations.

In contrast to PRP-17, which was shown to be part of the PRP19 complex and a splicing factor, UAF-1 and PRP-21 are "only" splicing factors (or at least shown to be) (Zahler 2012). The decrease of PRP-19 abundance might therefore result from a disruption of the splicing machinery that feeds back on either PRP-19 or the PRP-19 complex and the nuclear localization of GLP-1::GFP reflects a decrease in PRP-19 protein levels.
PRP-17 on the other hand, if it is indeed part of the PRP-19 complex, might predominantly function as part of the PRP-19 complex. Depletion of *prp-17* does not result in a decrease of PRP-19 abundance.
In this scenario, either *prp-17* depletion is not sufficient to disrupt the complex and thereby does not perturb PRP-19 stability or PRP-19 is also functioning without the complex and disruption of the complex therefore does not change the abundance of PRP-19.
Alternatively, PRP-17 might partially influence the activity of PRP-19 within or outside the complex resulting in the low penetrance of observed nuclear GLP-::GFP upon depletion of *prp-17.*
However, if PRP-17 is not part of the PRP-19 complex in *C. elegans*, the integrity of the PRP-19 complex might depend on splicing factors early in the splicing cycle (PRP-21 and UAF-1) and the activity of PRP-19 might be partially influenced by later steps in the splicing cascade. To test this hypothesis, we would need to look at PRP-19 abundance upon depletion of several additional splicing factors during the different steps in splicing.
Another possibility is that the co-transcriptional assembly of the spliceosome at the RNA polymerase somehow feeds back on the transcription factor that initiated transcription. Therefore, turnover of GLP-1 might ultimately not only be linked to the initiation of gene expression as shown before (Fryer, White et al. 2004), but also be dependent on the proper execution of events necessary for faithful mRNA production.
One of the putative PRP-19 complex members was shown to participate in transcription-related processes. SKIP, the homolog of SKP-1, was as mentioned above shown to interact with the intracellular domain of NOTCH (Zhou, Fujimuro et al. 2000). Since we do not know whether SKP-1 is associating with the PRP-19 complex in *C. elegans* one possibility for the observed stabilization of GLP-1::GFP in *skp-1*-depleted *glp-1::gfp* worms is that SKIP is indeed associating with the NICD itself to regulate turnover. This in turn might or might not be dependent on spliceosome formation and PRP-19. At least in one case SKIP was shown to coordinate transcription and splicing and this was shown to involve PRP19. SKIP is thought to selectively recruit U2AF65

(*uaf-1*) to the p21/Cip gene and mRNA. This process selectively requires PRP19 and DHX8 (Chen, Zhang et al. 2011). In *C. elegans* there is also at least one example that links PRP-19 with transcription and splicing. RSR-2, the homolog of the human splicing factor SRm300 was shown to be recruited to chromatin to interact with RNA Polymerase II and to influence the phosphorylation state of the CTD of the Polymerase. PRP-19 and PRP-8 were further demonstrated to be interaction partners of RSR-2 (Fontrodona, Porta-de-la-Riva et al. 2013).

The described scenarios are highly speculative. To understand whether or not PRP-19 functions as a E3 ligase on the GLP-1-ICD independent of the PRP-19 complex and how the observed nuclear localization of GLP-1::GFP is linked to splicing, if at all, needs careful and detailed investigations of the function of the PRP-19 complex in the *C. elegans* germline and the identification of PRP-19 complex members in *C. elegans*.

However, we can conclude that GLP-1 is dynamically regulated in the *C. elegans* germline and the regulation of GLP-1 signaling initiation and/or the turnover of the NICD differ between the larval and the adult germline. Furthermore, the stability of the GLP-1-ICD is regulated by the UPS. This might involve directly or indirectly the E3 ligase PRP-19.

5. Appendix

GLP-1 signaling antagonizes PRC2-mediated silencing

Introduction

GLP-1 signaling is well established as the master regulator of the decision proliferation versus differentiation in the *C. elegans* germline and was shown to mainly promote proliferation in this system. However, similarly to the situation in other types of stem cells that depend on Notch signaling (Liu, Sato et al. 2010), GLP-1 target genes in the germline were largely unknown at the time I started my PhD project.

To understand how GLP-1 affects gene expression in the germline Balazs Hargitai and Irene Adrian-Kalchhauser analyzed transcript abundance in germ cells with either active or inactive GLP-1 signaling. Using microarray analysis, they identified around 100 genes that are activated by GLP-1 signaling in the germline. Surprisingly, these Notch-activated genes were strikingly enriched on the sex (X) chromosome (Seelk, Adrian-Kalchhauser et al. 2016). This chromosome bias was unexpected as X-linked genes are largely silenced in the germline. The X chromosome silencing in the germline depends on MES (Maternal Effect Sterile) proteins (Fong, Bender et al. 2002, Kelly, Schaner et al. 2002). The MES-2 (Enhancer of zeste), MES-3 (novel), and MES-6 (Extra sex combs) proteins constitute the *C. elegans* counterpart of the Polycomb Repressive Complex 2 (PRC2), which contributes to repressive chromatin formation via histone H3 lysine 27 methylation (Bender, Cao et al. 2004). Another *mes* gene, *mes-4*, was shown to also contribute to X chromosome silencing in the germline largely by concentrating the PRC2 on the X (Bender, Suh et al. 2006, Gaydos, Rechtsteiner et al. 2012).
Again by microarray analysis on dissected gonads from *mes-2* and *mes-6* mutants Balazs Hargitai and Irene Adrian-Kalchhauser identified PRC2-repressed genes in the germline and found a striking overlap with GLP-1-activated genes, particularly of genes linked to the X chromosome. Nearly all of the X-linked GLP-1-activated genes were de-repressed upon the loss of PRC2 (Seelk, Adrian-Kalchhauser et al. 2016). Taken together, these findings suggested that GLP-1 is signaling to chromatin by changing the epigenetic landscape. How this works on a mechanistic level remains unclear.

Results and discussion

When I joined the project, we speculated that sequence features in the promoter regions of PRC2- and GLP-1-co-regulated genes are required to mediate the antagonistic regulation. We first looked at expression patterns of one PRC2- and GLP-1-co-regulated gene (*utx-1*) in the germline by expressing GFP-Histone-H2B from the respective promoter and controlled by an unregulated 3 `UTR (*tbb-2*), which we constructed by MosSCI (Frokjaer-Jensen, Davis et al. 2008).
Consistent with the expression patterns of the endogenous *utx-1* (Vandamme, Lettier et al. 2012) and of a GFP-fused functional *utx-1* transgene, the *utx-1* reporter was weakly expressed in the distal-most, proliferative part of the germline (Figure 20A and B). With progression through meiosis the reporter expression increased towards the proximal end of the gonad. The weak expression of *utx-1* in the distal-most gonad was somewhat surprising since GLP-1 is thought to function mostly in the stem cells. However, a similar expression pattern has been reported for another GLP-1 target gene, *lip-1* (Hajnal and Berset 2002, Lee, Hook et al. 2006). Consistent with the up-regulation of *utx-1* in microarrays on dissected gonads of *mes-2* and *mes-6* mutants, we observed up-regulation of the *utx-1* reporter upon RNAi against *mes-2, mes-3* and *mes-6* as well as against *mes-4* (Figure 20C).
In agreement with *utx-1* as a putative GLP-1 target gene, we detected very strong up-regulation of the *utx-1* reporter in the *glp-1* gain-of-function *(ar202)* background when these worms were raised at the restrictive temperature (Figure 20C). Taken together this confirmed that *utx-1* is co-regulated by the PRC2 and GLP-1 in the germline.

To study the sequence requirements of the dual regulation, we annotated published putative LAG-1 binding sites in the promoter region of *utx-1*. LAG-1 is the transcriptional co-activator of GLP-1 and is thought to mediate Notch target gene expression by binding to gene regulatory regions and recruiting the transcriptional machinery (Christensen, Kodoyianni et al. 1996, Wilson and Kovall 2006). Several binding sites for LAG-1 have been suggested so far: LBS (YRTGRGAA), GM1 (Greenwald Motif 1) (RTGMGCCTYYR) and GM2 (Greenwald Motif 2) (CYTCMYCCW) (Yoo, Bais et al. 2004). The *utx-1* promoter contains two LBSs within its 5`UTR and one LBS at the 5`-most region of the promoter as well as one GM1 and one GM2 site (Figure 21A).
Little is known about the binding requirements of the PRC2 in *C. elegans*. In *Drosophila* it was shown that Polycomb is recruited to DNA via Polycomb responsive elements, though the sequence requirements are not very well defined (Kassis and Brown 2013). We reasoned that sequences important for regulatory mechanism are well conserved over species. By sequence comparison with other closely related nematode species (*Pristionchus pacificus, C. remanei, C. japonica, C. briggsae, C. brenneri*) Balazs Hargitai

identified 5 additional conserved regions within the *utx-1* promoter, which we termed Motif 1-5 (M1-M5, Figure 21A) (for details see Materials and Methods). We then constructed several transcriptional reporter strains that drive GFP-Histone-H2B from different versions of the *utx-1* promoter, which were either mutated at one or more LBSs and/or lacking parts of the promoter that contained the respective conserved sequences (Figure 21A).
We hypothesized that removal of *utx-1* promoter regions that are required for GLP-1-dependent activation would lead to down-regulation of expression in untreated worms and would not make the reporter responsive to *glp-1* hyperactivation in the *glp-1* gain-of-function *(ar202)* background. Similar to this, we reasoned that removal of sequences required for PRC2-mediated silencing would lead to an up-regulation of the reporter in a wild-type background or at least render the reporter non-responsive to perturbations of the PRC2 complex.

All seven different versions of the *utx-1* transcriptional reporter were constructed with the gateway system and single-copy-integrated by MosSCI in Chromosome II with the help of Balazs Hargitai. Most of the constructed reporters showed a very high variability in expression pattern and intensity in the germline. One caveat of reporter analysis in the germline is the frequent occurrence of transgene silencing. This makes it difficult to interpret results. For most of the constructed reporters we could not observe consistent expression behavior neither in untreated worms nor in worms subjected to RNAi treatments. I will therefore hereafter briefly summarize a few findings that are more speculative and one key finding we were able to obtain with the only reporter that showed consistent expression.

The shortest version of the *utx-1* promoter (version 7) did not drive expression neither in the germline nor in somatic tissues likely because essential regulatory regions that are required for the recruitment of the transcriptional machinery are missing. Reporter versions 11 and 5 showed the highest frequency of silencing and were therefore not used in experiments. The reporter versions 1, 4 and 10 were somewhat consistent in their expression pattern and we therefore decided to use them in experiments. Reporter version 13, where we mutated all LBSs within the *utx-1* promoter showed the most consisting expression pattern (see below).
We subjected reporter versions 1, 4 and 10 to RNAi-mediated knock-down of the PRC2 components and *mes-4* as well as Notch pathway members (*glp-1, lag-1*, *sel-8* and *adm-4*) (Figure 21B-D).
Loss of GLP-1 signaling results in the loss of all germline cells and the differentiation of the remaining cells into sperm. Similarly, RNAi-mediated knock-down of essential GLP-1 pathway members (*glp-1*, *sel-8*, *lag-1)* resulted in germline phenotypes

reminiscent of the described loss of GLP-1 signaling. In RNAi experiments where we depleted GLP-1 pathway members we therefore analyzed gonads that escaped the *glp-1* phenotype to a certain extent. Therefore, it is possible that knock-down of GLP-1 pathway members was not fully penetrant in the gonads we analyzed. However, in a "population" of gonads we still expect to see changes in the expression of the reporters upon RNAi-mediated knock-down of GLP-1 signaling components or the PRC2 and *mes-4,* when the mutated regions within the used reporter are required for regulation by GLP-1 or the PRC2, respectively.

Reporter version 4 reacted strongly to the depletion of Notch pathway members in all regions of the germline (self-renewal, meiotic entry and pachytene), implicating that regulatory regions driving Notch-dependent gene expression are still present (Figure 21B). Most likely those regions correspond to the two LBSs in the 5`UTR. However, depletion of PRC2 members and *mes-4* did not result in strong de-repression as observed in the wild-type *utx-1* reporter. This implicated that regulatory regions required for PRC2-mediated co-regulation of *utx-1* might be located downstream of the promoter fragment used. In agreement with LBSs being required for Notch-dependent gene expression, reporter version 10 that harbors mutations in both LBSs of the 5`UTR was not able to react to depletion of Notch pathway components (Figure 21C). However, we still observed expression in the germline comparable to the wild-type reporter, implicating that the remaining upstream LBS is sufficient to drive expression.

Depletion of PRC2 members also resulted in de-repression of the reporter comparable to the observed de-repression in the wild-type reporter upon PRC2 knock-down. One explanation for the behavior of this reporter could be different affinities of the Notch ternary complex for LBSs. When the PRC2 is indeed competing with Notch for certain promoter regions, the dosage of both regulatory pathways might be decisive for the transcriptional output.

One possibility is that PRC2-mediated silencing is partially dependent on the Notch ternary complex that is present on regulatory regions. This would then mean that the PRC2 and Notch are only competing for available LBSs. When Notch pathway members are depleted, low levels of Notch are sufficient to drive the expression from the upstream LBS and to overcome the PRC2 to a certain degree. In the absence of the PRC2 the reporter is strongly up-regulated because the Notch ternary complex can fully utilize the upstream LBS.

However, when we looked at the expression of reporter version 1, where we would have expected to see a similar result as for version 4 if above-mentioned hypothesis holds true, we were surprised to see that depletion of PRC2, *mes-4* and GLP-1 signaling components resulted in de-repression of reporter version 1. It is therefore possible

that the regulatory sequences required for PRC2-mediated repression and the antagonism to GLP-1 signaling might not solely be dependent on a simple sequence stretch within the *utx-1* promoter, but might as well involve the coordinated utilization of multiple sites.

The requirements for a promoter to respond to GLP-1 signaling proved to be more straightforward to dissect, since LBSs are better studied than the sequence requirements for the PRC2

To confirm that *utx-1* is a target of GLP-1 in the germline, we mutated all three LBSs in the *utx-1* promoter (Version 13) (Figure 21A). GFP-H2B expression driven from this promoter was completely absent along the full-length of the germline and only detectable starting from the bend region (Figure 22). The observed expression of reporter version 13 in the bend region is in agreement with previous observations in a LBS-mutated reporter of a GLP-1 target. Similar to our observation, a transcriptional reporter driving GFP-H2B from the *sygl-1* promoter harboring mutations of the LBSs was only expressed within the germline from the bend region onwards and completely absent from the distal region (Kershner, Shin et al. 2014).

Version 13 of the reporter was additionally not de-repressed upon depletion of the PRC2 and not activated in the *glp-1* gain-of-function (*ar202*) background (data not shown). We therefore concluded that *utx-1* is a germline target of both GLP-1 and the PRC2 (Seelk, Adrian-Kalchhauser et al. 2016).

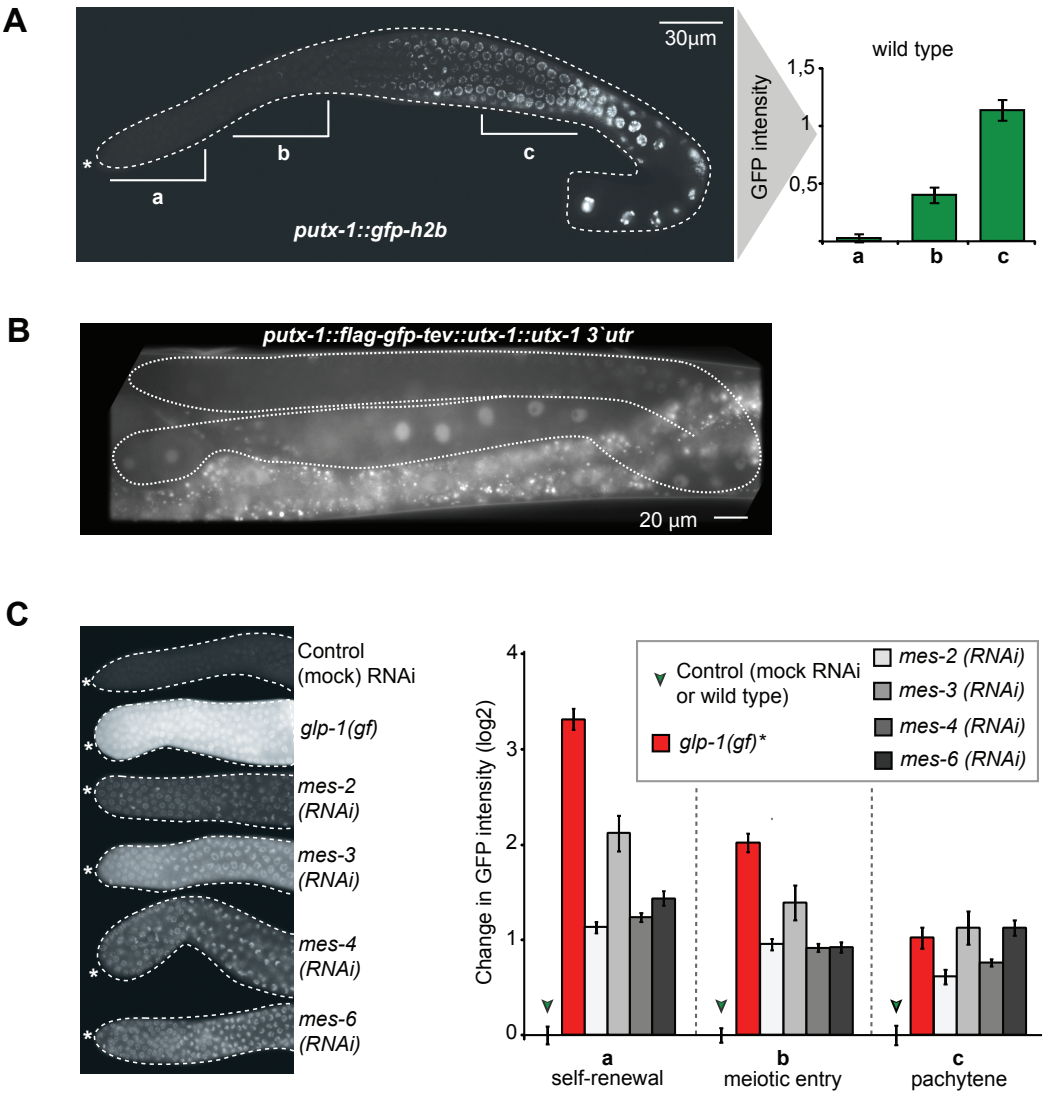

Figure 20: GLP-1 and the PRC2 transcriptionally co-regulate a common target.

(A) Expression of a GFP reporter driven from the promoter of the GLP-1-activated and PRC2-repressed gene, *utx-1.* Shown is a gonad of a *putx-1::gfp-h2b* transgenic adult. The diagram shows background-corrected relative GFP intensities in mitotic (a), early meiotic (transition zone) (b) and pachytene (c) nuclei (N=44). *Utx-1* is not expressed in the distal-most proliferative zone. Germ cells that progress through meiosis express *utx-1* progressively stronger. (B) Shown is an adult with an outlined gonad. The expression pattern of the full-length GFP-tagged functional UTX-1 transgene (*rrrSi189*) is identical with the pattern seen in the *utx-1* reporter strain. (C) The distal-most region of dissected gonads from *putx-1::gfp-h2b* worms treated with the indicated RNAi or in the *glp-1* gain-of-function (*gf*) (*ar202*) background are shown on the left. The corresponding GFP quantifications are shown on the right (N=55 for mock, N=36 for *glp-1* (*gf*), N=48 for *mes-2* (RNAi), N= 15 for *mes-3* (RNAi), N=74 for *mes-4* (RNAi), N= 29 for *mes-6* (RNAi)). Results are represented as average changes in the GFP intensity (relative to control wild types (for *glp-1* (*gf*)) or mock RNAi-treated animals). The error bars represent SEM. In *glp-1* (*gf*) and in different *mes* (RNAi) gonads the reporter was de-repressed in the proliferating cells (a) and increased in the more proximal region (b-c). *marks the distal end of the gonad.

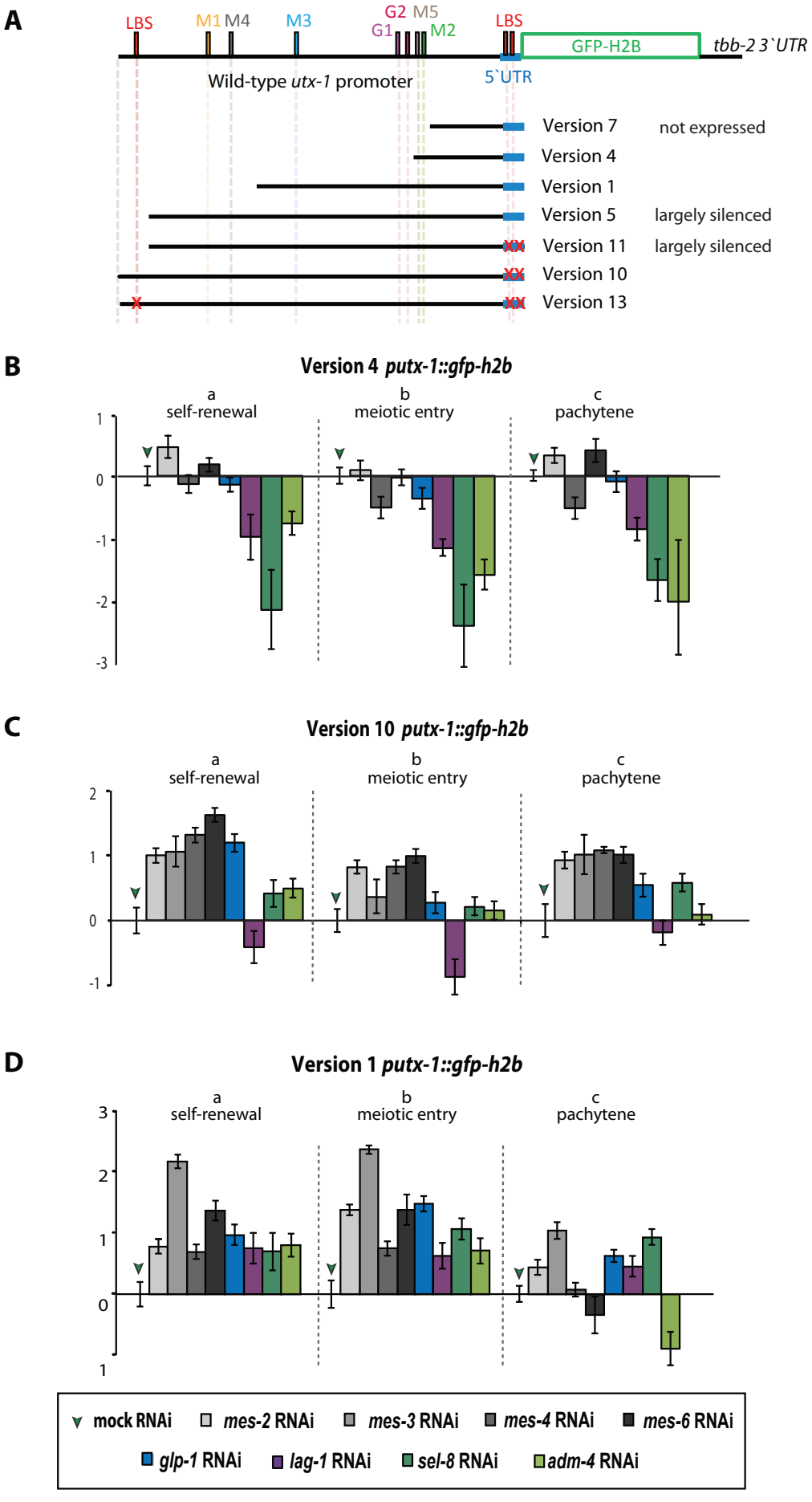
A
LBS
M1 M4
M3
G2 M5
G1
M2
LBS
GFP-H2B
tbb-2 3`UTR
Wild-type utx-1 promoter
5`UTR
Version 7
not expressed
Version 4
Version 1
Version 5
largely silenced
Version 11
largely silenced
Version 10
Version 13
B
Version 4 putx-1::gfp-h2b
a
self-renewal
b
meiotic entry
c
pachytene
C
Version 10 putx-1::gfp-h2b
a
self-renewal
b
meiotic entry
c
pachytene
D
Version 1 putx-1::gfp-h2b
a
self-renewal
b
meiotic entry
c
pachytene
mock RNAi
mes-2 RNAi
mes-3 RNAi
mes-4 RNAi
mes-6 RNAi
glp-1 RNAi
lag-1 RNAi
sel-8 RNAi
adm-4 RNAi

Figure 21: *putx-1* promoter dissection.
(A) Schematic representation of the putative *utx-1* promoter. Two LBSs are located in the 5 `UTR and one LBS in the 5`-most promoter region. Additionally proposed binding sites of LAG-1 are indicated (G1,G2) and motifs that were derived from sequence comparisons with other nematode species (M1-M5) (for details see text and Materials and Methods). (B)-(D) Results are represented as average changes in the GFP intensity (relative to mock RNAi-treated animals) in three different regions (see Figure 20) of dissected gonads of worms carrying the indicated reporter construct and treated with RNAi against PRC2 members, *mes-4* or Notch pathway components. Reporter Version 4 reacts strongly to depletion of the Notch pathway, but not to RNAi against the PRC2 or *mes-4*. Version 10 behaves exactly opposite to Version 4 and is not able to respond to alterations in the Notch pathway, while it is still de-repressed upon knock-down of the PRC2 and *mes-4*, as observed in the wild-type *utx-1*-reporter. The error bars represent SEM (N>20 for all conditions).

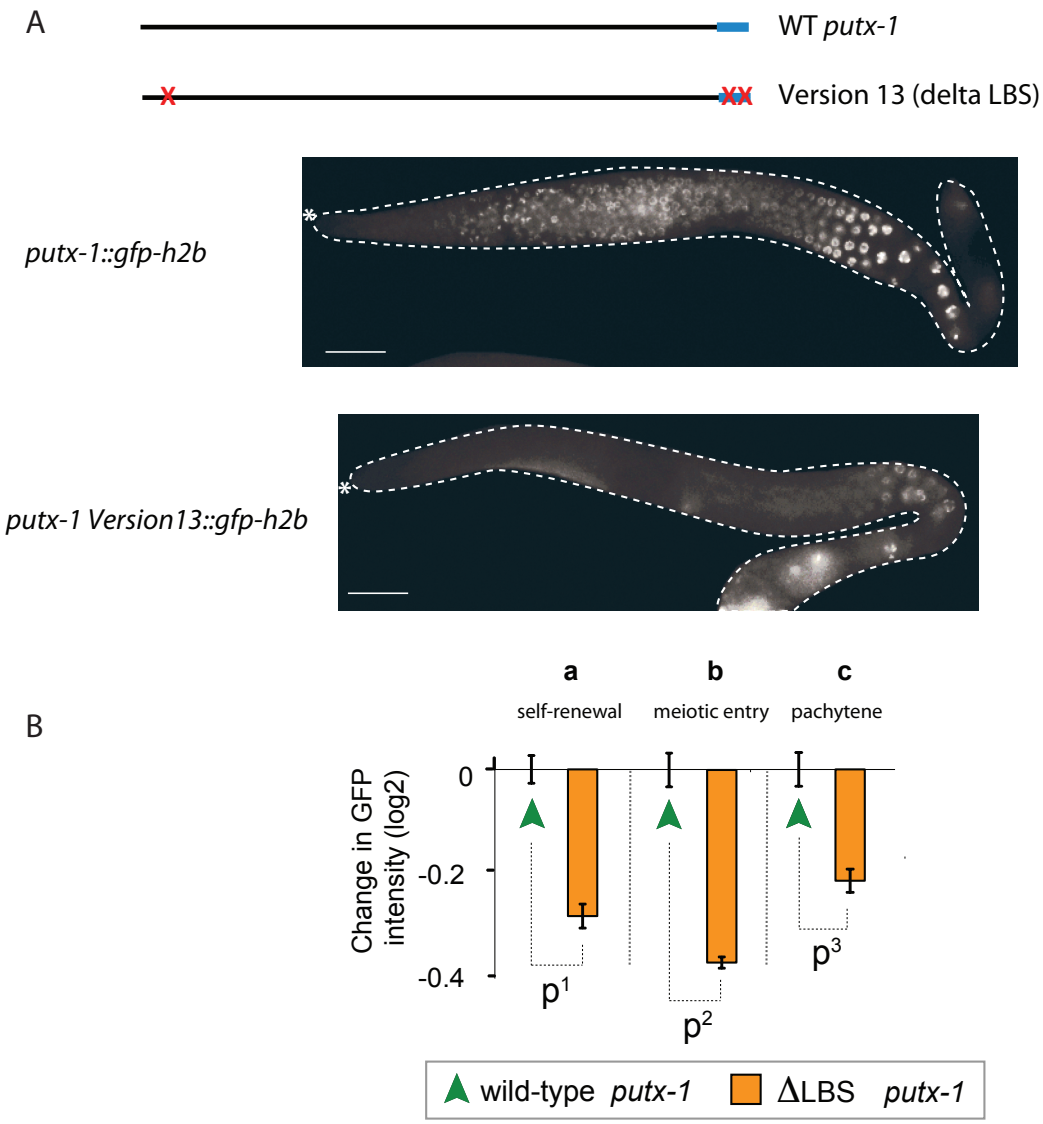

Figure 22: *utx-1* is a direct GLP-1 target.

(A) Shown are representative pictures of dissected gonads from worms carrying the indicated transgene. While the wild-type *utx-1* promoter drives expression of GFP-H2B in a gradient along the distal-proximal axis, the *utx-1* promoter carrying mutations in all three LBSs (Version 13) does not show expression along the full length of the gonad. Note that germ cell nuclei in the bend region occasionally showed GFP-H2B expression. (B) Average changes in GFP intensity (relative to the wild-type reporter construct) in three different regions (see Figure 20) of dissected gonads. The error bars represent SEM (N=20 for both strains). P1=4.85^{-13}, P2=1.38^{-20}, p3=1.18^{-7} *marks the distal end of gonads. Scale bar represents 30 µm.

6. References

Ambrosio, D. L., N. Badjatia and A. Gunzl (2015). "The spliceosomal PRP19 complex of trypanosomes." Mol Microbiol **95**(5): 885-901.
Andersen, P., H. Uosaki, L. T. Shenje and C. Kwon (2012). "Non-canonical Notch signaling: emerging role and mechanism." Trends Cell Biol **22**(5): 257-265.
Andersson, E. R. and U. Lendahl (2014). "Therapeutic modulation of Notch signalling--are we there yet?" Nat Rev Drug Discov **13**(5): 357-378.
Ariz, M., R. Mainpal and K. Subramaniam (2009). "C. elegans RNA-binding proteins PUF-8 and MEX-3 function redundantly to promote germline stem cell mitosis." Dev Biol **326**(2): 295-304.
Arribere, J. A., R. T. Bell, B. X. Fu, K. L. Artiles, P. S. Hartman and A. Z. Fire (2014). "Efficient marker-free recovery of custom genetic modifications with CRISPR/Cas9 in Caenorhabditis elegans." Genetics **198**(3): 837-846.
Aster, J. C., E. S. Robertson, R. P. Hasserjian, J. R. Turner, E. Kieff and J. Sklar (1997). "Oncogenic forms of NOTCH1 lacking either the primary binding site for RBP-Jkappa or nuclear localization sequences retain the ability to associate with RBP-Jkappa and activate transcription." J Biol Chem **272**(17): 11336-11343.
Aubin-Houzelstein, G. (2012). "Notch signaling and the developing hair follicle." Adv Exp Med Biol **727**: 142-160.
Austin, J. and J. Kimble (1987). "glp-1 is required in the germ line for regulation of the decision between mitosis and meiosis in C. elegans." Cell **51**(4): 589-599.
Barker, N. (2014). "Adult intestinal stem cells: critical drivers of epithelial homeostasis and regeneration." Nat Rev Mol Cell Biol **15**(1): 19-33.
Barker, N., M. van de Wetering and H. Clevers (2008). "The intestinal stem cell." Genes Dev **22**(14): 1856-1864.
Barolo, S., T. Stone, A. G. Bang and J. W. Posakony (2002). "Default repression and Notch signaling: Hairless acts as an adaptor to recruit the corepressors Groucho and dCtBP to Suppressor of Hairless." Genes Dev **16**(15): 1964-1976.
Bausek, N. (2013). "JAK-STAT signaling in stem cells and their niches in Drosophila." Jakstat **2**(3): e25686.
Bender, L. B., R. Cao, Y. Zhang and S. Strome (2004). "The MES-2/MES-3/MES-6 complex and regulation of histone H3 methylation in C. elegans." Curr Biol **14**(18): 1639-1643.
Bender, L. B., J. Suh, C. R. Carroll, Y. Fong, I. M. Fingerman, S. D. Briggs, R. Cao, Y. Zhang, V. Reinke and S. Strome (2006). "MES-4: an autosome-associated histone methyltransferase that participates in silencing the X chromosomes in the C. elegans germ line." Development **133**(19): 3907-3917.
Berdnik, D., T. Torok, M. Gonzalez-Gaitan and J. A. Knoblich (2002). "The endocytic protein alpha-Adaptin is required for numb-mediated asymmetric cell division in Drosophila." Dev Cell **3**(2): 221-231.
Berry, L. W., B. Westlund and T. Schedl (1997). "Germ-line tumor formation caused by activation of glp-1, a Caenorhabditis elegans member of the Notch family of receptors." Development **124**(4): 925-936.
Blaumueller, C. M., H. Qi, P. Zagouras and S. Artavanis-Tsakonas (1997). "Intracellular cleavage of Notch leads to a heterodimeric receptor on the plasma membrane." Cell **90**(2): 281-291.
Bray, S. J. (2006). "Notch signalling: a simple pathway becomes complex." Nat Rev Mol Cell Biol **7**(9): 678-689.

Brennan, K., M. Baylies and A. M. Arias (1999). "Repression by Notch is required before Wingless signalling during muscle progenitor cell development in Drosophila." Curr Biol **9**(13): 707-710.
Bres, V., N. Gomes, L. Pickle and K. A. Jones (2005). "A human splicing factor, SKIP, associates with P-TEFb and enhances transcription elongation by HIV-1 Tat." Genes Dev **19**(10): 1211-1226.
Brou, C., F. Logeat, N. Gupta, C. Bessia, O. LeBail, J. R. Doedens, A. Cumano, P. Roux, R. A. Black and A. Israel (2000). "A novel proteolytic cleavage involved in Notch signaling: the role of the disintegrin-metalloprotease TACE." Mol Cell **5**(2): 207-216.
Burger, J., J. Merlet, N. Tavernier, B. Richaudeau, A. Arnold, R. Ciosk, B. Bowerman and L. Pintard (2013). "CRL2(LRR-1) E3-ligase regulates proliferation and progression through meiosis in the Caenorhabditis elegans germline." PLoS Genet **9**(3): e1003375.
Bush, G., G. diSibio, A. Miyamoto, J. B. Denault, R. Leduc and G. Weinmaster (2001). "Ligand-induced signaling in the absence of furin processing of Notch1." Dev Biol **229**(2): 494-502.
Castel, D., P. Mourikis, S. J. Bartels, A. B. Brinkman, S. Tajbakhsh and H. G. Stunnenberg (2013). "Dynamic binding of RBPJ is determined by Notch signaling status." Genes Dev **27**(9): 1059-1071.
Chanarat, S. and K. Strasser (2013). "Splicing and beyond: the many faces of the Prp19 complex." Biochim Biophys Acta **1833**(10): 2126-2134.
Chen, N. and I. Greenwald (2004). "The lateral signal for LIN-12/Notch in C. elegans vulval development comprises redundant secreted and transmembrane DSL proteins." Dev Cell **6**(2): 183-192.
Chen, Y., L. Zhang and K. A. Jones (2011). "SKIP counteracts p53-mediated apoptosis via selective regulation of p21Cip1 mRNA splicing." Genes Dev **25**(7): 701-716.
Chitnis, A. (2006). "Why is delta endocytosis required for effective activation of notch?" Dev Dyn **235**(4): 886-894.
Christensen, S., V. Kodoyianni, M. Bosenberg, L. Friedman and J. Kimble (1996). "lag-1, a gene required for lin-12 and glp-1 signaling in Caenorhabditis elegans, is homologous to human CBF1 and Drosophila Su(H)." Development **122**(5): 1373-1383.
Cinquin, O., S. L. Crittenden, D. E. Morgan and J. Kimble (2010). "Progression from a stem cell-like state to early differentiation in the C. elegans germ line." Proc Natl Acad Sci U S A **107**(5): 2048-2053.
Corsi, A. K., B. Wightman and M. Chalfie (2015). "A Transparent window into biology: A primer on Caenorhabditis elegans." WormBook: 1-31.
Craig, K. L. and M. Tyers (1999). "The F-box: a new motif for ubiquitin dependent proteolysis in cell cycle regulation and signal transduction." Prog Biophys Mol Biol **72**(3): 299-328.
Crittenden, S. L., D. S. Bernstein, J. L. Bachorik, B. E. Thompson, M. Gallegos, A. G. Petcherski, G. Moulder, R. Barstead, M. Wickens and J. Kimble (2002). "A conserved RNA-binding protein controls germline stem cells in Caenorhabditis elegans." Nature **417**(6889): 660-663.
Crittenden, S. L., C. R. Eckmann, L. Wang, D. S. Bernstein, M. Wickens and J. Kimble (2003). "Regulation of the mitosis/meiosis decision in the Caenorhabditis elegans germline." Philos Trans R Soc Lond B Biol Sci **358**(1436): 1359-1362.

Crittenden, S. L., K. A. Leonhard, D. T. Byrd and J. Kimble (2006). "Cellular analyses of the mitotic region in the Caenorhabditis elegans adult germ line." Mol Biol Cell **17**(7): 3051-3061.
Crittenden, S. L., E. R. Troemel, T. C. Evans and J. Kimble (1994). "GLP-1 is localized to the mitotic region of the C. elegans germ line." Development **120**(10): 2901-2911.
D'Souza, B., A. Miyamoto and G. Weinmaster (2008). "The many facets of Notch ligands." Oncogene **27**(38): 5148-5167.
Davy, A., P. Bello, N. Thierry-Mieg, P. Vaglio, J. Hitti, L. Doucette-Stamm, D. Thierry-Mieg, J. Reboul, S. Boulton, A. J. Walhout, O. Coux and M. Vidal (2001). "A protein-protein interaction map of the Caenorhabditis elegans 26S proteasome." EMBO Rep **2**(9): 821-828.
de Almeida, R. A. and R. T. O'Keefe (2015). "The NineTeen Complex (NTC) and NTC-associated proteins as targets for spliceosomal ATPase action during pre-mRNA splicing." RNA Biol **12**(2): 109-114.
De Strooper, B., W. Annaert, P. Cupers, P. Saftig, K. Craessaerts, J. S. Mumm, E. H. Schroeter, V. Schrijvers, M. S. Wolfe, W. J. Ray, A. Goate and R. Kopan (1999). "A presenilin-1-dependent gamma-secretase-like protease mediates release of Notch intracellular domain." Nature **398**(6727): 518-522.
Deveraux, Q., V. Ustrell, C. Pickart and M. Rechsteiner (1994). "A 26 S protease subunit that binds ubiquitin conjugates." J Biol Chem **269**(10): 7059-7061.
Dickinson, D. J., J. D. Ward, D. J. Reiner and B. Goldstein (2013). "Engineering the Caenorhabditis elegans genome using Cas9-triggered homologous recombination." Nat Methods **10**(10): 1028-1034.
Doyle, T. G., C. Wen and I. Greenwald (2000). "SEL-8, a nuclear protein required for LIN-12 and GLP-1 signaling in Caenorhabditis elegans." Proc Natl Acad Sci U S A **97**(14): 7877-7881.
Eckmann, C. R., S. L. Crittenden, N. Suh and J. Kimble (2004). "GLD-3 and control of the mitosis/meiosis decision in the germline of Caenorhabditis elegans." Genetics **168**(1): 147-160.
Eckmann, C. R., B. Kraemer, M. Wickens and J. Kimble (2002). "GLD-3, a bicaudal-C homolog that inhibits FBF to control germline sex determination in C. elegans." Dev Cell **3**(5): 697-710.
Evans, T. C., S. L. Crittenden, V. Kodoyianni and J. Kimble (1994). "Translational control of maternal glp-1 mRNA establishes an asymmetry in the C. elegans embryo." Cell **77**(2): 183-194.
Fabrizio, P., J. Dannenberg, P. Dube, B. Kastner, H. Stark, H. Urlaub and R. Luhrmann (2009). "The evolutionarily conserved core design of the catalytic activation step of the yeast spliceosome." Mol Cell **36**(4): 593-608.
Ferrando, A. A. (2009). "The role of NOTCH1 signaling in T-ALL." Hematology Am Soc Hematol Educ Program: 353-361.
Fitzgerald, K. and I. Greenwald (1995). "Interchangeability of Caenorhabditis elegans DSL proteins and intrinsic signalling activity of their extracellular domains in vivo." Development **121**(12): 4275-4282.
Fitzgerald, K., H. A. Wilkinson and I. Greenwald (1993). "glp-1 can substitute for lin-12 in specifying cell fate decisions in Caenorhabditis elegans." Development **119**(4): 1019-1027.

Fong, Y., L. Bender, W. Wang and S. Strome (2002). "Regulation of the different chromatin states of autosomes and X chromosomes in the germ line of C. elegans." Science **296**(5576): 2235-2238.
Fontrodona, L., M. Porta-de-la-Riva, T. Moran, W. Niu, M. Diaz, D. Aristizabal-Corrales, A. Villanueva, S. Schwartz, Jr., V. Reinke and J. Ceron (2013). "RSR-2, the Caenorhabditis elegans ortholog of human spliceosomal component SRm300/SRRM2, regulates development by influencing the transcriptional machinery." PLoS Genet **9**(6): e1003543.
Fox, P. M., V. E. Vought, M. Hanazawa, M. H. Lee, E. M. Maine and T. Schedl (2011). "Cyclin E and CDK-2 regulate proliferative cell fate and cell cycle progression in the C. elegans germline." Development **138**(11): 2223-2234.
Francis, R., G. McGrath, J. Zhang, D. A. Ruddy, M. Sym, J. Apfeld, M. Nicoll, M. Maxwell, B. Hai, M. C. Ellis, A. L. Parks, W. Xu, J. Li, M. Gurney, R. L. Myers, C. S. Himes, R. Hiebsch, C. Ruble, J. S. Nye and D. Curtis (2002). "aph-1 and pen-2 are required for Notch pathway signaling, gamma-secretase cleavage of betaAPP, and presenilin protein accumulation." Dev Cell **3**(1): 85-97.
Frokjaer-Jensen, C., M. W. Davis, C. E. Hopkins, B. J. Newman, J. M. Thummel, S. P. Olesen, M. Grunnet and E. M. Jorgensen (2008). "Single-copy insertion of transgenes in Caenorhabditis elegans." Nat Genet **40**(11): 1375-1383.
Fryer, C. J., E. Lamar, I. Turbachova, C. Kintner and K. A. Jones (2002). "Mastermind mediates chromatin-specific transcription and turnover of the Notch enhancer complex." Genes Dev **16**(11): 1397-1411.
Fryer, C. J., J. B. White and K. A. Jones (2004). "Mastermind recruits CycC:CDK8 to phosphorylate the Notch ICD and coordinate activation with turnover." Mol Cell **16**(4): 509-520.
Fujita, M., T. Takasaki, N. Nakajima, T. Kawano, Y. Shimura and H. Sakamoto (2002). "MRG-1, a mortality factor-related chromodomain protein, is required maternally for primordial germ cells to initiate mitotic proliferation in C. elegans." Mech Dev **114**(1-2): 61-69.
Gause, M., J. C. Eissenberg, A. F. Macrae, M. Dorsett, Z. Misulovin and D. Dorsett (2006). "Nipped-A, the Tra1/TRRAP subunit of the Drosophila SAGA and Tip60 complexes, has multiple roles in Notch signaling during wing development." Mol Cell Biol **26**(6): 2347-2359.
Gaydos, L. J., A. Rechtsteiner, T. A. Egelhofer, C. R. Carroll and S. Strome (2012). "Antagonism between MES-4 and Polycomb repressive complex 2 promotes appropriate gene expression in C. elegans germ cells." Cell Rep **2**(5): 1169-1177.
Gissendanner, C. R., K. Kelley, T. Q. Nguyen, M. C. Hoener, A. E. Sluder and C. V. Maina (2008). "The Caenorhabditis elegans NR4A nuclear receptor is required for spermatheca morphogenesis." Dev Biol **313**(2): 767-786.
Gordon, W. R., K. L. Arnett and S. C. Blacklow (2008). "The molecular logic of Notch signaling--a structural and biochemical perspective." J Cell Sci **121**(Pt 19): 3109-3119.
Gordon, W. R., D. Vardar-Ulu, G. Histen, C. Sanchez-Irizarry, J. C. Aster and S. C. Blacklow (2007). "Structural basis for autoinhibition of Notch." Nat Struct Mol Biol **14**(4): 295-300.
Goutte, C., W. Hepler, K. M. Mickey and J. R. Priess (2000). "aph-2 encodes a novel extracellular protein required for GLP-1-mediated signaling." Development **127**(11): 2481-2492.

Graham, P. L. and J. Kimble (1993). "The mog-1 gene is required for the switch from spermatogenesis to oogenesis in Caenorhabditis elegans." Genetics **133**(4): 919-931.
Greenwald, I. (2005). "LIN-12/Notch signaling in C. elegans." WormBook: 1-16.
Groot, A. J., R. Habets, S. Yahyanejad, C. M. Hodin, K. Reiss, P. Saftig, J. Theys and M. Vooijs (2014). "Regulated proteolysis of NOTCH2 and NOTCH3 receptors by ADAM10 and presenilins." Mol Cell Biol **34**(15): 2822-2832.
Gupta, P., L. Leahul, X. Wang, C. Wang, B. Bakos, K. Jasper and D. Hansen (2015). "Proteasome regulation of the chromodomain protein MRG-1 controls the balance between proliferative fate and differentiation in the C. elegans germ line." Development **142**(2): 291-302.
Gupta-Rossi, N., O. Le Bail, H. Gonen, C. Brou, F. Logeat, E. Six, A. Ciechanover and A. Israel (2001). "Functional interaction between SEL-10, an F-box protein, and the nuclear form of activated Notch1 receptor." J Biol Chem **276**(37): 34371-34378.
Haas, A. L., J. V. Warms, A. Hershko and I. A. Rose (1982). "Ubiquitin-activating enzyme. Mechanism and role in protein-ubiquitin conjugation." J Biol Chem **257**(5): 2543-2548.
Haglund, K. and I. Dikic (2005). "Ubiquitylation and cell signaling." Embo j **24**(19): 3353-3359.
Hajnal, A. and T. Berset (2002). "The C.elegans MAPK phosphatase LIP-1 is required for the G(2)/M meiotic arrest of developing oocytes." Embo j **21**(16): 4317-4326.
Hansen, D., E. J. Hubbard and T. Schedl (2004). "Multi-pathway control of the proliferation versus meiotic development decision in the Caenorhabditis elegans germline." Dev Biol **268**(2): 342-357.
Hansen, D., L. Wilson-Berry, T. Dang and T. Schedl (2004). "Control of the proliferation versus meiotic development decision in the C. elegans germline through regulation of GLD-1 protein accumulation." Development **131**(1): 93-104.
Henderson, S. T., D. Gao, E. J. Lambie and J. Kimble (1994). "lag-2 may encode a signaling ligand for the GLP-1 and LIN-12 receptors of C. elegans." Development **120**(10): 2913-2924.
Hershko, A. and A. Ciechanover (1998). "The ubiquitin system." Annu Rev Biochem **67**: 425-479.
Hershko, A., H. Heller, S. Elias and A. Ciechanover (1983). "Components of ubiquitin-protein ligase system. Resolution, affinity purification, and role in protein breakdown." J Biol Chem **258**(13): 8206-8214.
Hogg, R., J. C. McGrail and R. T. O'Keefe (2010). "The function of the NineTeen Complex (NTC) in regulating spliceosome conformations and fidelity during pre-mRNA splicing." Biochem Soc Trans **38**(4): 1110-1115.
Hori, K., A. Sen, T. Kirchhausen and S. Artavanis-Tsakonas (2012). "Regulation of ligand-independent Notch signal through intracellular trafficking." Commun Integr Biol **5**(4): 374-376.
Hsieh, J. J., S. Zhou, L. Chen, D. B. Young and S. D. Hayward (1999). "CIR, a corepressor linking the DNA binding factor CBF1 to the histone deacetylase complex." Proc Natl Acad Sci U S A **96**(1): 23-28.
Hsu, Y. C., L. Li and E. Fuchs (2014). "Emerging interactions between skin stem cells and their niches." Nat Med **20**(8): 847-856.

Hu, Y., Y. Ye and M. E. Fortini (2002). "Nicastrin is required for gamma-secretase cleavage of the Drosophila Notch receptor." Dev Cell **2**(1): 69-78.
Hubbard, E. J. (2007). "Caenorhabditis elegans germ line: a model for stem cell biology." Dev Dyn **236**(12): 3343-3357.
Hubbard, E. J. and D. Greenstein (2005). "Introduction to the germ line." WormBook: 1-4.
Hubbard, E. J., G. Wu, J. Kitajewski and I. Greenwald (1997). "sel-10, a negative regulator of lin-12 activity in Caenorhabditis elegans, encodes a member of the CDC4 family of proteins." Genes Dev **11**(23): 3182-3193.
Ikeda, F. and I. Dikic (2008). "Atypical ubiquitin chains: new molecular signals. 'Protein Modifications: Beyond the Usual Suspects' review series." EMBO Rep **9**(6): 536-542.
Itoh, M., C. H. Kim, G. Palardy, T. Oda, Y. J. Jiang, D. Maust, S. Y. Yeo, K. Lorick, G. J. Wright, L. Ariza-McNaughton, A. M. Weissman, J. Lewis, S. C. Chandrasekharappa and A. B. Chitnis (2003). "Mind bomb is a ubiquitin ligase that is essential for efficient activation of Notch signaling by Delta." Dev Cell **4**(1): 67-82.
Jaenisch, R. and R. Young (2008). "Stem cells, the molecular circuitry of pluripotency and nuclear reprogramming." Cell **132**(4): 567-582.
Jan, E., C. K. Motzny, L. E. Graves and E. B. Goodwin (1999). "The STAR protein, GLD-1, is a translational regulator of sexual identity in Caenorhabditis elegans." Embo j **18**(1): 258-269.
Jarriault, S. and I. Greenwald (2005). "Evidence for functional redundancy between C. elegans ADAM proteins SUP-17/Kuzbanian and ADM-4/TACE." Dev Biol **287**(1): 1-10.
Jarriault, S., O. Le Bail, E. Hirsinger, O. Pourquie, F. Logeat, C. F. Strong, C. Brou, N. G. Seidah and A. Isra l (1998). "Delta-1 activation of notch-1 signaling results in HES-1 transactivation." Mol Cell Biol **18**(12): 7423-7431.
Jehn, B. M., I. Dittert, S. Beyer, K. von der Mark and W. Bielke (2002). "c-Cbl binding and ubiquitin-dependent lysosomal degradation of membrane-associated Notch1." J Biol Chem **277**(10): 8033-8040.
Jones, A. R. and T. Schedl (1995). "Mutations in gld-1, a female germ cell-specific tumor suppressor gene in Caenorhabditis elegans, affect a conserved domain also found in Src-associated protein Sam68." Genes Dev **9**(12): 1491-1504.
Jones, D., E. Crowe, T. A. Stevens and E. P. Candido (2002). "Functional and phylogenetic analysis of the ubiquitylation system in Caenorhabditis elegans: ubiquitin-conjugating enzymes, ubiquitin-activating enzymes, and ubiquitin-like proteins." Genome Biol **3**(1): Research0002.
Jung, T., B. Catalgol and T. Grune (2009). "The proteasomal system." Mol Aspects Med **30**(4): 191-296.
Kadam, S. and B. M. Emerson (2003). "Transcriptional specificity of human SWI/SNF BRG1 and BRM chromatin remodeling complexes." Mol Cell **11**(2): 377-389.
Kadyk, L. C. and J. Kimble (1998). "Genetic regulation of entry into meiosis in Caenorhabditis elegans." Development **125**(10): 1803-1813.
Kao, H. Y., P. Ordentlich, N. Koyano-Nakagawa, Z. Tang, M. Downes, C. R. Kintner, R. M. Evans and T. Kadesch (1998). "A histone deacetylase corepressor complex regulates the Notch signal transduction pathway." Genes Dev **12**(15): 2269-2277.
Kassis, J. A. and J. L. Brown (2013). "Polycomb group response elements in Drosophila and vertebrates." Adv Genet **81**: 83-118.

Katic, I. and H. Grosshans (2013). "Targeted heritable mutation and gene conversion by Cas9-CRISPR in Caenorhabditis elegans." Genetics **195**(3): 1173-1176.
Kato, H., Y. Taniguchi, H. Kurooka, S. Minoguchi, T. Sakai, S. Nomura-Okazaki, K. Tamura and T. Honjo (1997). "Involvement of RBP-J in biological functions of mouse Notch1 and its derivatives." Development **124**(20): 4133-4141.
Kelly, W. G., C. E. Schaner, A. F. Dernburg, M. H. Lee, S. K. Kim, A. M. Villeneuve and V. Reinke (2002). "X-chromosome silencing in the germline of C. elegans." Development **129**(2): 479-492.
Kerins, J. A., M. Hanazawa, M. Dorsett and T. Schedl (2010). "PRP-17 and the pre-mRNA splicing pathway are preferentially required for the proliferation versus meiotic development decision and germline sex determination in Caenorhabditis elegans." Dev Dyn **239**(5): 1555-1572.
Kershner, A. M., H. Shin, T. J. Hansen and J. Kimble (2014). "Discovery of two GLP-1/Notch target genes that account for the role of GLP-1/Notch signaling in stem cell maintenance." Proc Natl Acad Sci U S A **111**(10): 3739-3744.
Kidd, S. and T. Lieber (2002). "Furin cleavage is not a requirement for Drosophila Notch function." Mech Dev **115**(1-2): 41-51.
Kiger, A. A., D. L. Jones, C. Schulz, M. B. Rogers and M. T. Fuller (2001). "Stem cell self-renewal specified by JAK-STAT activation in response to a support cell cue." Science **294**(5551): 2542-2545.
Kim, H. T., K. P. Kim, F. Lledias, A. F. Kisselev, K. M. Scaglione, D. Skowyra, S. P. Gygi and A. L. Goldberg (2007). "Certain pairs of ubiquitin-conjugating enzymes (E2s) and ubiquitin-protein ligases (E3s) synthesize nondegradable forked ubiquitin chains containing all possible isopeptide linkages." J Biol Chem **282**(24): 17375-17386.
Kimble, J. and S. L. Crittenden (2005). "Germline proliferation and its control." WormBook: 1-14.
Kimble, J. E. and J. G. White (1981). "On the control of germ cell development in Caenorhabditis elegans." Dev Biol **81**(2): 208-219.
Kipreos, E. T. (2005). "Ubiquitin-mediated pathways in C. elegans." WormBook: 1-24.
Kipreos, E. T., L. E. Lander, J. P. Wing, W. W. He and E. M. Hedgecock (1996). "cul-1 is required for cell cycle exit in C. elegans and identifies a novel gene family." Cell **85**(6): 829-839.
Kirkpatrick, D. S., N. A. Hathaway, J. Hanna, S. Elsasser, J. Rush, D. Finley, R. W. King and S. P. Gygi (2006). "Quantitative analysis of in vitro ubiquitinated cyclin B1 reveals complex chain topology." Nat Cell Biol **8**(7): 700-710.
Knoblich, J. A. (2008). "Mechanisms of asymmetric stem cell division." Cell **132**(4): 583-597.
Knust, E. and J. A. Campos-Ortega (1989). "The molecular genetics of early neurogenesis in Drosophila melanogaster." Bioessays **11**(4): 95-100.
Krek, W. (1998). "Proteolysis and the G1-S transition: the SCF connection." Curr Opin Genet Dev **8**(1): 36-42.
Kumsta, C. and M. Hansen (2012). "C. elegans rrf-1 mutations maintain RNAi efficiency in the soma in addition to the germline." PLoS One **7**(5): e35428.
Kuraoka, I., S. Ito, T. Wada, M. Hayashida, L. Lee, M. Saijo, Y. Nakatsu, M. Matsumoto, T. Matsunaga, H. Handa, J. Qin, Y. Nakatani and K. Tanaka (2008).

"Isolation of XAB2 complex involved in pre-mRNA splicing, transcription, and transcription-coupled repair." J Biol Chem **283**(2): 940-950.
Kurooka, H., K. Kuroda and T. Honjo (1998). "Roles of the ankyrin repeats and C-terminal region of the mouse notch1 intracellular region." Nucleic Acids Res **26**(23): 5448-5455.
Lai, E. C., G. A. Deblandre, C. Kintner and G. M. Rubin (2001). "Drosophila neuralized is a ubiquitin ligase that promotes the internalization and degradation of delta." Dev Cell **1**(6): 783-794.
Lai, E. C. and G. M. Rubin (2001). "neuralized functions cell-autonomously to regulate a subset of notch-dependent processes during adult Drosophila development." Dev Biol **231**(1): 217-233.
Lake, R. J., L. M. Grimm, A. Veraksa, A. Banos and S. Artavanis-Tsakonas (2009). "In vivo analysis of the Notch receptor S1 cleavage." PLoS One **4**(8): e6728.
Lambie, E. J. and J. Kimble (1991). "Two homologous regulatory genes, lin-12 and glp-1, have overlapping functions." Development **112**(1): 231-240.
Lamont, L. B., S. L. Crittenden, D. Bernstein, M. Wickens and J. Kimble (2004). "FBF-1 and FBF-2 regulate the size of the mitotic region in the C. elegans germline." Dev Cell **7**(5): 697-707.
Le Borgne, R., S. Remaud, S. Hamel and F. Schweisguth (2005). "Two distinct E3 ubiquitin ligases have complementary functions in the regulation of delta and serrate signaling in Drosophila." PLoS Biol **3**(4): e96.
Lee, C., E. B. Sorensen, T. R. Lynch and J. Kimble (2016). "C. elegans GLP-1/Notch activates transcription in a probability gradient across the germline stem cell pool." Elife **5**.
Lee, M. H., B. Hook, L. B. Lamont, M. Wickens and J. Kimble (2006). "LIP-1 phosphatase controls the extent of germline proliferation in Caenorhabditis elegans." Embo j **25**(1): 88-96.
Levitan, D., G. Yu, P. St George Hyslop and C. Goutte (2001). "APH-2/nicastrin functions in LIN-12/Notch signaling in the Caenorhabditis elegans somatic gonad." Dev Biol **240**(2): 654-661.
Li, X. and I. Greenwald (1997). "HOP-1, a Caenorhabditis elegans presenilin, appears to be functionally redundant with SEL-12 presenilin and to facilitate LIN-12 and GLP-1 signaling." Proc Natl Acad Sci U S A **94**(22): 12204-12209.
Liu, J., C. Sato, M. Cerletti and A. Wagers (2010). "Notch signaling in the regulation of stem cell self-renewal and differentiation." Curr Top Dev Biol **92**: 367-409.
Logeat, F., C. Bessia, C. Brou, O. LeBail, S. Jarriault, N. G. Seidah and A. Israel (1998). "The Notch1 receptor is cleaved constitutively by a furin-like convertase." Proc Natl Acad Sci U S A **95**(14): 8108-8112.
Lowry, W. E. and L. Richter (2007). "Signaling in adult stem cells." Front Biosci **12**: 3911-3927.
Macdonald, L. D., A. Knox and D. Hansen (2008). "Proteasomal regulation of the proliferation vs. meiotic entry decision in the Caenorhabditis elegans germ line." Genetics **180**(2): 905-920.
MacQueen, A. J. and A. M. Villeneuve (2001). "Nuclear reorganization and homologous chromosome pairing during meiotic prophase require C. elegans chk-2." Genes Dev **15**(13): 1674-1687.
Makarov, E. M., O. V. Makarova, H. Urlaub, M. Gentzel, C. L. Will, M. Wilm and R. Luhrmann (2002). "Small nuclear ribonucleoprotein remodeling during catalytic activation of the spliceosome." Science **298**(5601): 2205-2208.

Makarova, O. V., E. M. Makarov, H. Urlaub, C. L. Will, M. Gentzel, M. Wilm and R. Luhrmann (2004). "A subset of human 35S U5 proteins, including Prp19, function prior to catalytic step 1 of splicing." Embo j **23**(12): 2381-2391.
Mango, S. E., E. M. Maine and J. Kimble (1991). "Carboxy-terminal truncation activates glp-1 protein to specify vulval fates in Caenorhabditis elegans." Nature **352**(6338): 811-815.
Mango, S. E., C. J. Thorpe, P. R. Martin, S. H. Chamberlain and B. Bowerman (1994). "Two maternal genes, apx-1 and pie-1, are required to distinguish the fates of equivalent blastomeres in the early Caenorhabditis elegans embryo." Development **120**(8): 2305-2315.
Mantina, P., L. MacDonald, A. Kulaga, L. Zhao and D. Hansen (2009). "A mutation in teg-4, which encodes a protein homologous to the SAP130 pre-mRNA splicing factor, disrupts the balance between proliferation and differentiation in the C. elegans germ line." Mech Dev **126**(5-6): 417-429.
Marin, V. A. and T. C. Evans (2003). "Translational repression of a C. elegans Notch mRNA by the STAR/KH domain protein GLD-1." Development **130**(12): 2623-2632.
Matsumoto, A., I. Onoyama, T. Sunabori, R. Kageyama, H. Okano and K. I. Nakayama (2011). "Fbxw7-dependent degradation of Notch is required for control of "stemness" and neuronal-glial differentiation in neural stem cells." J Biol Chem **286**(15): 13754-13764.
McGill, M. A. and C. J. McGlade (2003). "Mammalian numb proteins promote Notch1 receptor ubiquitination and degradation of the Notch1 intracellular domain." J Biol Chem **278**(25): 23196-23203.
Mello, C. C., B. W. Draper and J. R. Priess (1994). "The maternal genes apx-1 and glp-1 and establishment of dorsal-ventral polarity in the early C. elegans embryo." Cell **77**(1): 95-106.
Merritt, C., D. Rasoloson, D. Ko and G. Seydoux (2008). "3' UTRs are the primary regulators of gene expression in the C. elegans germline." Curr Biol **18**(19): 1476-1482.
Mickey, K. M., C. C. Mello, M. K. Montgomery, A. Fire and J. R. Priess (1996). "An inductive interaction in 4-cell stage C. elegans embryos involves APX-1 expression in the signalling cell." Development **122**(6): 1791-1798.
Moore, R. and L. Boyd (2004). "Analysis of RING finger genes required for embryogenesis in C. elegans." Genesis **38**(1): 1-12.
Morgan, D. E., S. L. Crittenden and J. Kimble (2010). "The C. elegans adult male germline: stem cells and sexual dimorphism." Dev Biol **346**(2): 204-214.
Morrison, S. J. and J. Kimble (2006). "Asymmetric and symmetric stem-cell divisions in development and cancer." Nature **441**(7097): 1068-1074.
Mukhopadhyay, D. and H. Riezman (2007). "Proteasome-independent functions of ubiquitin in endocytosis and signaling." Science **315**(5809): 201-205.
Nadarajan, S., J. A. Govindan, M. McGovern, E. J. Hubbard and D. Greenstein (2009). "MSP and GLP-1/Notch signaling coordinately regulate actomyosin-dependent cytoplasmic streaming and oocyte growth in C. elegans." Development **136**(13): 2223-2234.
Nicholson, S. C., B. N. Nicolay, M. V. Frolov and K. H. Moberg (2011). "Notch-dependent expression of the archipelago ubiquitin ligase subunit in the Drosophila eye." Development **138**(2): 251-260.

Ninov, N., M. Borius and D. Y. Stainier (2012). "Different levels of Notch signaling regulate quiescence, renewal and differentiation in pancreatic endocrine progenitors." Development **139**(9): 1557-1567.
Nusser-Stein, S., A. Beyer, I. Rimann, M. Adamczyk, N. Piterman, A. Hajnal and J. Fisher (2012). "Cell-cycle regulation of NOTCH signaling during C. elegans vulval development." Mol Syst Biol **8**: 618.
Oberg, C., J. Li, A. Pauley, E. Wolf, M. Gurney and U. Lendahl (2001). "The Notch intracellular domain is ubiquitinated and negatively regulated by the mammalian Sel-10 homolog." J Biol Chem **276**(38): 35847-35853.
Ogura, K., N. Kishimoto, S. Mitani, K. Gengyo-Ando and Y. Kohara (2003). "Translational control of maternal glp-1 mRNA by POS-1 and its interacting protein SPN-4 in Caenorhabditis elegans." Development **130**(11): 2495-2503.
Ohta, T., J. J. Michel, A. J. Schottelius and Y. Xiong (1999). "ROC1, a homolog of APC11, represents a family of cullin partners with an associated ubiquitin ligase activity." Mol Cell **3**(4): 535-541.
Oswald, F., U. Kostezka, K. Astrahantseff, S. Bourteele, K. Dillinger, U. Zechner, L. Ludwig, M. Wilda, H. Hameister, W. Knochel, S. Liptay and R. M. Schmid (2002). "SHARP is a novel component of the Notch/RBP-Jkappa signalling pathway." Embo j **21**(20): 5417-5426.
Oswald, F., M. Winkler, Y. Cao, K. Astrahantseff, S. Bourteele, W. Knochel and T. Borggrefe (2005). "RBP-Jkappa/SHARP recruits CtIP/CtBP corepressors to silence Notch target genes." Mol Cell Biol **25**(23): 10379-10390.
Overstreet, E., E. Fitch and J. A. Fischer (2004). "Fat facets and Liquid facets promote Delta endocytosis and Delta signaling in the signaling cells." Development **131**(21): 5355-5366.
Pagan, J., T. Seto, M. Pagano and A. Cittadini (2013). "Role of the ubiquitin proteasome system in the heart." Circ Res **112**(7): 1046-1058.
Pan, D. and G. M. Rubin (1997). "Kuzbanian controls proteolytic processing of Notch and mediates lateral inhibition during Drosophila and vertebrate neurogenesis." Cell **90**(2): 271-280.
Pasternak, B. and P. Aspenberg (2009). "Metalloproteinases and their inhibitors-diagnostic and therapeutic opportunities in orthopedics." Acta Orthop **80**(6): 693-703.
Pavlopoulos, E., C. Pitsouli, K. M. Klueg, M. A. Muskavitch, N. K. Moschonas and C. Delidakis (2001). "neuralized Encodes a peripheral membrane protein involved in delta signaling and endocytosis." Dev Cell **1**(6): 807-816.
Pepper, A. S., D. J. Killian and E. J. Hubbard (2003). "Genetic analysis of Caenorhabditis elegans glp-1 mutants suggests receptor interaction or competition." Genetics **163**(1): 115-132.
Petcherski, A. G. and J. Kimble (2000). "LAG-3 is a putative transcriptional activator in the C. elegans Notch pathway." Nature **405**(6784): 364-368.
Pickart, C. M. and D. Fushman (2004). "Polyubiquitin chains: polymeric protein signals." Curr Opin Chem Biol **8**(6): 610-616.
Pickart, C. M. and I. A. Rose (1985). "Functional heterogeneity of ubiquitin carrier proteins." J Biol Chem **260**(3): 1573-1581.
Priess, J. R. (2005). "Notch signaling in the C. elegans embryo." WormBook: 1-16.
Priess, J. R. and J. N. Thomson (1987). "Cellular interactions in early C. elegans embryos." Cell **48**(2): 241-250.

Pushpa, K., G. A. Kumar and K. Subramaniam (2013). "PUF-8 and TCER-1 are essential for normal levels of multiple mRNAs in the C. elegans germline." Development **140**(6): 1312-1320.
Qiao, L., J. L. Lissemore, P. Shu, A. Smardon, M. B. Gelber and E. M. Maine (1995). "Enhancers of glp-1, a gene required for cell-signaling in Caenorhabditis elegans, define a set of genes required for germline development." Genetics **141**(2): 551-569.
Qiu, L., C. Joazeiro, N. Fang, H. Y. Wang, C. Elly, Y. Altman, D. Fang, T. Hunter and Y. C. Liu (2000). "Recognition and ubiquitination of Notch by Itch, a hect-type E3 ubiquitin ligase." J Biol Chem **275**(46): 35734-35737.
Racher, H. and D. Hansen (2012). "PUF-8, a Pumilio homolog, inhibits the proliferative fate in the Caenorhabditis elegans germline." G3 (Bethesda) **2**(10): 1197-1205.
Richards, G. S. and B. M. Degnan (2009). "The dawn of developmental signaling in the metazoa." Cold Spring Harb Symp Quant Biol **74**: 81-90.
Roehl, H., M. Bosenberg, R. Blelloch and J. Kimble (1996). "Roles of the RAM and ANK domains in signaling by the C. elegans GLP-1 receptor." Embo j **15**(24): 7002-7012.
Romito, A. and G. Cobellis (2016). "Pluripotent Stem Cells: Current Understanding and Future Directions." Stem Cells Int **2016**: 9451492.
Rudel, D. and J. Kimble (2001). "Conservation of glp-1 regulation and function in nematodes." Genetics **157**(2): 639-654.
Ryder, S. P., L. A. Frater, D. L. Abramovitz, E. B. Goodwin and J. R. Williamson (2004). "RNA target specificity of the STAR/GSG domain post-transcriptional regulatory protein GLD-1." Nat Struct Mol Biol **11**(1): 20-28.
Safdar, K., A. Gu, X. Xu, V. Au, J. Taylor, S. Flibotte, D. G. Moerman and E. M. Maine (2016). "UBR-5, a Conserved HECT-Type E3 Ubiquitin Ligase, Negatively Regulates Notch-Type Signaling in Caenorhabditis elegans." G3 (Bethesda) **6**(7): 2125-2134.
Sandy, A. R., M. Jones and I. Maillard (2012). "Notch signaling and development of the hematopoietic system." Adv Exp Med Biol **727**: 71-88.
Sapra, A. K., P. Khandelia and U. Vijayraghavan (2008). "The splicing factor Prp17 interacts with the U2, U5 and U6 snRNPs and associates with the spliceosome pre- and post-catalysis." Biochem J **416**(3): 365-374.
Sarikas, A., T. Hartmann and Z. Q. Pan (2011). "The cullin protein family." Genome Biol **12**(4): 220.
Scadden, D. T. (2006). "The stem-cell niche as an entity of action." Nature **441**(7097): 1075-1079.
Scheckel, C., D. Gaidatzis, J. E. Wright and R. Ciosk (2012). "Genome-wide analysis of GLD-1-mediated mRNA regulation suggests a role in mRNA storage." PLoS Genet **8**(5): e1002742.
Schlesinger, D. H., G. Goldstein and H. D. Niall (1975). "The complete amino acid sequence of ubiquitin, an adenylate cyclase stimulating polypeptide probably universal in living cells." Biochemistry **14**(10): 2214-2218.
Schreiner, P., X. Chen, K. Husnjak, L. Randles, N. Zhang, S. Elsasser, D. Finley, I. Dikic, K. J. Walters and M. Groll (2008). "Ubiquitin docking at the proteasome through a novel pleckstrin-homology domain interaction." Nature **453**(7194): 548-552.

Schroeter, E. H., J. A. Kisslinger and R. Kopan (1998). "Notch-1 signalling requires ligand-induced proteolytic release of intracellular domain." Nature **393**(6683): 382-386.
Schweisguth, F. (1999). "Dominant-negative mutation in the beta2 and beta6 proteasome subunit genes affect alternative cell fate decisions in the Drosophila sense organ lineage." Proc Natl Acad Sci U S A **96**(20): 11382-11386.
Seelk, S., I. Adrian-Kalchhauser, B. Hargitai, M. Hajduskova, S. Gutnik, B. Tursun and R. Ciosk (2016). "Increasing Notch signaling antagonizes PRC2-mediated silencing to promote reprograming of germ cells into neurons." Elife **5**.
Shao, G., J. Patterson-Fortin, T. E. Messick, D. Feng, N. Shanbhag, Y. Wang and R. A. Greenberg (2009). "MERIT40 controls BRCA1-Rap80 complex integrity and recruitment to DNA double-strand breaks." Genes Dev **23**(6): 740-754.
Shaye, D. D. and I. Greenwald (2002). "Endocytosis-mediated downregulation of LIN-12/Notch upon Ras activation in Caenorhabditis elegans." Nature **420**(6916): 686-690.
Shaye, D. D. and I. Greenwald (2005). "LIN-12/Notch trafficking and regulation of DSL ligand activity during vulval induction in Caenorhabditis elegans." Development **132**(22): 5081-5092.
Shiimori, M., K. Inoue and H. Sakamoto (2013). "A specific set of exon junction complex subunits is required for the nuclear retention of unspliced RNAs in Caenorhabditis elegans." Mol Cell Biol **33**(2): 444-456.
Smith, D. M., S. C. Chang, S. Park, D. Finley, Y. Cheng and A. L. Goldberg (2007). "Docking of the proteasomal ATPases' carboxyl termini in the 20S proteasome's alpha ring opens the gate for substrate entry." Mol Cell **27**(5): 731-744.
Song, E. J., S. L. Werner, J. Neubauer, F. Stegmeier, J. Aspden, D. Rio, J. W. Harper, S. J. Elledge, M. W. Kirschner and M. Rape (2010). "The Prp19 complex and the Usp4Sart3 deubiquitinating enzyme control reversible ubiquitination at the spliceosome." Genes Dev **24**(13): 1434-1447.
Song, W., P. Nadeau, M. Yuan, X. Yang, J. Shen and B. A. Yankner (1999). "Proteolytic release and nuclear translocation of Notch-1 are induced by presenilin-1 and impaired by pathogenic presenilin-1 mutations." Proc Natl Acad Sci U S A **96**(12): 6959-6963.
Sternberg, P. W. (2005). "Vulval development." WormBook: 1-28.
Sternberg, P. W. and H. R. Horvitz (1989). "The combined action of two intercellular signaling pathways specifies three cell fates during vulval induction in C. elegans." Cell **58**(4): 679-693.
Sterner, D. E., P. A. Grant, S. M. Roberts, L. J. Duggan, R. Belotserkovskaya, L. A. Pacella, F. Winston, J. L. Workman and S. L. Berger (1999). "Functional organization of the yeast SAGA complex: distinct components involved in structural integrity, nucleosome acetylation, and TATA-binding protein interaction." Mol Cell Biol **19**(1): 86-98.
Struhl, G. and A. Adachi (1998). "Nuclear access and action of notch in vivo." Cell **93**(4): 649-660.
Sun, L. and Z. J. Chen (2004). "The novel functions of ubiquitination in signaling." Curr Opin Cell Biol **16**(2): 119-126.
Sun, X. and S. Artavanis-Tsakonas (1996). "The intracellular deletions of Delta and Serrate define dominant negative forms of the Drosophila Notch ligands." Development **122**(8): 2465-2474.

Sundaram, M. and I. Greenwald (1993). "Suppressors of a lin-12 hypomorph define genes that interact with both lin-12 and glp-1 in Caenorhabditis elegans." Genetics **135**(3): 765-783.
Szilagyi, Z. and C. M. Gustafsson (2013). "Emerging roles of Cdk8 in cell cycle control." Biochim Biophys Acta **1829**(9): 916-920.
Tamura, K., Y. Taniguchi, S. Minoguchi, T. Sakai, T. Tun, T. Furukawa and T. Honjo (1995). "Physical interaction between a novel domain of the receptor Notch and the transcription factor RBP-J kappa/Su(H)." Curr Biol **5**(12): 1416-1423.
Tanaka, K., A. Kumatori, K. Ii and A. Ichihara (1989). "Direct evidence for nuclear and cytoplasmic colocalization of proteasomes (multiprotease complexes) in liver." J Cell Physiol **139**(1): 34-41.
Tang, H., S. B. Rompani, J. B. Atkins, Y. Zhou, T. Osterwalder and W. Zhong (2005). "Numb proteins specify asymmetric cell fates via an endocytosis- and proteasome-independent pathway." Mol Cell Biol **25**(8): 2899-2909.
Taniguchi, Y., T. Furukawa, T. Tun, H. Han and T. Honjo (1998). "LIM protein KyoT2 negatively regulates transcription by association with the RBP-J DNA-binding protein." Mol Cell Biol **18**(1): 644-654.
Tetzlaff, M. T., W. Yu, M. Li, P. Zhang, M. Finegold, K. Mahon, J. W. Harper, R. J. Schwartz and S. J. Elledge (2004). "Defective cardiovascular development and elevated cyclin E and Notch proteins in mice lacking the Fbw7 F-box protein." Proc Natl Acad Sci U S A **101**(10): 3338-3345.
Tian, X., D. Hansen, T. Schedl and J. B. Skeath (2004). "Epsin potentiates Notch pathway activity in Drosophila and C. elegans." Development **131**(23): 5807-5815.
Tsunematsu, R., K. Nakayama, Y. Oike, M. Nishiyama, N. Ishida, S. Hatakeyama, Y. Bessho, R. Kageyama, T. Suda and K. I. Nakayama (2004). "Mouse Fbw7/Sel-10/Cdc4 is required for notch degradation during vascular development." J Biol Chem **279**(10): 9417-9423.
Tulina, N. and E. Matunis (2001). "Control of stem cell self-renewal in Drosophila spermatogenesis by JAK-STAT signaling." Science **294**(5551): 2546-2549.
Ulbright, T. M. (2005). "Germ cell tumors of the gonads: a selective review emphasizing problems in differential diagnosis, newly appreciated, and controversial issues." Mod Pathol **18 Suppl 2**: S61-79.
van den Heuvel, S. (2004). "Protein degradation: CUL-3 and BTB--partners in proteolysis." Curr Biol **14**(2): R59-61.
van Tetering, G., P. van Diest, I. Verlaan, E. van der Wall, R. Kopan and M. Vooijs (2009). "Metalloprotease ADAM10 is required for Notch1 site 2 cleavage." J Biol Chem **284**(45): 31018-31027.
Vandamme, J., G. Lettier, S. Sidoli, E. Di Schiavi, O. Norregaard Jensen and A. E. Salcini (2012). "The C. elegans H3K27 demethylase UTX-1 is essential for normal development, independent of its enzymatic activity." PLoS Genet **8**(5): e1002647.
Vander Kooi, C. W., M. D. Ohi, J. A. Rosenberg, M. L. Oldham, M. E. Newcomer, K. L. Gould and W. J. Chazin (2006). "The Prp19 U-box crystal structure suggests a common dimeric architecture for a class of oligomeric E3 ubiquitin ligases." Biochemistry **45**(1): 121-130.
Vassin, H., K. A. Bremer, E. Knust and J. A. Campos-Ortega (1987). "The neurogenic gene Delta of Drosophila melanogaster is expressed in neurogenic territories and encodes a putative transmembrane protein with EGF-like repeats." Embo j **6**(11): 3431-3440.

Verma, R., L. Aravind, R. Oania, W. H. McDonald, J. R. Yates, 3rd, E. V. Koonin and R. J. Deshaies (2002). "Role of Rpn11 metalloprotease in deubiquitination and degradation by the 26S proteasome." Science **298**(5593): 611-615.
Vought, V. E., M. Ohmachi, M. H. Lee and E. M. Maine (2005). "EGO-1, a putative RNA-directed RNA polymerase, promotes germline proliferation in parallel with GLP-1/notch signaling and regulates the spatial organization of nuclear pore complexes and germline P granules in Caenorhabditis elegans." Genetics **170**(3): 1121-1132.
Wahl, M. C., C. L. Will and R. Luhrmann (2009). "The spliceosome: design principles of a dynamic RNP machine." Cell **136**(4): 701-718.
Wallberg, A. E., K. Pedersen, U. Lendahl and R. G. Roeder (2002). "p300 and PCAF act cooperatively to mediate transcriptional activation from chromatin templates by notch intracellular domains in vitro." Mol Cell Biol **22**(22): 7812-7819.
Wang, L., C. R. Eckmann, L. C. Kadyk, M. Wickens and J. Kimble (2002). "A regulatory cytoplasmic poly(A) polymerase in Caenorhabditis elegans." Nature **419**(6904): 312-316.
Wang, W. and G. Struhl (2004). "Drosophila Epsin mediates a select endocytic pathway that DSL ligands must enter to activate Notch." Development **131**(21): 5367-5380.
Wang, X., F. Wu, Q. Xie, H. Wang, Y. Wang, Y. Yue, O. Gahura, S. Ma, L. Liu, Y. Cao, Y. Jiao, F. Puta, C. R. McClung, X. Xu and L. Ma (2012). "SKIP is a component of the spliceosome linking alternative splicing and the circadian clock in Arabidopsis." Plant Cell **24**(8): 3278-3295.
Wen, C., M. M. Metzstein and I. Greenwald (1997). "SUP-17, a Caenorhabditis elegans ADAM protein related to Drosophila KUZBANIAN, and its role in LIN-12/NOTCH signalling." Development **124**(23): 4759-4767.
Weng, A. P., A. A. Ferrando, W. Lee, J. P. t. Morris, L. B. Silverman, C. Sanchez-Irizarry, S. C. Blacklow, A. T. Look and J. C. Aster (2004). "Activating mutations of NOTCH1 in human T cell acute lymphoblastic leukemia." Science **306**(5694): 269-271.
Westlund, B., D. Parry, R. Clover, M. Basson and C. D. Johnson (1999). "Reverse genetic analysis of Caenorhabditis elegans presenilins reveals redundant but unequal roles for sel-12 and hop-1 in Notch-pathway signaling." Proc Natl Acad Sci U S A **96**(5): 2497-2502.
Wilkinson, H. A., K. Fitzgerald and I. Greenwald (1994). "Reciprocal changes in expression of the receptor lin-12 and its ligand lag-2 prior to commitment in a C. elegans cell fate decision." Cell **79**(7): 1187-1198.
Wilson, J. J. and R. A. Kovall (2006). "Crystal structure of the CSL-Notch-Mastermind ternary complex bound to DNA." Cell **124**(5): 985-996.
Wu, G., S. Lyapina, I. Das, J. Li, M. Gurney, A. Pauley, I. Chui, R. J. Deshaies and J. Kitajewski (2001). "SEL-10 is an inhibitor of notch signaling that targets notch for ubiquitin-mediated protein degradation." Mol Cell Biol **21**(21): 7403-7415.
Wu, L., T. Sun, K. Kobayashi, P. Gao and J. D. Griffin (2002). "Identification of a family of mastermind-like transcriptional coactivators for mammalian notch receptors." Mol Cell Biol **22**(21): 7688-7700.
Wu, M., G. Chen and Y. P. Li (2016). "TGF-beta and BMP signaling in osteoblast, skeletal development, and bone formation, homeostasis and disease." Bone Res **4**: 16009.

Xie, T. (2008). Germline stem cell niches. StemBook. Cambridge (MA), Harvard Stem Cell Institute
Copyright: (c) 2008 Ting Xie.
Xie, T. and A. C. Spradling (2000). "A niche maintaining germ line stem cells in the Drosophila ovary." Science **290**(5490): 328-330.
Xu, P., D. M. Duong, N. T. Seyfried, D. Cheng, Y. Xie, J. Robert, J. Rush, M. Hochstrasser, D. Finley and J. Peng (2009). "Quantitative proteomics reveals the function of unconventional ubiquitin chains in proteasomal degradation." Cell **137**(1): 133-145.
Yamanaka, A., M. Yada, H. Imaki, M. Koga, Y. Ohshima and K. Nakayama (2002). "Multiple Skp1-related proteins in Caenorhabditis elegans: diverse patterns of interaction with Cullins and F-box proteins." Curr Biol **12**(4): 267-275.
Yochem, J. and I. Greenwald (1989). "glp-1 and lin-12, genes implicated in distinct cell-cell interactions in C. elegans, encode similar transmembrane proteins." Cell **58**(3): 553-563.
Yoo, A. S., C. Bais and I. Greenwald (2004). "Crosstalk between the EGFR and LIN-12/Notch pathways in C. elegans vulval development." Science **303**(5658): 663-666.
Yu, G., M. Nishimura, S. Arawaka, D. Levitan, L. Zhang, A. Tandon, Y. Q. Song, E. Rogaeva, F. Chen, T. Kawarai, A. Supala, L. Levesque, H. Yu, D. S. Yang, E. Holmes, P. Milman, Y. Liang, D. M. Zhang, D. H. Xu, C. Sato, E. Rogaev, M. Smith, C. Janus, Y. Zhang, R. Aebersold, L. S. Farrer, S. Sorbi, A. Bruni, P. Fraser and P. St George-Hyslop (2000). "Nicastrin modulates presenilin-mediated notch/glp-1 signal transduction and betaAPP processing." Nature **407**(6800): 48-54.
Zahler, A. M. (2012). "Pre-mRNA splicing and its regulation in Caenorhabditis elegans." WormBook: 1-21.
Zhou, S., M. Fujimuro, J. J. Hsieh, L. Chen and S. D. Hayward (2000). "A role for SKIP in EBNA2 activation of CBF1-repressed promoters." J Virol **74**(4): 1939-1947.
Zhou, S., M. Fujimuro, J. J. Hsieh, L. Chen, A. Miyamoto, G. Weinmaster and S. D. Hayward (2000). "SKIP, a CBF1-associated protein, interacts with the ankyrin repeat domain of NotchIC To facilitate NotchIC function." Mol Cell Biol **20**(7): 2400-2410.
Zhou, S. and S. D. Hayward (2001). "Nuclear localization of CBF1 is regulated by interactions with the SMRT corepressor complex." Mol Cell Biol **21**(18): 6222-6232.

Webpages:

Wormbase:

http://www.wormbase.org

Wormatlas:

http://www.wormatlas.org/hermaphrodite/somatic%20gonad/mainframe.htm

Acknowledgements

First and foremost, I would like to thank Rafal Ciosk for giving me the opportunity to do my PhD in his lab, for his constant support and trust in me even when projects proved to be less straightforward.
I also want to thank my PhD committee members, Susan Gasser and Alex Hajnal, for fruitful discussions during our meetings.
Special thanks go to all the FMI facilities that provided me with scientific advice and technical support. Special thanks to Heinz Gut (protein structure facility) for modeling the position of GFP within GLP-1, to Iskra Katic (worm facility), who was of tremendous help in all the transgenesis I ever attempted, be it cloning of constructs, giving me advices on new methods and most importantly injecting a large proportion of the strains I generated in this work. Also, thanks to Daniel Hess and Vytautas Iesmantavicius (proteomics and protein analysis facility) for technical advises on IPs and performing the mass spec analysis. Thanks to Laurent Gelman and Steven Bourke (FAIM) who helped me become a very big fan of the W1 spinning disc microscope. Special thanks also to the FMI IT support, who I could always bother with my more or less "serious" computer problems. Thanks also to the media kitchen, who always supplied me with a huge amount of plates.
A very special thanks goes to all the Ciosk lab members, present and past ones. It was and still will be a pleasure to work with you guys! I really appreciate it to not only have you as my colleagues, but also as friends.
A few Cioskies I would like to specially thank. Jorge Merlet for (h)is (that typo is for the French…) constant support even after he left the lab, his motivation and enthusiasm that kept me going. Janosch Stöcklin for performing a large part of the E3 ligase screen, thanks for this huge amount of work. Balazs (Balzyly) Hargitai, who started the *utx-1* promoter dissection and who annotated the conserved domains within the promoter. Thanks also for being my supervisor when I started in the lab and for introducing me to the world of *C. elegans*.
Thanks to my family, my mum, my dad and my sister, who always supported me, and to my friends, near and far, that made my life outside the lab a blast.
Thanks to the SBB for being mostly on time and even apologizing for a 2 min delay, as a commuter I really appreciate that. Thanks also to the guy at the "Guudy" coffee shop at the Zurich train station for getting my morning coffee and Gipfeli ready as soon as he sees me approaching. Last but not least I would like to specially thank Jan, who not only commutes with me to Basel (solidarity!!) and turns train rides sometimes in inspiring philosophical and political discussions, but who became one of my best friends over the years, one I could always count on.